Energy Utilities from Low Temperature Industrial Waste Heat: Analysis of a Few Cycles

Thesis submitted by

Subha Mondal

Doctor of Philosophy (Engineering)

Department of Mechanical Engineering,
Faculty Council of Engineering & Technology
Jadavpur University
Kolkata, India

2019

JADAVPUR UNIVERSITY

KOLKATA-700032, INDIA

INDEX NO. 61/15/E

1. Title of the thesis: **Energy Utilities from Low Temperature Industrial Waste Heat: Analysis of a Few Cycles.**

2. Name, Designation & Institution of the Supervisor/s:
Dr. Sudipta De,
Professor,
Department of Mechanical Engineering,
Jadavpur University

3. List of publication:

International Journal

I. Mondal S, Alam S, De S. Performance assessment of a low grade waste heat driven organic flash cycle (OFC) with ejector. ***Energy* (*Elsevier)*** 163(2018)849-862.

II. Mondal S, De S. Ejector based organic flash combined power and refrigeration cycle (EBOFCP&RC) –A scheme for low grade waste heat recovery. **Energy (*Elsevier)*** 134 (2017) 638-648.

III. Mondal S, De S. Power by waste heat recovery from low temperature industrial flue gas by Organic Flash Cycle (OFC) and Transcritical-CO2 power cycle: a comparative study through combined thermodynamic and economic analysis. ***Energy (Elsevier)*** 121(2017) 832-840.

IV. Mondal S, De S. CO2 based Power cycle with multi-stage compression and intercooling for low temperature waste heat recovery. ***Energy (Elsevier)*** 90 (2015) 1132-1143.

V. Mondal S, De S. Transcritical CO2 power cycle – effects of regenerative heating using turbine bleed gas at intermediate pressure. ***Energy (Elsevier)*** *87* (2015) 95-103

Book Chapter

I. Mondal S, De S. Power and Other Energy Utilities From Low Grade Waste Heat – Novel Technologies to Reduce Carbon Footprint. ***Reference Module in Materials Science and Materials Engineering (Elsevier)***2018

4. List of Patents: Nil

5 List of Presentation in National/ International /conferences/ Workshops:

I. Mondal S, De S, Ashadi M. CO2 based combined power and refrigeration cycle - a scheme for low grade waste heat recovery. Proceedings of the International Conference on Sustainable Energy and Environmental Challenges (***SEEC-2017***), Mohali, India.

CERTIFICATE FROM THE SUPERVISOR

This is to certify that the thesis entitled "**Energy Utilities from Low Temperature Industrial Waste Heat: Analysis of a Few Cycles"** submitted by Shri Subha Mondal who got his name registered on 29/01/2015 for the award of Ph.D. (Engg) degree of Jadavpur University is absolutely based upon his own work under my supervision and that neither his thesis nor any part of the thesis has been submitted for any degree/diploma or any other academic award anywhere before.

(Sudipta De)
Signature of sole Supervisor
and date with office Seal

Dedicated to
My Father

Acknowledgements

During my journey of PhD work, there were many ups and downs. I would like to express my sincere gratitude to those people who helped me to overcome all the hurdles throughout my PhD period.

First and foremost, I would like to gratefully acknowledge my PhD supervisor, Prof. Sudipta De for his continuous support and guidance. It is not an exaggeration to say that my curiosity and eagerness in research was evoked by Prof. Sudipta De. He provided me all the necessary facilities and support. Apart from the facility, his valuable suggestion and guidance improved my research a lot. Without his support it was not possible to complete this thesis.

I would like to acknowledge Head of Mechanical Engineering Department and Laboratory-in-charge of Heat Power Laboratory, Mechanical Engineering Department, Jadavpur University, for providing me the infrastructure support during the PhD work. I would also like to express my gratitude to the staff of Heat Power Laboratory and my lab mates, especially Mr. Avishek Ray, for making the time happy and enjoyable in the laboratory.

I would like to express my sincere gratitude to my research committee for their valuable suggestions. Last but not least, I owe my greatest gratitude to my family for their continuous support.

(Subha Mondal)

Abstract

Global demand for secondary energy is increasing steadily with time. Most of this global demand is catered to by fossil fuel based power plants.These fossil fuel based power plants are responsible for the most of the greenhouse gas emission. Fossil fuel resources are also finite in nature. Extensive production of secondary energy using renewable resources may reduce fossil fuel consumption and corresponding greenhouse gas emission to some extent. Satisfying global demand for secondary energy with minimum environmental impact is very challenging. Though installed capacity of renewable energy is increasing, it is not possible to replace fossil fuel based power plant by renewable one in near future. As substantial part of industrial energy input through combustion of fuel is rejected as waste heat, this waste heat can also be utilized to produce secondary energy through innovative cycles. This would reduce fossil fuel consumption and corresponding emission of greenhouse gases to some extent. It should be noted that steam based Rankine cycle is the best possible option for producing power from any heat source available at or above 200°C. Conversion of available waste heat into power is very challenging if temperature of the heat source is below 200°C. In the present study, low grade heat driven cycles (power cycles as well as combined power & refrigeration cycle) are proposed to achieve better thermodynamic performance. The cycles are assumed to be driven by low grade heat of the flue gas with temperature ranging from 150°C to 200°C.

It is observed during the analysis that 1^{st} and 2^{nd} law efficiencies of a regenerative transcritcal CO_2 power cycle can be improved appreciably by using an additional regenerator with turbine bleeding. Cycle performance of a regenerative CO_2 power cycle (expressed in terms of specific work output, 1^{st} law efficiency and 2^{nd} law efficiency) also improves by the adoption of multistage compression with intercooling.

While recovering waste heat of the flue gas, free from SO_2, an organic flash cycle (OFC) produces power output, which is comparable to the power output of a transcritical CO_2 power cycle without regeneration. However, the OFC exhibits economically superior performance than the transcritical CO_2 power cycle without regeneration. The thermodynamic performance of an OFC can also be improved by replacing the low-pressure throttle valve of the OFC with an ejector.

List of publication:

International Journal

1. Mondal S, Alam S, De S. Performance assessment of a low grade waste heat driven Organic flash cycle with ejector. ***Energy* (*Elsevier)*** 163(2018)849-862.
2. Mondal S, De S. Ejector based organic flash combined power and refrigeration cycle (EBOFCP&RC) –A scheme for low grade waste heat recovery. ***Energy* (*Elsevier)***134 (2017) 638-648.
3. Mondal S, De S. Power by waste heat recovery from low temperature industrial flue gas by Organic Flash Cycle (OFC) and Transcritical-CO2 power cycle: a comparative study through combined thermodynamic and economic analysis. ***Energy (Elsevier)***121(2017) 832-840.
4. Mondal S, De S. CO2 based Power cycle with multi-stage compression and intercooling for low temperature waste heat recovery. ***Energy (Elsevier)***90 (2015) 1132-1143.
5. Mondal S, De S. Transcritical CO2 power cycle – effects of regenerative heating using turbine bleed gas at intermediate pressure. ***Energy (Elsevier)*** *87* (2015) 95-103

International Conference

1. Mondal S, De S, Asadi M. CO2 based combined power and refrigeration cycle - a scheme for low grade waste heat recovery. Proceedings of the International Conference on Sustainable Energy and Environmental Challenges (***SEEC-2017***), Mohali, India.

Book chapter published

1. Mondal S, De S. Power and Other Energy Utilities From Low Grade Waste Heat – Novel Technologies to Reduce Carbon Footprint. ***Reference Module in Materials Science and Materials Engineering(Elsevier)***2018.

Contents

List of Tables

List of Figures

Nomenclature

Symbols

c_P	Specific heat (kJ $kg^{-1}K$)
C_P^0	Basic equipment cost ($)
E	Exergy (kW or kJ kg^{-1} of FG or kJ kg^{-1} of working fluid)
h	Enthalpy (kJ kg^{-1} K)
I	Irreversibility (kW or kJ kg^{-1} of FG or kJ kg^{-1} of working fluid)
$\dot{m}$	Mass flow rate (kg s^{-1})
NTU	Number of transfer unit (dimension less)
P	Pressure (MPa)
r	Bleed ratio (dimension less)
R	Mass fraction(dimension less)
$\dot{Q}$	Heat flow rate (kW)
q	Heat input (kJ kg^{-1} of working fluid)
s	Entropy (kJ kg^{-1} K)
T	Temperature (K)
t	Temperature (^oC)
u	Fluid velocity (m s^{-1})
Δt_{Pinch}	Pinch point temperature difference (^oC)
Δt_{LTE}	Terminal temperature difference at the low temperature end (°C)
U	Over all heat transfer coefficient ($wm^{-2}K$)
$\dot{W}$	Power (kW)
W	Work (kJ $kg^{-1}$of FG)
W_{NET}	Work output (kJ $kg^{-1}$of FG)
w	Work (kJ kg^{-1} of working fluid)
$\dot{W}_{REF}$	Equivalent power input for a vapour compression refrigeration (kW)
$w_{SPEcIFIC}$	Specific work output (kJ $kg^{-1}$of working fluid)
x	Quality (Dimension less)

Greek letter

η	Efficiency (Dimension less)

α	Convective heat transfer coefficient (wm^{-2} °C)
μ	Ejector entrainment ratio (Dimension Less)

Subscripts

CON	condenser
CO	Cooler
Cr	Critical point
D	Diffuser
E	Evaporator
F	Flash pressure
gi	Flue gas inlet
go	Flue gas outlet
C	Compressor
COM	Compressor exit
HPC	High pressure compressor
HPT	High pressure throttle valve
Ci	i^{th}stage of compression
HRU	Heat recovery Unit
HTR	High temperature regenerator
LPC	Low pressure compressor
LPTV	Low pressure throttle valve.
LTR	Low temperature regenerator
m	Mixing
N	nozzle
P	Pump
R	Regenerator
RE	Refrigeration effect
T	Turbine
TE	Turbine exit
d	Diffuser
I	1st law
II	2nd Law
i	Intermediate

0	Ambient condition

Abbreviation

AUTI	Area utilization temperature indicator
BMC	Bare module cost
CFCs	Chlorofluorocarbons
(CAEBOFCP&RC).	compressor assisted ejector based organic flash combined power and refrigeration cycle
EBOFCP&RC	Ejector based organic flash combined power and refrigeration cycle
FG	Flue gas
HCFCs	Hydrochloroflurocarbons
HFCs	Hydroflurocarbons
HFOs	Hydrofluroolefins
GWP	Global warming potential
HRU	Heat recovery unit
HP	High pressure
HT	High temperature
IP	Intermediate pressure
LT	Low temperature
LP	Low pressure
NTU	Number of transfer unit
ODP	Ozone depletion potential
OFC	Organic Flash Cycle
ORC	Organic Rankine Cycle
T-CO_2	Transcritical CO_2.

1. Introduction

The rise of global average temperature due to excessive emission of greenhouse gases (specifically CO_2) due to combustion of fossil fuel is an issue of great concern for the survival of future generation. Fossil fuel based power plants are responsible for the majority of this CO_2 emission. However, fossil fuel burning is unavoidable for a considerable period in future to maintain a steady energy supply for desirable industrial growth and improved living standard.

Though renewable power generation is steadily increasing worldwide, the majority of the global demand for electricity is still being supplied by coal based power plants. There is a major gap between possible generation of secondary energy using renewable resources and corresponding global demand of the same for a sustainable development. In this situation, replacement of older coal based power plants with an improved natural gas based power plants, retrofitting of existing low efficient power plants for better efficiency, incorporating CO_2 capture and sequestrations are some possible better options to continue with fossil fuel and simultaneously to fight against the threat of global warming. However, all of these are capital intensive options with a larger time frame to implement.

On the other hand, generally a large part of all industrial energy inputs through combustion of fuels is finally released to the local atmosphere as waste heat for many existing plants. This waste heat may be utilized to produce more electricity introducing suitable retrofitting for this purpose. Thus, the additional amount of fossil fuel burning required for generating that amount of power will be reduced and corresponding CO_2 emission will not be there.

If waste heat is available above 300°C, steam based Rankine cycle is the well established technology for converting waste heat into secondary energy say, electricity. Steam based CCGT (Combined Cycle Gas Turbine) may be cited as an example in this respect. However; new innovation is required to generate secondary energy from waste heat available below 200°C.

1.1 Review of energy scenario worldwide and share of fossil fuel

Global energy consumption is ever increasing. It is reported in International energy outlook, 2017 (2017) that between 2015 to 2040 world energy consumption will increase by 28%. More than half of this increment in energy consumption will be in non-OECD Asia (including India and China) due to the rapid economic growth of these countries. It is predicted in this report that there will be 51% increment in energy demand in non-OECD Asia. In Africa and Middle

East, this growth will be 51% and 45% respectively. Industrial sector that consumes more than 50% of the world energy production appears to be a major end user of global energy supply.

Though, global contribution of renewable energy is increasing steadily, fossil fuels like liquid fuel (including petroleum), coal and natural gas are the major sources that still contribute to most of the global energy demand. World energy council reported in 2016 (2016) that oil accounts for 32.9% of global energy demand. On the other hand, coal accounts for about 30% of global basic energy consumption. 40% of the global secondary energy demand is by coal based power plants. Natural gas is the third major contributor to global primary and secondary energy demands. As still fossil fuel-based power plant caters to majority of global secondary energy demand, electricity production units are responsible for more than 40% of the global CO_2 emission as shown Fig. 1.1.

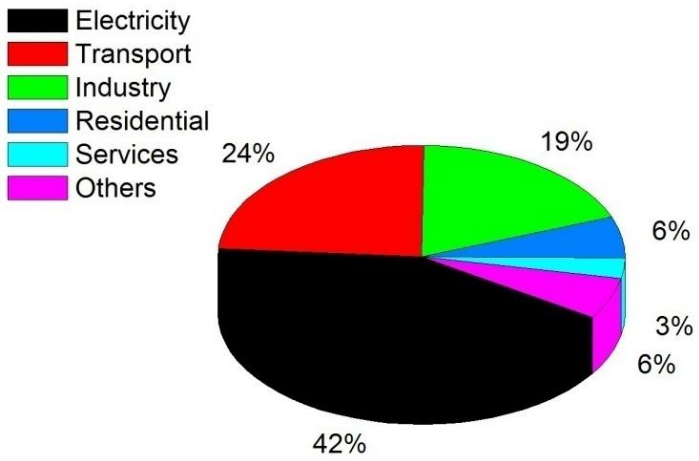

Fig. 1.1: Global CO_2 emission by different sector in 2015 (IEA Statistics, 2017)

1.2 Status of renewable energy and gap between demand and supply

As discussed in the previous section, it is clear that the power sector is responsible for more than 40% of the global CO_2 emission. So instead of burning fossil fuels it is better to concentrate on renewable resources like Solar, wind, hydro power etc. Wind, solar and nuclear energy are the forms of energy that can effectively reduce global CO_2 emission.

However, improved technology for large power generation at lower cost is the critical challenge for wide spread power harvesting from renewable sources.

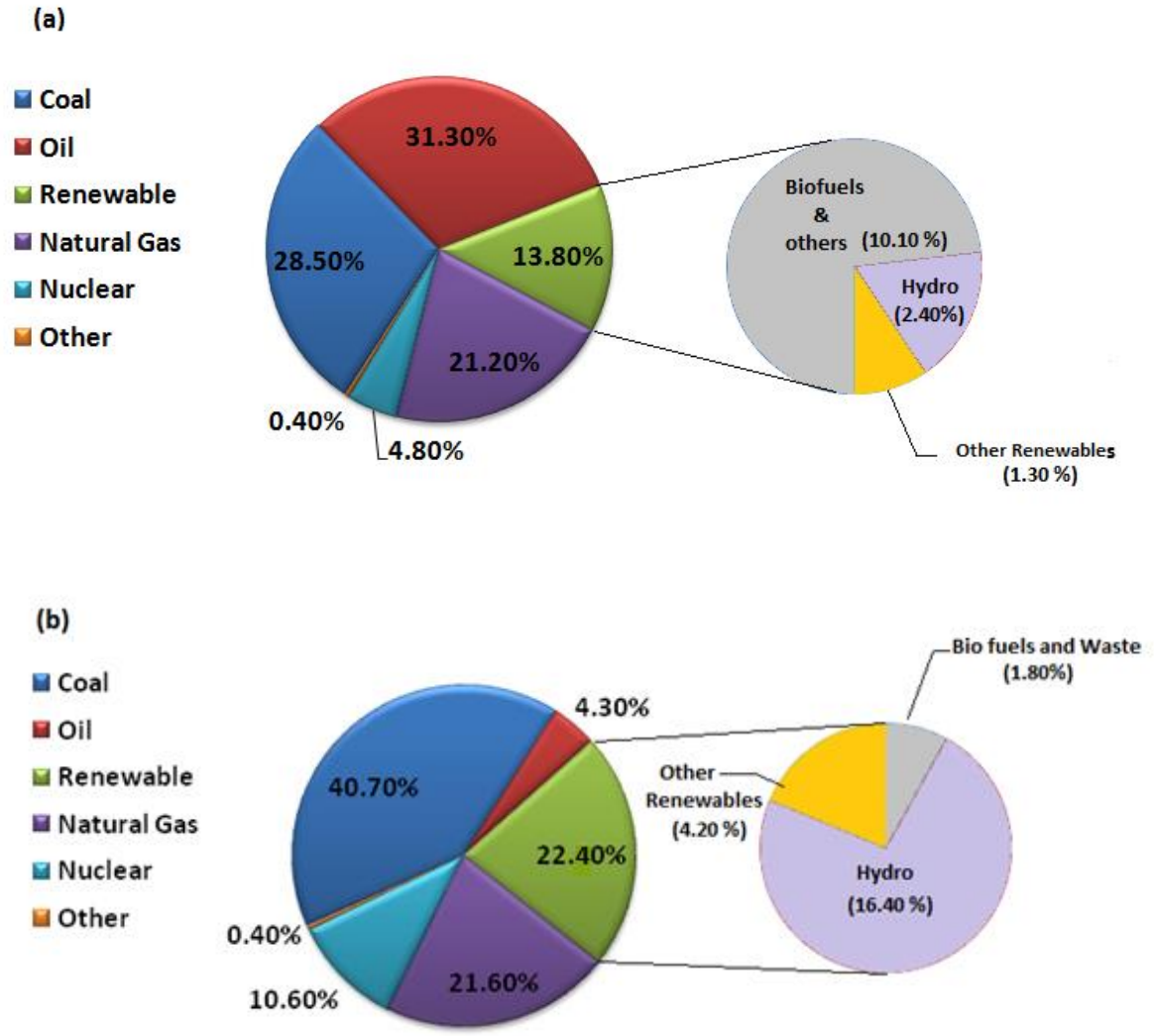

Fig. 1.2 (a): Fuel shares for global primary energy supply of 2014 (b) Fuel shares for global secondary energy supply of 2014 (IEA Statistics, 2016).

It was reported by IEA (2016) that in the year 2014, only 13.8% of global primary energy was produced from Renewable resources. For electrical energy supply, corresponding value was 22.4% of global electricity production as shown in Fig. 1.2 (b). Out of this 22.4%, 16.4%

were only from hydro power and 1.8% was from bio fuel and available waste. Thus, in the year 2014, only 4.2% of global demand of electricity was from geothermal, solar, wind and tidal resources.

IEO (2017) reported that between 2015 and 2040 renewable energy use will grow at an average rate of 2.8% per year. During this period global share of coal based power will decline from 40% in 2015 to 31% in 2040. In the year 2040, renewable resources will contribute 31% of the global demand for secondary energy. Among non hydro-power renewable resources, solar and wind are two fastest growing sectors- global capacity of these two resources will be 2.5 and 1.4 trillion kWh respectively in the year 2040. However, global electricity demand will rise from about 22 trillion kWh in 2015 to about 33 trillion kWh in 2040 and about 57% of this demand will be from coal and natural gas based power plants. Corresponding CO2 emission will also be an issue of great concern. Moreover the availability of renewable resources greatly depends on location and environmental condition. Fluctuating supply of electricity from renewable resources is a great challenge for its successful utilization. Thus, in addition to the progress of renewable power generation technology other possible options are to be explored to reduce carbon footprint resulting from burning of fossil fuels. Innovation for improved utilization of fossil fuels for lower CO_2 emission appears to be a critical need at present.

1.3 Energy efficiency through waste heat recovery

Most of the industrial units require thermal energy input in some form for their operation. It was presented by Rosen (2013) that in the year 2005 total industrial energy input was about 87.6 Exa Joule (EJ). Out of this energy input only 44.6EJ was utilized. Thus, nearly 50% of the industrial energy input remained un-utilized and ultimately released into the local environment as waste heat. Obviously there is wide variation in quality (basically its temperature) and quantity of waste heat released from different industries.

Utilization of industrial waste heat to meet a part of local electricity demand or to supply auxiliary power to run plant equipment may enhance overall utilization efficiency of input fossil fuel and hence, reduce carbon footprint for same utility services through less fossil fuel consumption. It should be noted that performance of a waste heat recovery unit greatly depends on quality of waste heat used and local ambient condition. Proper selection of technology with suitable working fluid is also very critical for the successful implementation of waste heat recovery process.

1.3.1 Classification of waste heat recovery and its challenges and issues

It is important to note that the majority of waste heat is carried away by the flue gas streams and released finally to the local atmosphere. Industrial waste heat can be grossly classified into three different categories depending on their temperature as shown in table1.1

Table 1.1 Waste heat classification

Waste heat temperature range (°C)	Waste heat category
300-500	High grade
200-299	Medium Grade
100-199	Low grade

About 66% of the industrial heat released to ambient is low grade heat as presented in Fig.1.3. Being of large quantity, systematic utilization of this low grade waste heat would reduce green house gas emission significantly by reducing fossil fuel consumption.

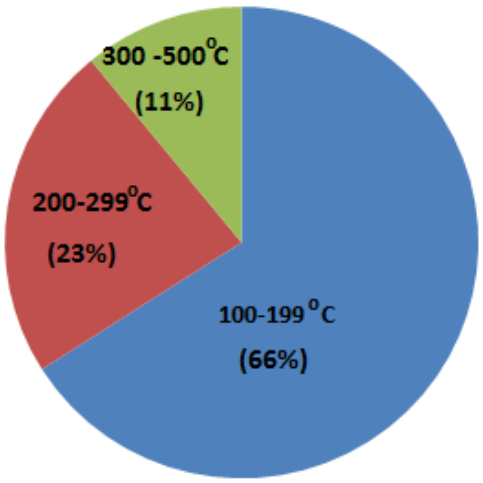

Fig. 1.3: Temperature distribution for the industrial waste heat (Haddad et al. 2014)

Majority of the industrial waste heat is carried away by exhaust flue gas. The quality of waste heat can be determined by the flue gas temperature and can alternately be represented by its exergy value. Exergy is the theoretically maximum useful work obtainable from a given heat source. It depends on flue gas temperature as well as the temperature of the immediate surroundings as shown in equation -1.1:

$$e_g = c_{pg}\left(T_g - T_0\right) - c_{pg}\ln\left(\frac{T_g}{T_0}\right) \qquad (1.1)$$

Variation of exergy of a flue gas stream with a varying flue gas temperature at different ambient temperatures is demonstrated in Fig. 1.4. It is evident from Fig. 1.4 that exergy or the quality of the flue gas decreases with a decrease in flue gas temperature.

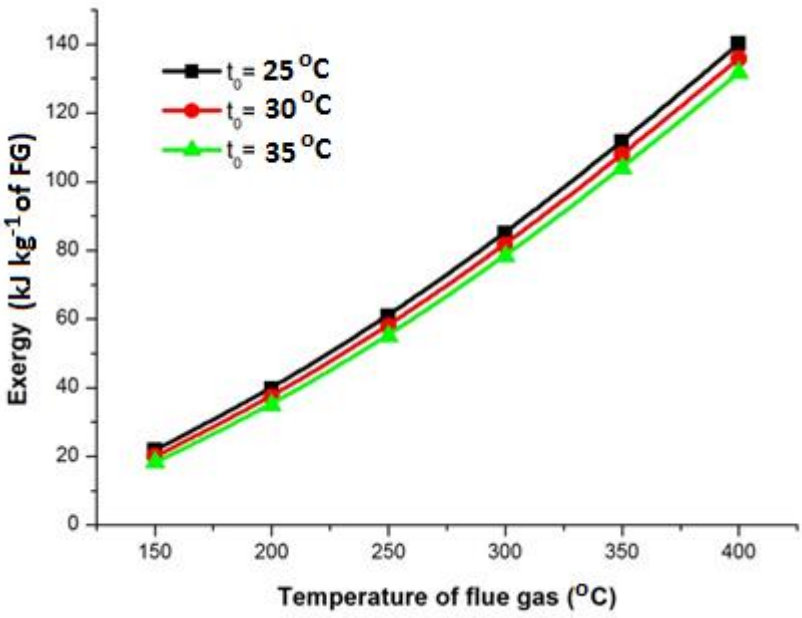

Fig. 1.4: Exergy variation with varying temperature of flue gas

The most effective way of utilizing waste heat is to produce secondary energy through some thermodynamic cycles. For fixed heat source and sink temperatures, theoretically most efficient thermodynamic cycle for generating power is Carnot cycle. As during the execution of any real cycle, certain finite temperature difference between the flue gas and the working fluid during heat transfer is always be there, the efficiency of the any actually executed cycle is always less than that of the Carnot cycle. Efficiency of any power cycle

sharply decreases with a decrease in heat source temperature. As a result waste heat recovery becomes more challenging as flue gas temperature decreases. This challenge is even more for the ambient temperature being higher.

Besides flue gas temperature, composition of the flue gas is another major factor for the selection of suitable waste heat recovery scheme. If some amount of SO_2 is present in the flue gas then SO_2 reacts with moisture and produces sulphuric acid. Reaction of sulphuric acid formation is presented as follows:

$$SO_2 + \frac{1}{2}O_2 = SO_3$$

$$SO_3 + H_2O = H_2SO_4$$

Acid dew point temperature (i.e. Sulphuric acid condensation temperature) of the flue gas varies between 115 to 160ºC depending on the SO_2 content in the flue gas. As Sulphuric acid is highly corrosive, cooling of the flue gas in the waste heat recovery unit (HRU) below the acid dew point temperature must be avoided to ensure longer life. Thus, for the flue gas containing SO_2, improving 1st law or thermal efficiency of a thermodynamic cycle is the prime objective as for a specified mass flow rate and temperature of the flue gas, waste heat available is fixed. However, if the flue gas is free from SO_2, it is better to cool it to a much lower temperature as it would increase the power output from same available heat of the flue gas. Thus, for SO_2 free flue gas, maximizing work output per kg of flue gas flow is the objective instead of improving thermal efficiency of conversion of waste heat to work. While improving cycle performance, economical aspect must also be considered.

1.3.2 Selection of working fluid for low temperature waste heat recovery

Selection of suitable working fluid with zero ODP, low GWP and reasonable thermodynamic performance is another challenging task. CFCs (Chlorofluorocarbons) had been most preferred working fluids since 1930. However, Montreal protocol decided to phase out production of CFCs by 2010 due to high ozone depletion potential of CFCs. Soon HCFCs (Hydrochlorofluorocarbons) appeared as alternatives of CFCs. But due to very high GWP use of HCFCs will not be permitted after 2030 in developed countries and after 2040 in developing countries (Powell, 2002). HFCs are to be phased out by the year 2047 according to Kigali amendment to the Montreal protocol introduced in 2016. In this situation, natural

refrigerants, Hydrocarbons, and some of the HFCs (Hydrofluorocarbons) with low GWP are the possible working fluids for waste heat recovery as listed in table 1.2 (Calm and Hourahan, 2011).

Table-1.2: Environmental and safety data of selected refrigerant (Calm and Hourahan, 2011).

Category	Refrigerant	Critical temperature (° C)	Critical pressure (MPa)	ODP	GWP in 100years	ASHRAE safety group
Natural refrigerant	CO_2 (R744)	30.978	7.38	0	1	A1
	Ammonia (R717)			0	0	B2
	N_2O (R744A)	36.425	7.254	0.017	298	A1
HC	Butane (R600)	152.01	3.796	0		A3
	Isobutane (R600A)	134.7	3.64	0	~20	A3
	Pentane (R601)	196.56	3.358	0	~20	A3
	Isopentane (R601A)	187.78	3.358	0	~20	A3
	Propane (R290)	96.7	4.248	0	~20	A3
HFC	Difluoromethane (R32)	78.11	5.782	0	675	A2L
	1,1,1,2-tetrafluroethene (R134a)	101.06	4.059	0	1430	A1
	1,1-Difluroethene (R152a)	113.26	4.517	0	124	A2
	Fluroethane (R161)	102.22	4.702	0	12	-
	1,1,1,3,3,3-Hexafluropropane (R236ea)	139.29	3.502	0	1370	-
	1,1,1,3,3-Pentafluropropane R245fa	154.05	3.64	0	1030	B1

Both CO2 and NH_3 are in use since the 19th century. However, high toxicity of ammonia is an issue of great concern for their utilization in the HRU (Heat Recovery Unit). On the other hand, CO2 is a non-flammable and non toxic working fluid. Due to lower critical temperature, CO_2 at supercritical state can be utilized for the recovery of low grade waste heat. This eliminates the pinch limitation of the subcritical HRU. Supercritical CO_2 has a concave shaped temperature profile as shown in Fig.1.5. This allows operation of the HRU with smaller terminal temperature differences by maintaining a feasible size of the HRU. Thus, CO_2 can be heated closer to the flue gas inlet temperature to achieve higher 1st law efficiency. High operating pressure (>10MPa) of CO_2 inside the HRU is a disadvantage of the CO_2 power cycle. However, CO_2 may be considered as the most preferable working fluid after steam if thermodynamic, environmental and safety issues are considered together. For low grade waste heat recovery, CO_2 is emerging as a better option than steam as the working fluid.

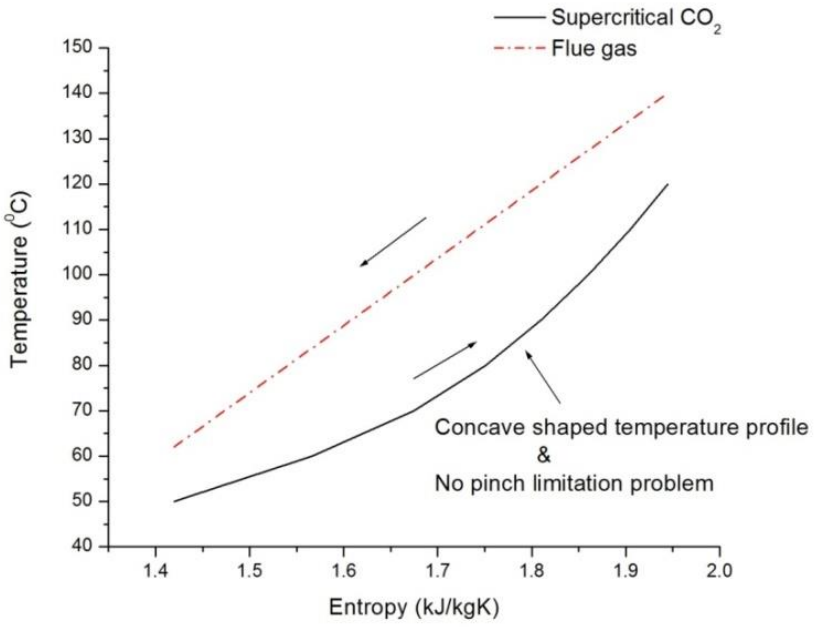

Fig. 1.5: Temperature profile of supercritical CO_2

Hydrocarbons as working fluids yield satisfactory thermodynamic performance for low temperature waste heat recovery. They are non toxic and with zero ODP and negligible GWP.

However, they fall in A3 safety category which means they are highly flammable gases. Thus, possible safety measures are to be ensured to eliminate the accidental explosion while using HCs as working fluids.

HFCs are having higher GWP compared to HCs. However, they are favoured due to their excellent thermodynamic properties and less chance of explosion. For an example, R32 is slightly flammable and R245fa is non-flammable. But R245fa is toxic to some extent.

Besides refrigerants listed in table 1.2, recently some of the HFOs (Hydrofluroolefins) may be considered for future use as working fluids. As listed in table 1.3 these working fluids are less flammable compared to hydrocarbon as well as having zero ODP and lower GWP. However, they are still not available commercially.

Table 1.3: Environmental and safety data for HFO refrigerant.

Refrigerant	Critical temperature(^{0} C)	Critical pressure(MPa)	ODP	GWP in 100years	ASHRAE safety group
R1234yf	94.7	3.3822	0	04	A2L
R1234ze(E)	109.36	3.6349	0	06	A2L
R1234ze(Z)	150.12	3.53	0	<10	A2L

Finally, it should be noted that saturated vapour lines of some of the working fluids (R600, R600a, and R245fa etc.) have positive slope. These working fluids are known as dry working fluids. Some of the working fluids which are having almost vertical vapour lines are known as isentropic working fluids. With the use of dry or isentropic working fluids, compulsory requirement of a super heater in conventional ORC can be eliminated.

1.4 Literature review on low grade heat recovery

About 50% of the energy input in industrial processes through the combustion of fuel is finally rejected as waste heat. Utilization of this waste heat for producing different energy utilities is one of the possible sustainable ways for reducing fossil fuel consumption and corresponding greenhouse gas emission.

1.4.1 Steam vs. organic working fluids

Producing power through steam-based Rankine cycle is the most preferable option if waste heat temperature is above 230^0C. Combined cycle gas turbine (CCGT) may be cited as one of the suitable examples in this respect (Kehlhofer 1991). Steam is non-flammable and non-toxic. Leakage of steam does not cause any adverse effect on the environment like global warming, ozone layer depletion etc. Low power consumption in recirculation pump and high chemical stability are other two desirable properties of steam as the working fluid.

Though steam is the most desirable working fluid for available heat at a higher temperature, the performance of the steam-based Rankine cycle drops noticeably if heat is available at or below 200°C. This is because with heat available at or below 200°C it is not possible to maintain the desired pressure in the heat recovery steam generator (HRSG) along with the required degree of superheating. This limitation of steam based Rankine cycle may be addressed by replacing steam with some alternative (say, organic) working fluids. Zhang et al. (2016) demonstrated that among steam Rankine cycle (SRC), Organic Rankine Cycle (ORC) and Steam-organic Rankine cycle (S-ORC), ORC yielded highest thermal efficiency, exergy efficiency and power output for the heat source temperature ranging between 150 to 200^oC. Quoilin et al. (2013) pointed out some advantages of organic fluid over steam as the working fluid of a Rankine cycle. The possibility of air infiltration into the condenser of the steam based Rankine cycle can be eliminated by using organic working fluids as for most of the organic working fluids condensing pressures corresponding to heat rejection temperatures are higher compared to atmospheric pressure. The Organic Rankine cycle also allows the use of once-through type heat recovery unit instead of the drum-based boiler with recirculation. Some of the organic working fluids are having saturation vapour lines with positive slope. These working fluids are termed as dry working fluids. Use of these working fluids for low grade heat recovery eliminates the compulsory requirement of the super-heater of the steam-based Rankine cycle. Mago et al. (2008) also demonstrated that with superheating of dry working fluid thermal efficiency of the Rankine cycle remains almost constant.

1.4.2 Review on low temperature organic Rankine cycles (ORCs)

1.4.2.1 Literature on modified Layout of ORCs

Though a basic ORC can convert low grade heat into power more effectively compared to that of an SRC, many researchers proposed modifications of the basic ORC configuration to achieve improved thermodynamic performances. Peris et al. (2013) analysed performances of five different configurations of ORCs – namely basic ORC, regenerative ORC, double regenerative ORC, reheat regenerative ORC and ejector ORC. All ORCs were driven by the heat of cooling water of an IC engine. For the specified operating condition the double regenerative ORC with SES36 working fluid yielded the highest net electrical efficiency. Xi et al. (2013) successfully implemented the genetic algorithm (GA) to explore optimum values of operating parameters for the basic ORC (BORC), single stage regenerative ORC and double stage regenerative ORC. It was observed that for a specified heat source temperature the double stage regenerative ORC yielded the highest exergy efficiency followed by the single stage regenerative ORC. Thermal efficiency of a basic ORC could also be improved by using an internal heat exchanger (Li 2016). Bina et al. (2017) reported that an ORC with internal heat exchanger could produce a larger power output at a lower cost. Use of internal heat exchanger also reduced CO_2 emission by cutting down the fuel consumption. Saleh (2007) pointed out that the use of an internal heat exchanger would be advantageous if the superheated working fluid were available at the exit of the turbine. However, Marver et al. (2014) pointed out that there was no need of recuperator if the lower limit of heat source exit temperature was not assigned by any constraint (say acid dew point). Braimakis and Karella (2018) concluded that the use of dry working fluid would be advantageous for both the recuperative and the regenerative ORCs. Those ORCs also exhibited improved performance with working fluids having higher critical temperatures.

Some of the researchers also proposed to use transcritical ORCs for low grade heat recovery. Baik et al. (2013) claimed that an R125 based transcritical ORC could produce higher power output compared to those of subcritical ORCs using R134a, R245fa and R152a as working fluids. In this study, geothermal water available at 100^0C was utilized as the heat source. Use of the trascritcal ORC ensured greater waste heat recovery from a varying temperature heat source (Saleh et al. 2007).

1.4.2.2 Literature on ORCs with different pure working fluids

Performances of ORCs (Both basic as well as modified) greatly depend on the selection of suitable working fluids. Many of the researchers identified certain characteristics of working fluids that would optimize the energetic performance of a low grade heat driven ORC for specified operating conditions. Liu et al. (2004) analyzed the performance of the basic ORC by using seven different working fluids. They concluded that working fluids with Hydrogen bonds would not be suitable for ORCs. This is because the presence of hydrogen bond in working fluids results in higher enthalpy of evaporation. Saleh et al. (2007) analyzed performances of different ORC configurations using thirty-one pure working fluids. All cycles were assumed to be operated between 100 and 30^{o}C. They revealed that the use of dry working fluids in a subcritical cycle with internal heat exchanger would yield highest thermal efficiency. They also presented that combining superheating with internal heat exchanger would lead to appreciable improvement in thermal efficiency of a subcritical ORC using wet working fluid. White et al. (2017) reported that a low grade heat driven ORC would yield optimum performance by using working fluids with simple molecular structure (such as propane and propene).

Besides energetic performance, environmental and Safety parameters of working fluids are also to be considered for successful implementation of ORCs. Since 1930 CFCs were most preferred working fluids due to easy availability and their excellent thermodynamic properties. Due to nontoxic and non-flammable nature, use of CFCs ensured a longer life of equipment along with safe operation. However, due to high ozone depletion potential, commercial production and use of CFCs were restricted by the Montreal protocol in 1987 (Benhadid-Dib and Benzaoui, 2012). Though HCFCs appeared as good alternatives of CFCs, most of the HCFCs are having appreciably higher global warming potential. Due to very high GWP, use of HCFCs will not be permitted after 2030 in developed countries and after 2040 in developing countries (Powell, 2002). HFCs are also to be phased out by 2047 according to the Kigali amendment to the Montreal protocol, 2016. In this situation, Hydrocarbons, and some of the HFCs (Hydroflurocarbons) with low GWP were considered as working fluids of ORCs by many of the researchers. Galloni et al. (2015) conducted an experimental analysis of an ORC utilizing R245fa as the working fluid. They varied heat source temperature in the range of 75-95^{o}C. The highest cycle efficiency of the experimental setup was slightly higher than 9%. Wei et al. (2007) optimized an exhaust heat driven ORC

using R245fa as the working fluid. They concluded that the peak efficiency and power output would be achieved by keeping the degree of subcooling in the condenser in the range of 0.5-0.6K. According to the investigation conducted by Tchanche et al. (2009) out of 20 considered working fluids R134a appeared as the most suitable working fluid for a low temperature solar driven ORC. Wang et al. (2011) recommended R245fa and R245ca as the most environment-friendly working fluids for an engine waste heat driven ORC out of nine selected working fluids. Varga and Csaba (2018) considered isobutene, butane, isopentane and pentane as working fluids of an ORC, driven by the heat of an air-cooler. As concluded from the analysis, cycle with isobutene yielded highest power output. Zhai et al. (2014) analyzed the performance of a geothermal heat driven ORC by using HC as well as HFC as working fluids. They recommended the use of R32, R134a and propylene as they were capable of extracting larger energy from the given heat source. GWP of these working fluids were less than 1500. Liu et al. (2013) analyzed the performance of a geothermal heat driven ORC using five different hydrocarbons (butane, isobutane, pentane, isopentane and hexane) and one HFC (R245fa) as the working fluid. The cycle with isobutane yielded the highest power output. Aljundi (2011) recommended iso-pentane as the possible alternative of R113. He also showed that ORC with n-butane would exhibit better thermal efficiency compared to those of ORCs using R245fa, R236fa and RC318 respectively. Mikielewicz et al. (2016) analyzed the performance of an ORC utilizing waste heat of water available at 90^{o}C. The heat of bleed steam from a steam turbine was also utilized to improve the evaporation temperature of working fluids. They considered n-pentane, ethanol, R236ea and R245fa as working fluids during the analysis.

1.4.2.3 Literature on ORCs with mixtures of HCs and inert working fluids

Though HCs are having lower GWP compared to HCFCs, most of the HCs are highly flammable. Recent studies indicated that mixing of a non-flammable working fluid (say R245fa, CO_2 etc.) with a highly flammable HC would avoid possible accidental flame propagation during the use of an HC as the working fluid of an ORC. The mixture would have reasonably lower GWP. Le et al. (2014) revealed that ORC with a mixture of n-Pentane and R245fa containing 0.1 mass fraction of R45fa could yield thermodynamic and economic performances which were comparable with that of the ORC using pure n-Pentane as the working fluid. Garg et al. (2013a) proposed a mixture of Isopentane and R245fa in 0.7/0.3 mole fraction ratio to reduce GWP of R245fa as well as the chance of the possible explosion

in ORC operating with pure Isopentane. Kang et al. (2015) reported that a mixture of R245fa/ R600a in (0.9/0.1) mass ratio could produce a satisfactory performance combining issues related to flammability, power output and environmental impact. Xi et al. (2017) optimized the performance of the ORC utilizing R245fa as the flame retardant in mixtures of working fluids. Song and GU (2015) utilized R141B and R11 as the retardants for suppressing the flammability of the hydrocarbons. Garg et al. (2013b) considered mixtures of CO2 and hydrocarbons to address the very high flammability of hydrocarbons.

1.4.2.4 Literature on ORCs with other Zeotropic mixtures of pure working fluids

It was also observed in the literature that utilization of zeotropic mixtures as the working fluid improved performance of an ORC in some specified cases. According to the study conducted by Baik et al. (2013), a transcritical ORC operating with an optimized mixture of R125-R245fa yielded higher power than that of the transcritical ORC operating with R134a. An experimental study conducted by Pang et al. (2017) indicated that ORC with a mixture of R245fa and R123 in a mass ratio of 2:1 could produce 1.66kW power with 4.4% electrical efficiency. The corresponding heat source was at 120°C. Shu et al. (2014) conducted an analysis of ORC, considering R11 and R123 as diluents to reduce the flammability of hydrocarbons. During the analysis, improved thermal efficiency was noted for a particular composition of the zeotropic mixtures. Abadi and Kim (2017) concluded that the ORCs using zeotropic mixtures as working fluid would require larger sized evaporator and condenser compared to those of the ORC using a pure working fluid.

1.4.2.5 Literature on ORCs with HFO working fluids

Recently, some of the researchers proposed the use of HFO working fluids as alternatives to HFCs. HFOs are having zero ODP and very low GWP(<10). They are less flammable compared to HCs. Invernizzi et al. (2016) reported that the net power output of a geothermal driven ORC reduced by 13% as HFC-134a was replaced by HFO-1234yf. The corresponding reduction was 1% if the replacement was done with HFO-1234ze (E). Yamada et al. (2012) claimed that a low or medium temperature heat driven ORC with HFO-1234yf would deliver a thermal efficiency which was comparable to the same delivered with R134a. Eyerer et al. (2016) reported that R1233zd-E would be a good replacement of R245fa in already existing ORC system. Petr and Rabbe (2015) considered R1234ze (Z) as the possible alternative of R245fa. It was observed that ORC with R245fa yielded slightly higher power

output for the heat source temperature ranging between 100 to 182^{o}C. However, power output with R245fa was substantially higher compared to the same with R1234ze (Z) if the temperature of the heat source was in between 182 to 224^{o}C.

1.4.3 Literature on CO_2 based power cycles

CO_2 based power cycle became subject of interest of many of the researchers due to non-flammable, non toxic and environment friendly nature of CO_2 as well as easy availability. High chemical stability is another desirable property of CO_2 as a working fluid. As critical temperature of CO_2 is close to 31^{o}C, the heat recovery unit of a CO_2 based power cycle can be operated at a supercritical pressure even with a lower heat source temperature. This eliminates the pinch limitation of a conventional ORC and also helps to reduce irreversibility in waste heat recovery gas heater by better matching of its temperature profile with temperature profile of the heat source (Chen and Lundqvist, 2011). Supercritical CO_2 is having a concave shaped temperature profile. Thus, the use of super critical CO_2 instead of any subcritical organic fluid results in smaller terminal temperature differences in the HRU. Conventionally, CO_2 based power cycles were considered to be suitable for high temperature applications. Dostal et al. (2004) recommended use of the supercritical CO_2 power cycle in the next generation nuclear reactor. Yoon et al. (2012) reported that a supercritical CO_2 power cycle would yield higher thermal efficiency compared to that of the steam Rankine cycle if the operating temperature was above 500^{o}C. Moullec (2013) showed that a coal power plant with a supercritical CO_2 Brayton cycle could achieve a net efficiency of 50% for maximum cycle temperature and pressure of 620^{0}C and 300 bar respectively. Some of the recent studies indicated CO_2 based power cycle was also capable of producing reasonably good power output from low grade heat. Chen et al. (2006) demonstrated that with same mean heat rejection temperature, transcritical CO_2 cycle yielded slightly higher power output than that of the R123 based ORC. Flue gas available at 150^{o}C was considered as the heat source during this comparative study. It was concluded by Garg et al. (2014) that transcritical CO_2 cycle was more compact than the transcritical steam cycle with comparable thermal efficiency. Thermo-economic comparison between transcritical CO_2 cycle and Kalina cycle for low temperature heat sources revealed that the Kalina cycle exhibited comparatively better economic performance (Li and Dai, 2014). However, high toxicity of ammonia was a major drawback of the Kalina cycle. Li et al. (2016) conducted a comparative study between a Transcritical CO_2 power cycle and an R245fa based ORC.

Under the assumed operating condition the ORC with R245fa yielded slightly higher energy and exergy efficiencies compared to those of the Transcritical CO_2 power cycle. According to the study conducted by Li et al. (2014) a transcritical CO_2 power cycle was an economically better option for the conversion of low grade geothermal heat into power compared to those of ORCs using R600, R601, R123 and R245fa as working fluids. Guo et al. (2010) reported that a transcritical CO_2 power cycle could produce larger power output compared to that of the subcritical power cycle using R245fa. They also pointed out that transcritical CO_2 power cycle would require a smaller sized turbine and larger sized heat recovery unit made of high strength material. Zhang et al. (2007) conducted numerical analysis of a supercritical CO_2 Rankine cycle driven by solar energy. The analysis conducted by Zhang et al. (2007) showed that solar driven Rankine cycle utilizing CO_2 as working fluid could yield thermal efficiency which is comparable with the efficiency of solar cells. A solar driven Rankine cycle utilizing CO_2 as the working fluid was analysed experimentally by Yamaguchi et al. (2006). During the experiment, CO_2 was heated in an evacuated tube solar collector to convert a part of solar energy to electricity. In the experimental setup, as a throttle valve was put in place of the turbine, no power output was obtained from the proposed experimental setup. By utilizing measured experimental data the cycle was evaluated thermodynamically by using PROPATH 12.1. From the analysis, it was demonstrated that solar energy based transcritical CO_2 power cycle could produce heat and power simultaneously with reasonable efficiency. Considering exergy efficiency as the objective function; a genetic algorithm based parametric optimization of Supercritical CO_2 cycle was done by Wang et al. (2010). Bryant et al. (2011) showed that supercritical CO_2 cycle exhibited better performance compared to that of simple supercritical CO_2 cycle provided larger heat transfer area is associated with recuperator of recompression cycle. Sarkar and Bhattacharyya (2009) optimized the performance of a recompression CO_2 power cycle with reheat and also developed an empirical correlation for optimum intermediate pressure. Banik et al. (2016) concluded that for a low temperature cycle, increasing recompression ratio would be beneficial only if the precooler inlet temperature remained constant. Cayer et al. (2009) demonstrated that the incorporation of an internal heat exchanger marginally improved energy and exergy efficiency of a T-CO_2 power cycle operating at low temperature environment. However, this reduced optimum pressure corresponding to maximum efficiencies. Tuo (2013) found a critical turbine inlet pressure above which transcritical reheat CO_2 cycle was more cost-effective than the cycle without

reheat. Dai et al. (2014) evaluated performances of transcritical Rankine cycles using blends of CO_2 with low GWP working fluids. It was observed that R161-CO_2 blend with 0.5 CO_2 mass fraction yielded higher thermal efficiency even at lower turbine inlet pressure. Song et al. (2012) analysed a solar driven transcritical CO_2 cycle using liquefied natural gas (LNG) as the heat sink. Wang et al. (2014) conducted multi objective optimisation of geothermal power plant operating in transcritical CO_2 cycle and utilizing LNG as the heat sink. Ge et al. (2018) developed an experimental setup of a transcritical CO_2 power cycle to demonstrate effects of varying source and sink parameters on system performance. During the experiment, the overall turbine efficiency appeared to be smaller compared to isentropic efficiency. Thus, mechanical and electrical efficiencies of the turbine would be improved further to achieve better overall turbine efficiency. It is important to note that though there is no commercial installation of transcritical CO_2 power cycle still now, it may be a future possible technology due to its simplicity and highly compact turbo machinery (Sarkar, 2015).

1.4.4 Literature on organic flash cycles (OFCs)

Though T-CO_2 power cycle is evolving as one of the promising technologies for low grade heat recovery, there is a possibility of working fluid leakage through various valves and joints in pipelines due to the appreciably high operating pressure of the CO_2 based power cycle. Besides T-CO_2 power cycle, Organic Flash Cycle (OFC) is another possible option that can avoid the pinch limitation of the conventional ORC. The pressure of working fluid in the HRU of an OFC is also appreciably smaller compared to that of the T-CO_2 power cycle. Ho et al. (2012a) revealed that utilization efficiency of OFC was comparable with that of optimized ORC while utilizing the heat of medium and high temperature sources. They also improved performance of the single organic flash cycle by splitting expansion process in two steps and replacing the throttle valve of flash evaporation process by two phase expander (2012b). Thus the system consisted of one two phase expander, one high pressure expander and one low pressure expander. Lee et al. (2016) conducted a comparison between basic OFC, OFC with two phase expander and ORC operating in a low temperature environment. Analysis revealed that OFC could efficiently produce power from low grade heat source. Baccioli et al. (Applied Energy 2017; 199: 69-87) demonstrated that incorporation of a direct contact heat exchanger into the system layout would reduce installation cost of the OFC.

1.4.5 Literature on ejector assisted cycles

Low grade heat source is also capable of producing refrigeration effects by using either vapour absorption refrigeration cycle or ejector based refrigeration cycle. It may be noted that one major advantage of the ejector based refrigeration cycle is the capability of utilizing the wide range of working fluids as refrigerants. Mazzelli and Milazzo (2015) conducted both numerical and experimental analyses of a heat source driven supersonic ejector chiller using R245fs as the working fluid. Analysis conducted by Mansour et al. (2014) revealed that an ejector assisted mechanical compression system could improve the COP of a conventional vapour compression refrigeration cycle operating at similar working condition. Wang et al. (2015) compared performances among transcritical ejector refrigeration cycles using CO_2, R1270, R32, R143a, R125 and R115 as refrigerants. It was observed that the cycle using R1270 as the working fluid yielded the highest COP for a specified heat source condition. Kasperski and Gil (2014) revealed that for fixed ejector geometry, COPs of heavier hydrocarbon based refrigeration cycles became a maximum at specific generator temperatures. A multi temperature combined compression /ejection refrigeration cycle was proposed by Lontsi et al. (2016). Bilir and Ersoy (2009) improved performance of a vapour compression refrigeration cycle by using two phase constant area ejector. Chen et al. (2017) analyzed the performance of a two stage ejector refrigeration cycle driven by dual heat sources experimentally.

Some of the recent studies indicated that a power cycle could be modified by incorporating an ejector into the system. The modified cycle would produce power and refrigeration effects simultaneously. This would be a preferred option as installation and maintenance costs of an ejector based system is significantly small (2015) due to the presence of a lesser number of moving parts. Yang et al. (2016) proposed a combined power and ejector refrigeration cycle in which turbine exhaust of an ORC was utilized to entrain the refrigerant mass coming out from the evaporator. Ghaebi et al. (2017) combined a Kalina cycle with an ejector based refrigeration cycle for producing simultaneous power and cooling effect. Wang et al. (2009) analyzed the performance of a combined power refrigeration cycle in which fluid mass extracted at an intermediate pressure of turbine expansion was utilized as the primary flow to run the ejector. Oliveira et al. (2002) integrated an ejector based heat pump with a Rankine cycle matching heat and power load of a building. The combined system was solar energy and gas driven. Chen et al. (2018) demonstrated that the poor performance of an ORC arising

due to low pumping efficiency could be improved appreciably by using a vapour-liquid ejector. Xu and He (2011) proposed to use an injector as the regenerator in an ORC that exhibited better thermal efficiency compared to a basic ORC when turbine exit pressure was less than 390 kPa.

1.4.6 Identification of research objective from the literature review

From the extensive literature review, it is observed that Organic Rankine cycle, CO_2 based power cycle; organic flash cycles are some of the possible technologies for producing power from low grade heat available at or below 200^{o}C. Energetic performances of these cycles can be improved further by some modifications of system layouts. Most of the low-grade heat sources considered in the literature are either solar or geothermal heat sources. Numbers of studies performed on utilization of low grade waste heat of flue gas are not very appreciable. However, substantial part of the industrial waste heat is carried away by exhaust flue gas and rejected to the immediate surroundings.

The objective of the present study is to suggest some modifications of a few existing power cycles for achieving improved energetic and exergetic performances. The cycles are assumed to be driven by low grade waste heat of the industrial flue gas with temperature ranging from 150°C to 200°C. It is important to note that while utilizing industrial flue gas as heat sources, besides temperature of the flue gas, the composition (i.e. SO_2 content) of the flue gas also plays a vital role for selecting a suitable waste heat recovery scheme.

1.5 Overview of contents in chapters

In chapter-1, background and motivation behind the adoption of the present work are explored. In this chapter, through an extensive literature review possible research gaps are identified to fix the thesis objective.

In chapter-2, a transcritical CO_2 power cycle with two stage regeneration is proposed and corresponding energetic and exergetic performances are evaluated.

In chapter-3, effects of adopting multi-stage compression with intercooling on a regenerative CO_2 power cycle are analyzed. Initially, the performance is evaluated with two-stage compression and intercooling and effects of multi-staging are also evaluated at a later stage of the study.

In chapter-4, energetic and economic performances of an organic flash cycle (OFC) are compared with those of a transcritical CO_2 power cycle. Both of the cycles are assumed to be driven by the waste heat of SO_2 free flue gas available at 150°C.

In chapter-5, the low pressure throttle valve of an organic flash cycle (OFC) is replaced with an ejector to improve the turbine power output. The ejector utilizes the energy of the saturated liquid exiting the vapour separator to entrain exhaust mass of working fluid exiting the turbine at a pressure which is lower than the saturation pressure corresponding to condenser temperature.

In chapter-6 the low pressure throttle valve of an organic flash cycle (OFC) is replaced with an ejector to produce additional cooling effects without affecting the power output of the OFC. The saturated liquid stream exiting the vapour separator is accelerated in the nozzle of the ejector to entrain the dry saturated vapour mass leaving the evaporator of the refrigerator.

In chapter-7, major findings of analyses carried out in chapters 2 to 7 are summarised and possible scopes for future research are identified

2. Transcritical CO_2 power cycle with two stage regeneration

2.1 Objective of the work

In this chapter, a regenerative transcritical CO_2 power cycle is considered as the baseline cycle. The cycle is assumed to be driven by low grade heat of flue gas available at 200^{o}C. As flue gas is assumed to contain some amount of SO_2, the flue gas cannot be cooled below the acid dew point temperature. Thus the base line cycle should be modified to achieve a higher 1st law or thermal efficiency. To improve the thermal efficiency of the base line cycle an additional regenerator is introduced into the system layout. This additional regenerator is driven by the heat of the bleed CO_2 stream extracted at some intermediate pressure of turbine expansion.

2.2 System description

The layout of the proposed transcritical CO_2 power cycle with regenerative heating and corresponding Temperature-entropy diagrams are shown in the Fig. 2.1 (a) and 2.1 (b) respectively.

CO_2 at Supercritical condition from the Heat Recovery Unit (HRU) expands in the turbine. Some CO_2 is extracted at an intermediate stage of the turbine for heating in the high temperature (HT) regenerator. The HT regenerator is a counter flow heat exchanger in which the main CO_2 stream is heated utilizing heat of the extracted CO_2 stream from the turbine. During this regenerative heating bleed CO_2 is cooled from temperature t_8 to t_9. The intermediate pressure (P_i) at which CO_2 is extracted from the turbine for the purpose of regenerative heating is termed as bleed pressure. The ratio of the mass rate of CO_2 extracted to the total CO_2 mass flow rate entering to the turbine is termed as the bleed ratio (r). CO_2 stream coming out of the HT regenerator (at state-9) is compressed to pressure P_1 (state-10) before it mixes with the main CO_2 stream (at state-7). After mixing total CO_2 mass enters the HRU (at state-11) and heated up to turbine inlet temperature (i.e. t_1) by utilizing waste heat of finite quantity flue gas available at 200^{0}C. A low temperature (LT) regenerator is utilized to heat the cold stream coming out of the low pressure (LP) compressor (process 5-6) by the heat (process2-3) from the hot CO_2 stream at the exit of the turbine. 3-4 and 4-5 represent the processes of pre-cooling/condensation and LP compression process respectively.

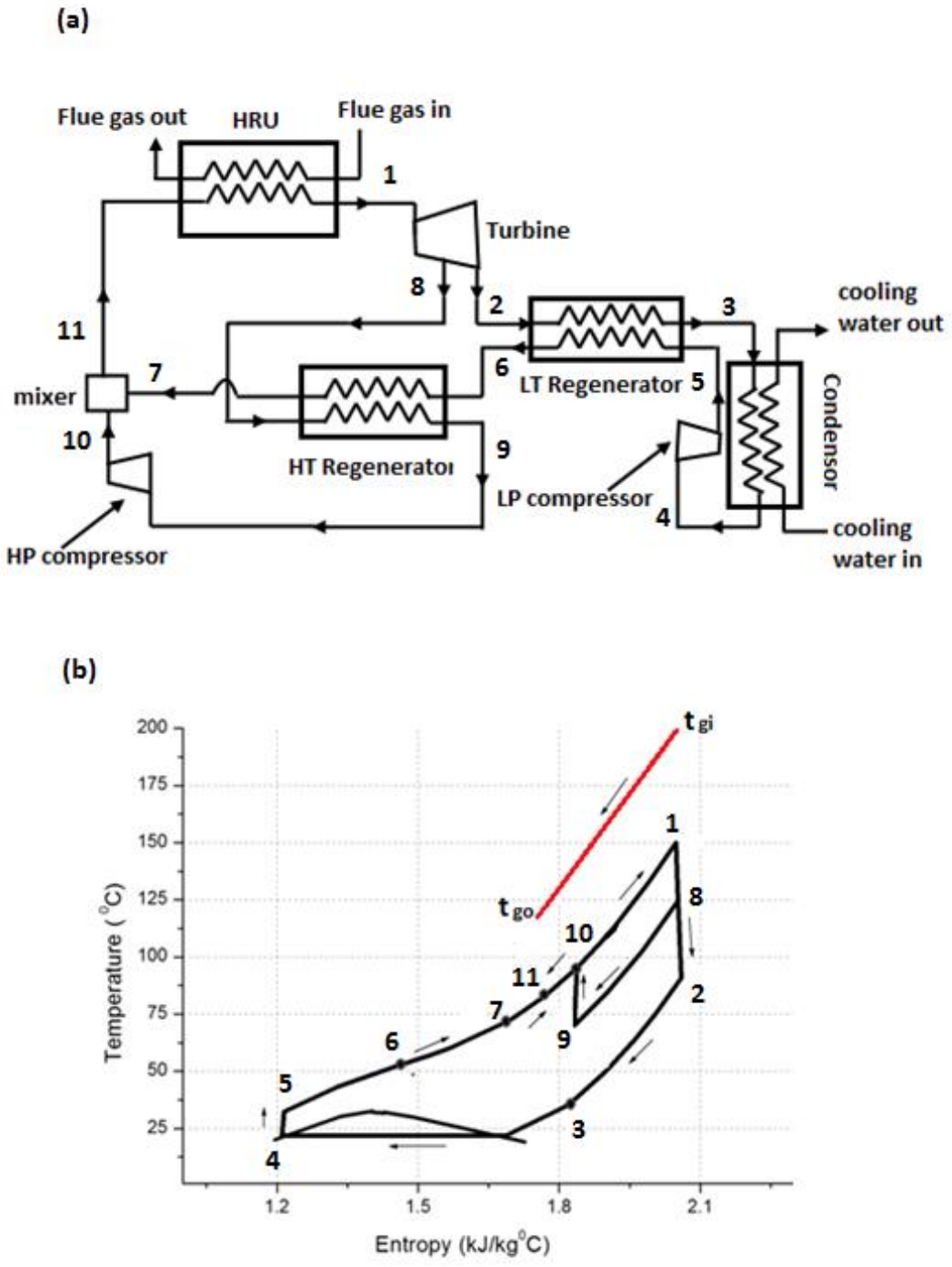

Fig. 2.1 (a): Layout of T-CO_2 Power cycle with two stage regeneration. (b): Temperature-entropy diagram of T-CO_2 Power cycle with two stage regeneration.

2.3 System modelling

A mathematical model has been developed based on 1st law and 2nd law of thermodynamics to study effects of various operating parameters of regenerative heating process on the cycle performance. The performance of the proposed cycle is estimated by both 1st law and 2nd law efficiencies. CO_2 properties are calculated using REFPROP7 (Lemmon et al. 2002). While carrying on system modelling following assumptions are made:

i. There is no extraneous heat loss from the system except heat rejection in pre-cooler and condenser.
ii. Frictional pressure drop is negligible
iii. Specific heat of assumed waste flue gas is constant in its composition. Composition of flue gas is provided in table 2.1.
iv. Finite quantity (25kg s^{-1}) of flue gas is available at 200^{o}C as heat source.
v. Assuming small amount of SO_2 present in the flue gas minimum flue gas exit temperature is 120^{o}C to avoid sulphuric acid condensation.
vi. Turbine efficiency is assumed to be 90%.
vii. Compressor efficiency is considered to be 85%
viii. The effectiveness of LT regenerator is 90%
ix. Minimum terminal temperature difference is greater than 25^{o}C in the HRU
x. Local ambient condition is specified as 15^{o}C and 1bar
xi. Kinetic and potential energy of fluid streams are neglected.
xii. Turbine inlet and exit pressures are 12 MPa and 6 MPa respectively. Turbine inlet temperature is fixed at 150^{o}C

Table 2.1 Flue Gas composition (Milewski et al. 2014)

Composition	% of volume	Specific heat
CO2	12.6%	1.063kJ kg^{-1} K
N2	76.6%	
O2	4.4%	
H2O	6.2	
SO2	0.1%	
NO_x	0.1%	

2.3.1 1st law efficiency (η_I)

From energy balance across the turbine

$$\dot{W}_T = \dot{m}_{CO_2}(h_1 - h_8) + \dot{m}_{CO_2}(1-r)(h_8 - h_2) \quad (2.1)$$

Low pressure and high pressure compressor power input can be represented by the following equations,

$$\dot{W}_{LPC} = \dot{m}_{CO_2}(1-r)(h_5 - h_4) \quad (2.2)$$

$$\dot{W}_{HPC} = \dot{m}_{CO_2} r(h_{10} - h_9) \quad (2.3)$$

By energy balance across the HRU total waste heat input to the cycle is:

$$\dot{Q} = \dot{m}_{CO_2}(h_1 - h_{11}) = \dot{m}_g C_{Pg}\left(T_{gi} - T_{go}\right) \quad (2.4)$$

Hence 1st law efficiency is:

$$\eta_I = \frac{\dot{W}_T - \dot{W}_{LPC} - \dot{W}_{HPC}}{\dot{Q}} \quad (2.5)$$

Following expression for NTU_{HTR} is obtained by considering energy balance across the regenerator

$$NTU_{HTR} = \frac{\dot{m}_{CO_2} r(h_8 - h_9)}{C_{CO_2 min} LMTD_R} \quad (2.6)$$

In the above equation, $C_{CO_2 min}$ is the minimum heat capacity of CO_2 streams entering to the HT regenerator.

If gas is heated from state-i to state-j isobaric specific heat of CO_2 streams are calculated as

$$c_p = \frac{h_j - h_i}{t_j - t_i} \quad (2.7)$$

Energy balance across the HRU yields

$$NTU_{HRU} = \frac{\dot{Q}}{C_{min}\, LMTD_{HRU}} \quad (2.8)$$

In the above equation C_{min} is the smaller value of heat capacity between CO_2 and flue gas.

2.3.2 2nd law efficiency (η_{II})

Neglecting kinetic and potential energy changes, exergy flow with fluid stream at any state 'i' can be represented as

$$E_i = \dot{m}\{(h_i - h_0) - T_o(s_i - s_0)\} \quad (2.9)$$

Now exergy destruction or irreversibility in any component in which fluids are entering at state 'a' and leaving at state 'b' can be calculated as

$$I = E_a - E_b - \dot{W}_{ab} \quad (2.10)$$

Applying equation (2.10) irreversibility for different components can be calculated as

$$I_T = \dot{m}_{CO_2} T_0\{(s_8 - s_1) + (1 - r)(s_2 - s_8)\} \quad (2.11)$$

$$I_{LTR} = \dot{m}_{CO_2} T_0(1 - r)\{(s_3 - s_2) + (s_6 - s_5)\} \quad (2.12)$$

$$I_{CON/PC} = \dot{m}_{CO_2}(1 - r)\{(h_3 - h_4) - T_0(s_3 - s_4)\} \quad (2.13)$$

$$I_{LPC} = \dot{m}_{CO_2}(1 - r)T_0(s_5 - s_4) \quad (2.14)$$

$$I_{HTR} = \dot{m}_{CO_2}(1 - r)T_0(s_7 - s_6) + \dot{m}_{CO_2} T_0 r(s_9 - s_8) \quad (2.15)$$

$$I_{HPC} = \dot{m}_{CO_2} T_0 r(s_{10} - s_9) \quad (2.16)$$

$$I_M = \dot{m}_{CO_2} T_0\{s_{11} - rs_{10} - (1 - r)s_7\} \quad (2.17)$$

$$I_{HRU} = \dot{m}_g C_{pg} T_0 \ln\frac{T_{go}}{T_{gi}} + \dot{m}_{CO_2} T_0(s_1 - s_{11}) \quad (2.18)$$

Exergy entering and leaving with the flue gas are expressed by the equations (2.19) and (2.20) respectively.

$$E_{in} = \dot{m}_g C_{pg}\left(T_{gi} - T_0\right) - \dot{m}_g C_{pg} T_0 \ln\frac{T_{gi}}{T_0} \quad (2.19)$$

$$E_{out} = \dot{m}_g C_{pg}\left(T_{go} - T_0\right) - \dot{m}_g C_{pg} T_0 \ln\frac{T_{go}}{T_0} \quad (2.20)$$

Hence, 2nd law efficiency is (Wang et al. 2010),

$$\eta_{II} = \frac{E_{in} - E_{out} - \sum I}{E_{in}} \quad (2.21)$$

2.4 Results and discussion

Results are obtained from this developed model. The study is concentrated on the effects of bleeding CO_2 gas for regenerative heating on the performance of the power cycle. Parameters of bleeding that affect the performance of the cycle are considered. Effects of variation of these parameters on both the 1st and 2nd law efficiencies are reported.

2.4.1 1st law Efficiency(η_I):

Bleed ratio (r), exit temperature of bleed stream from the regenerator (t_9) and bleed pressure (P_i) are the parameters to influence the cycle performance when turbine inlet and outlet conditions are specified.

Figure 2.2 shows variation of power for varying bleed ratio- Fig. 2.2 (a) for power inputs and Fig. 2.2 (b) for corresponding outputs. As shown in the Fig. 2.2(a) for a increase in bleedratio (r) power input to HP compressor ($\dot{W}_{HPC}$) increases due to higher mass flow rate of CO_2 gas. However, corresponding LP compressor work ($\dot{W}_{LPC}$) does not vary significantly. It should be noted that though total mass flow rate increasses with increase in bleed ratio, flow rate through the LP compressor does not vary significantly as higher fraction of mass enters to the HT regnerator. For lower bleed gas exit temperature (t_9) HP compresssor power input ($\dot{W}_{HPC}$) decreases, though more significant for higher bleed ratio. Similar effect on LP compressor power input (($\dot{W}_{LPC}$) is insignificant as shown in Fig. 2.2(a).

Figure 2.2(b) shows the effects of bleed ratio (r) on power outputs. With increasing bleed ratio, turbine power output ($\dot{W}_T$) increases as total mass flow rate of CO_2 increases. However the effect of t_9 is insignificant on this power output. The net output also increases for higher bleed ratio as shown in Fig. 2.2 (b). The increase of power output in turbine dominates over the corresponding increase of power inputs in LP and HP compressors. The net power output is also influenced by t_9, though this effect is not significant as shown in Fig. 2.2(b). Also for specified bleed ratio, variation in exit temperature (t_9) of bleed gas coming out of the HT regenerator does not significantly affect LP compressor power input and corresponding turbine power output because total energy added to the main stream of CO_2

entering to HRU remains almost constant with variation of t_9 within specified range due to the presence of the mixer.

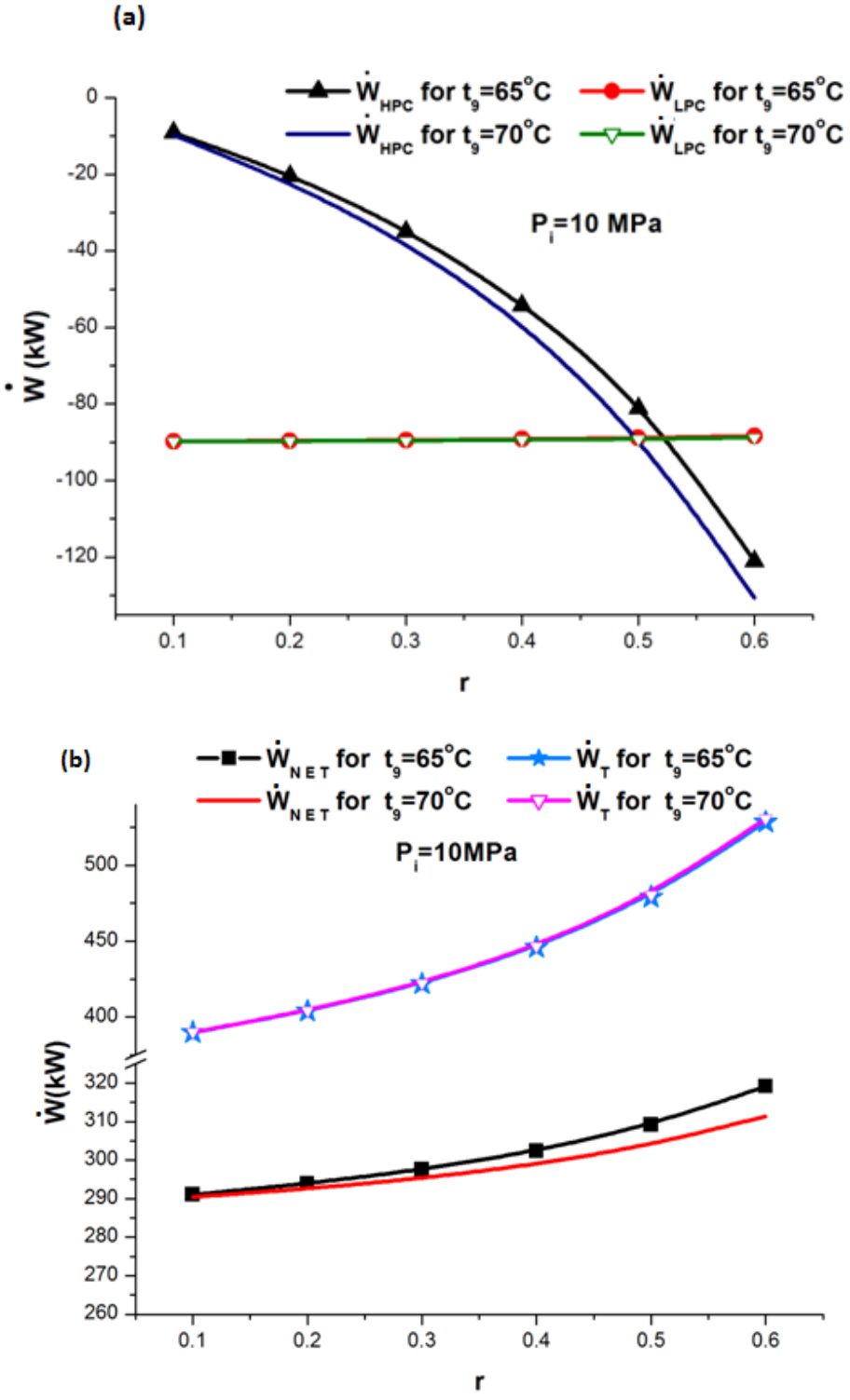

Fig. 2.2 (a): Power input vs. bleed ratio. (b): Power output vs. bleed ratio.

Figure 2.3 shows the variation of 1st law efficiency (η_I) with varying bleed ratio. It is noted from the Fig. 2.3 that the 1st law efficiency increases with an increase in bleed ratio (r) as available waste heat is utilized to heat the larger mass of CO_2 without altering the turbine inlet condition. It is also clear from Fig. 2.3 that above a certain value of the bleed ratio, 1st law efficiency increases significantly with reduction in bleed gas temperature at the HT regenerator exit. The horizontal line in Fig. 2.3 is representing the 1st law efficiency for a baseline cycle without turbine bleeding ($\eta_{I,WOTB}$).

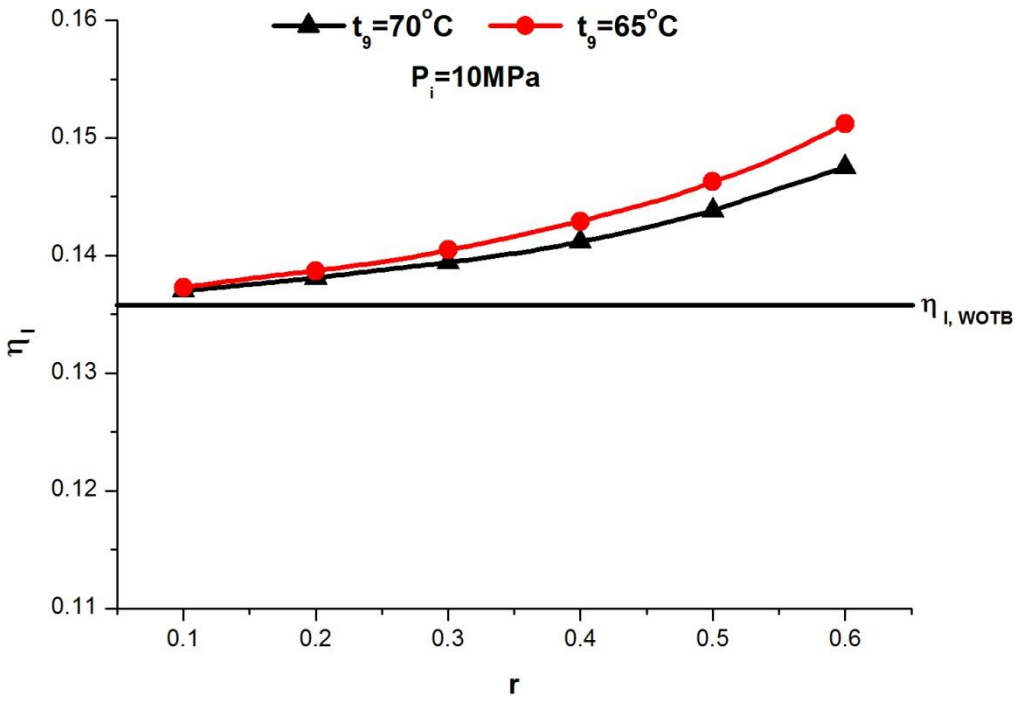

Fig. 2.3: 1st law efficiency vs. bleed ratio

Figure 2.4 shows the effect of varying bleed ratio on NTU of the HT regenerator. It should be noted that improving 1st law efficiency with higher bleed ratio for a specified bleed gas temperature (t_9) at the HT regenerator exit, is restricted by the size of the HT regenerator as shown in the Fig. 2.4. It is observed that NTU of the HT regenerator initially increases at a lower rate as rate of temperature rise of the main CO_2 stream is very small. The higher specific heat of the inlet main stream and lower mass flow rate of bleed stream are mainly responsible for this phenomenon. In other words, effective temperature difference between hot and cold streams remains sufficiently large with lower value of r. However, this effective

temperature difference starts to decrease rapidly as r is allowed to increase beyond a certain value –at this level due to higher heat transfer from the bleed stream and reduction of specific heat of main stream temperature profiles come closer to one another.

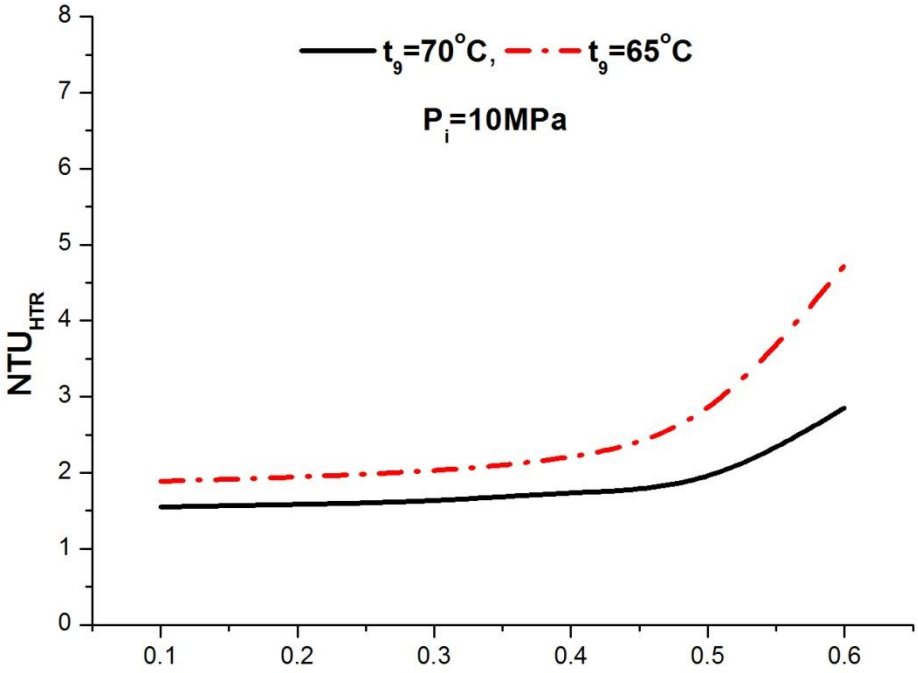

Fig. 2.4: NTU of high temperature (HT) regenerator vs. bleed ratio

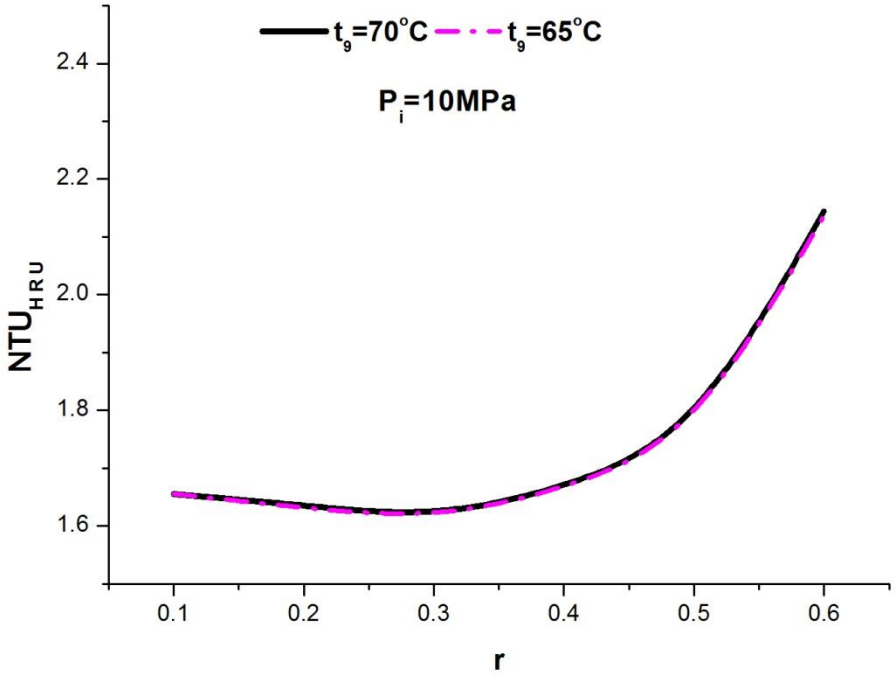

Fig. 2.5: NTU of the Heat recovery unit (HRU) vs. bleed ratio

The effect of varying bleed ratio on Number of Transfer Unit of the HRU (NTU_{HRU}) is shown in Fig. 2.5. Increment in bleed ratio initially helps to reduce the overall size of the HRU but ultimately it requires a larger heat transfer area for the HRU. It should be noted that the initial reduction in NTU of the HRU is due to the large specific heat of CO_2 near the critical point. With a specified value of r, variation in t_9 with in specified range will have little effect on the HRU sizing as it has no significant effect on flow rate or inlet condition of CO_2 to t he HRU.

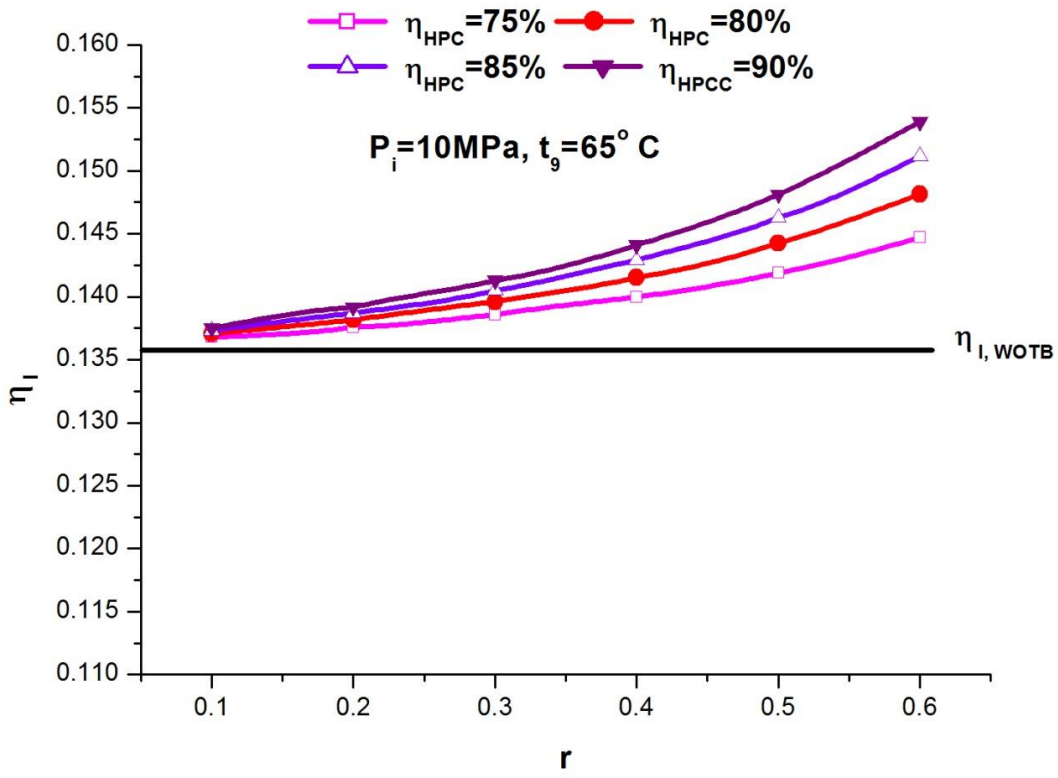

Fig. 2.6: 1st law efficiency vs. bleed ratio for various High pressure (HP) compressor efficiencies

As the HP compressor is not an essential part of a basic regenerative T-CO_2 power cycle, the effects of varying efficiency of this component on 1st and 2nd law efficiencies should be discussed. Figure 2.6 shows effect of variation in bleed ratio (r) on 1st law efficiencies for different HP compressor efficiencies (η_{HPC}). Results show that for specified bleed ratio with increase in HP compressor efficiency, 1st law efficiency increases due to lesser power requirement of the compressor. However, this effect is more significant for higher values of bleed ratios.

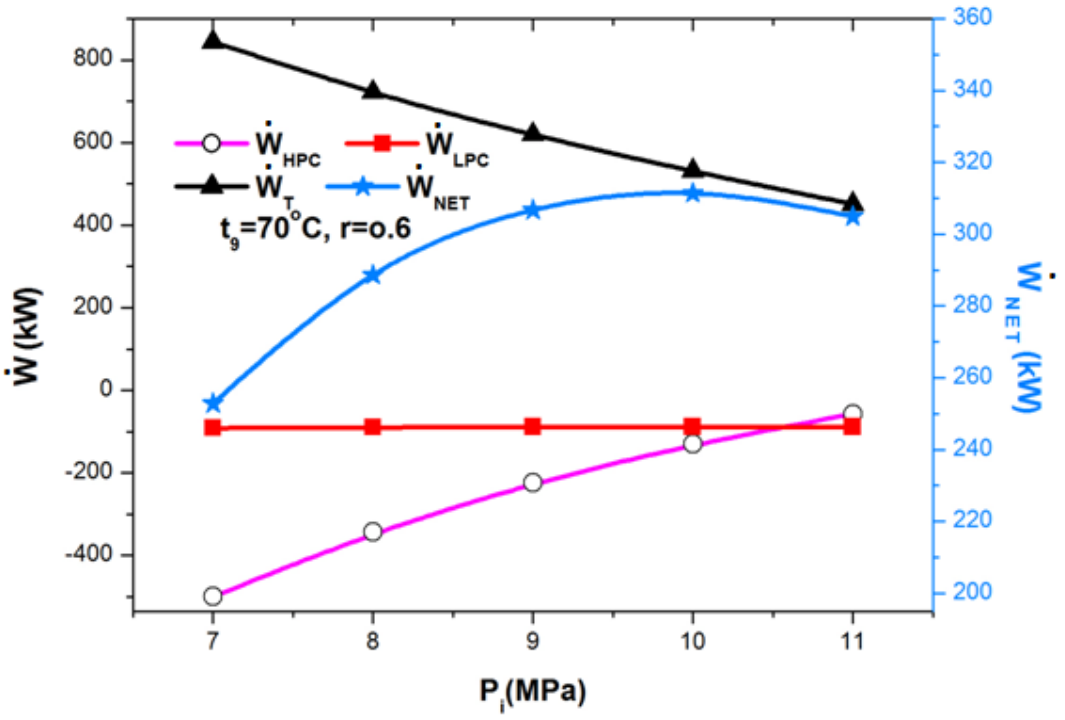

Fig. 2.7: Power vs. bleed pressure

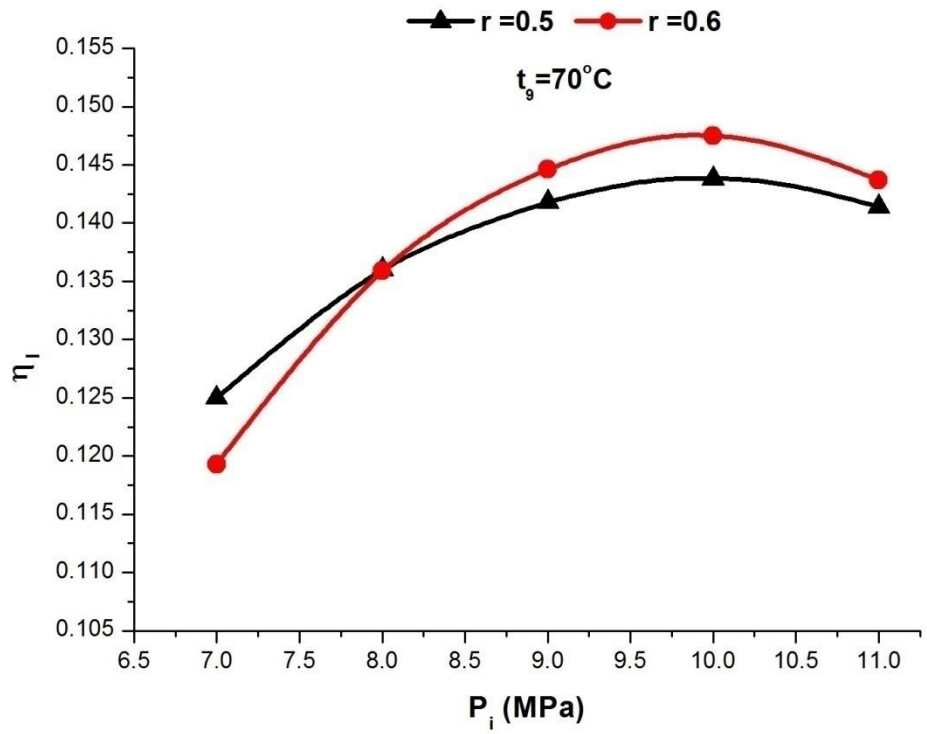

Fig. 2.8: 1st law efficiency vs. bleed pressure

Another parameter that significantly influences net power output and overall efficiency of the cycle is the intermediate pressure at which CO_2 is extracted for regenerative heating. This pressure is termed as bleed pressure (P_i) in this study. The effect of bleed pressure on cycle power and 1st law efficiencies are shown in Fig. 2.7 and 2.8 respectively. It is observed that at lower bleed pressure, turbine power output is significantly large. However, this is not that useful as the majority of this power is utilized to run the HP compressor. With increase in bleed pressure, turbine output as well as HP compressor input decreases. Initial increase in bleed pressure is beneficial as turbine output decreases at a lesser rate than the input to the HP compressor. However, for specified r above certain bleed pressure, just reverse phenomenon is observed. Thus, for given r value as well as turbine inlet and outlet conditions, it is possible to obtain an optimum bleed pressure corresponding to which net power output and 1st law efficiency are maximum as shown in the Fig. 2.7 and 2.8 respectively.

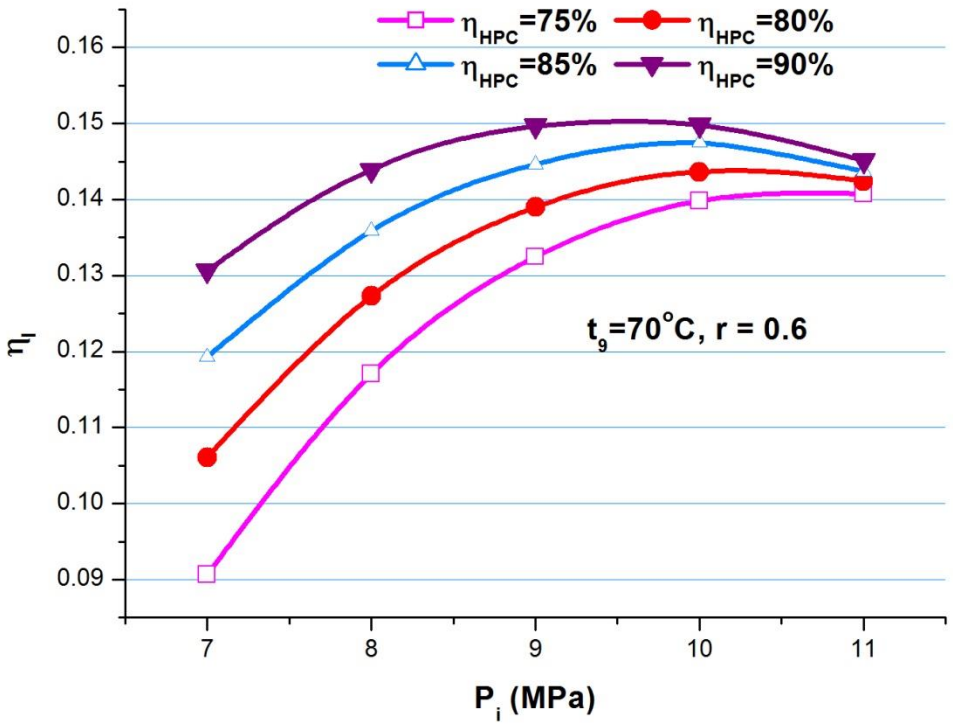

Fig. 2.9: 1st law efficiency vs. bleed pressure for various HP compressor efficiencies

Figure 2.9 shows variation in 1st law efficiency with varying bleed pressure at different HP compressor efficiencies. It is observed that 1st law efficiency decreases with reduction in HP compressor efficiency. However, variation in HP compressor efficiency is having larger impact on 1st law efficiency for lower values of bleed pressures (P_i). It is also found in the Fig. 2.9 that optimum bleed pressure corresponding to maximum cycle efficiency decreases with higher HP compressor efficiency.

2.4.2 2nd law efficiency (η_{II})

The proposed cycle includes extra devices than that without regeneration using turbine bleed gas like HP compressor, HT regenerator and mixer. Each device has its associated irreversibility. However, this hardly matters as irreversibility associated with the heat recovery unit (HRU) substantially reduces with the incorporation of turbine bleeding to the baseline cycle. Irreversibility of different components with varying r is presented in Fig. 2.10.

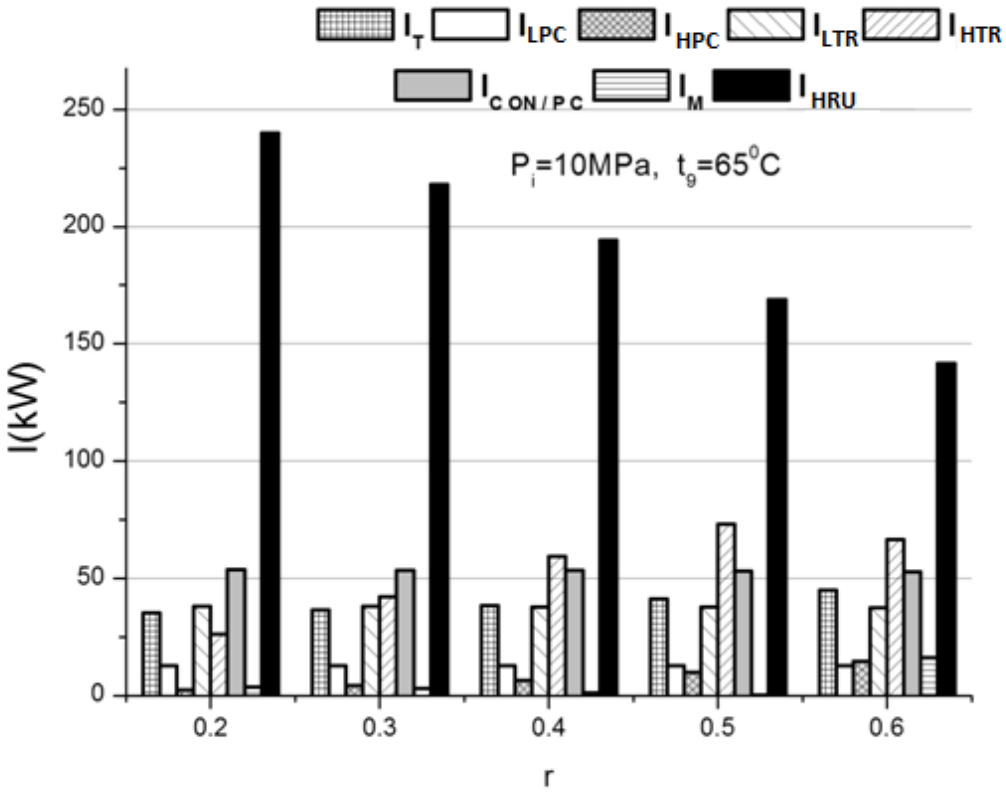

Fig. 2.10: Component Irreversibility vs. bleed ratio

It is observed from Fig. 2.10 that HRU and HT regenerator are two major contributors to the total irreversibility. Irreversibility of HRU decreases rapidly with higher value of r due to higher inlet temperature of CO_2 entering to the device. Irreversibility associated with the HT regenerator shows an increasing trend with r. However, at certain r value, it reaches the peak and then with further increment of r a decreasing trend is observed. Irreversibility of HT regenerator initially increase as temperature rise per unit heat input is significantly small for main CO_2 stream. However, above a particular r value this is not significant as mean specific heat of CO_2 decrease due to comparatively higher mean temperature of colder stream. As irreversibility of HRU decreases rapidly with r, some improvement in second law efficiency will be achieved as shown in the Fig. 2.11. Some improvement in 2nd law efficiency is observed with reduction in t_9 as this helps to reduce irreversibility associated with the HP compressor and HT regenerator. The horizontal line is showing the 2nd law efficiency for base line cycle without regenerative heating using bleed gas.

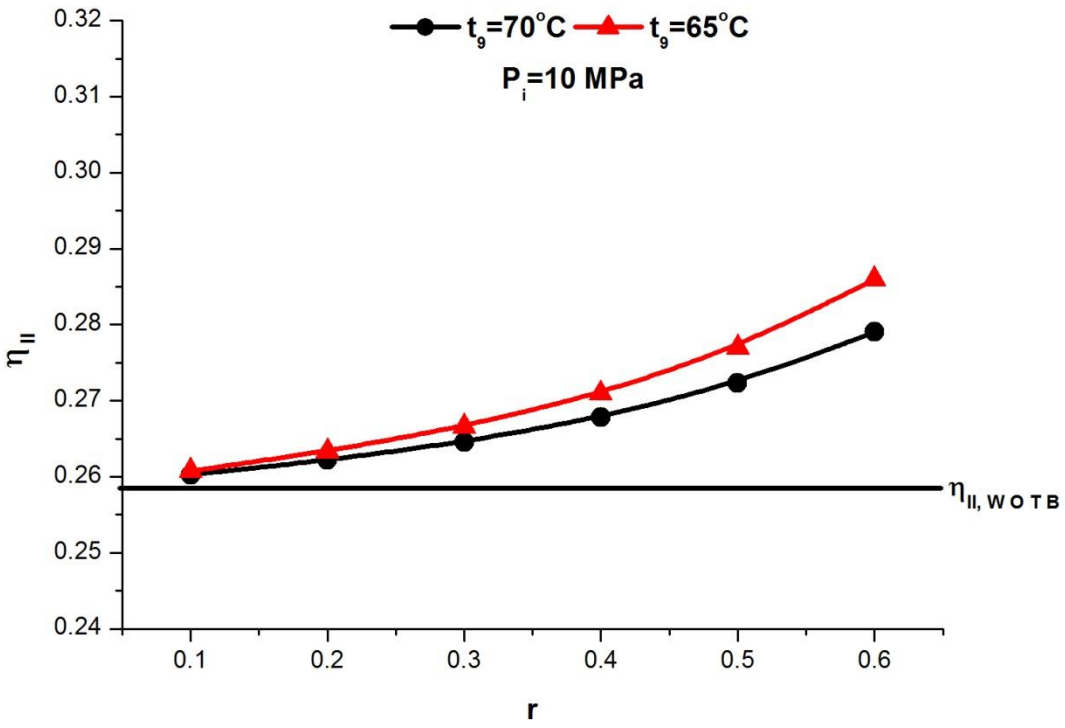

Fig. 2.11: 2nd law efficiency vs. bleed ratio

By plotting 2nd law efficiency vs. bleed ratio for various compressor efficiencies in Fig. 2.12, it is observed that higher efficiency of the HP compressor helps to improve 2nd law efficiency as it reduces irreversibility associated with the compressor.

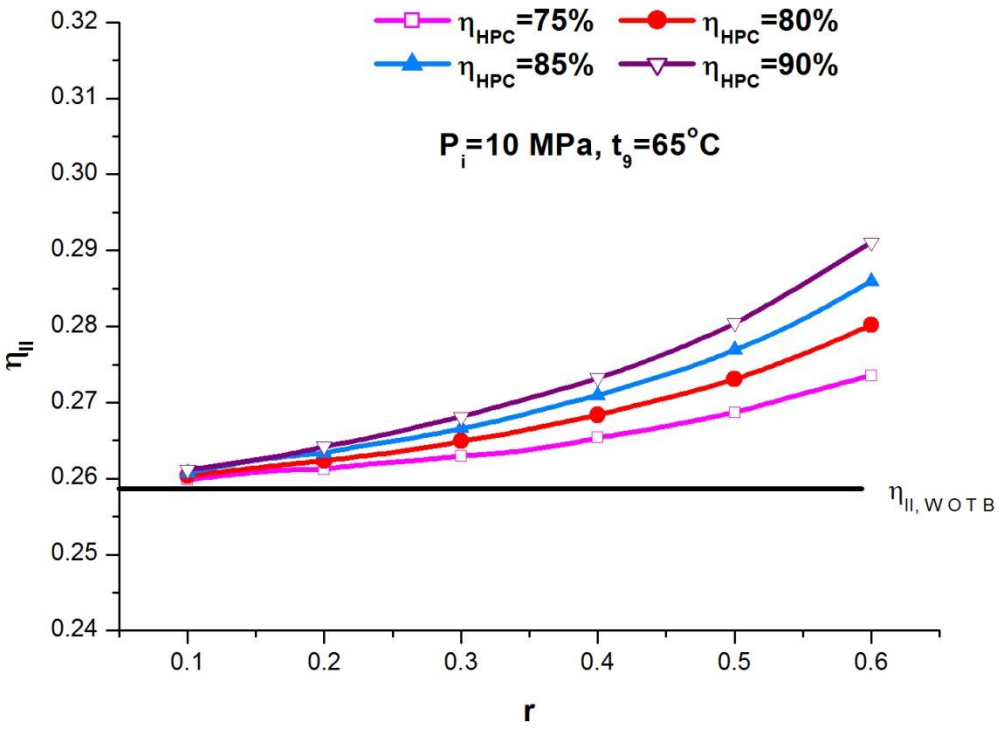

Fig. 2.12: 2nd law efficiency vs. bleed ratio for various HP compressor efficiencies

Effects of varying bleed pressure on component irreversibilities are presented in Fig. 2.13. Figure 2.13 shows that irreversibility associated with HRU does not vary much with bleed pressure as temperature of the CO_2 stream entering to HRU remains almost constant if bleed gas temperature at HT regenerator exit is specified. This is due to the fact that there is little variation in total overall energy input (Heat + HP compressor work) to the main stream with variation in bleed pressure. It is also evident from the Fig. 2.14 that there is an optimum bleed pressure for minimum total system irreversibility when bleed ratio (r), bleed gas exit temperature at HT regenerator exit (t_9), turbine inlet and exit conditions are specified. It is also observed that the nature of total irreversibility variation with bleed pressure (P_i) is mainly controlled by decreasing and increasing trends of turbine irreversibility and HT regenerator irreversibility respectively. Bleed pressure corresponding to minimum total cycle irreversibility also yields a peak value of 2nd law efficiency as shown in the Fig. 2.15.

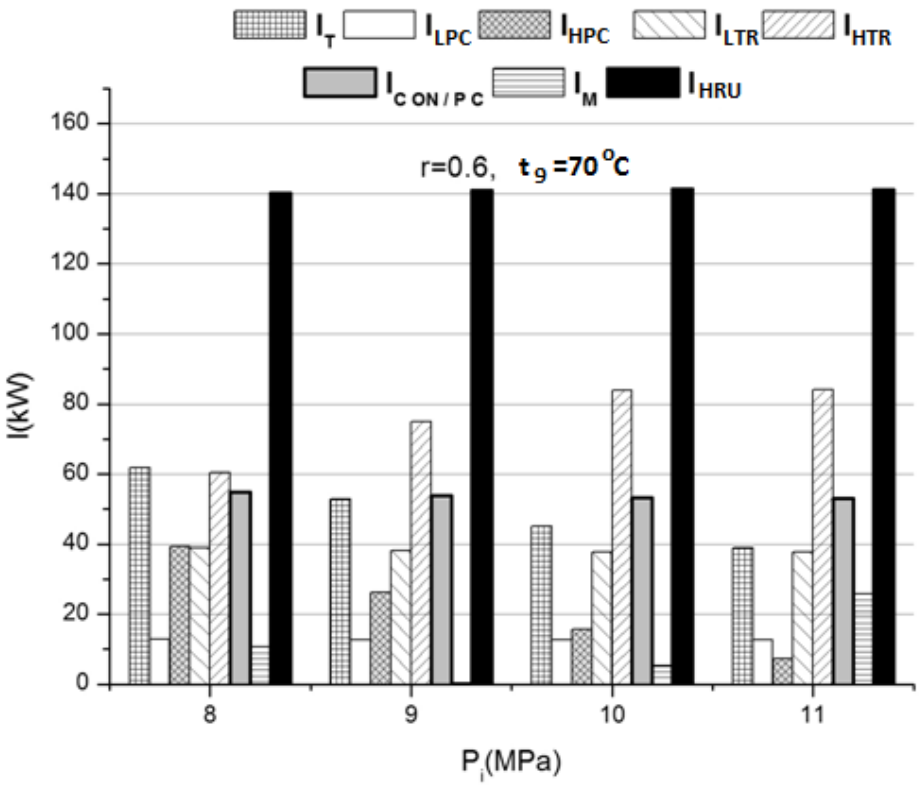

Fig. 2.13: Component Irreversibility vs. bleed pressure

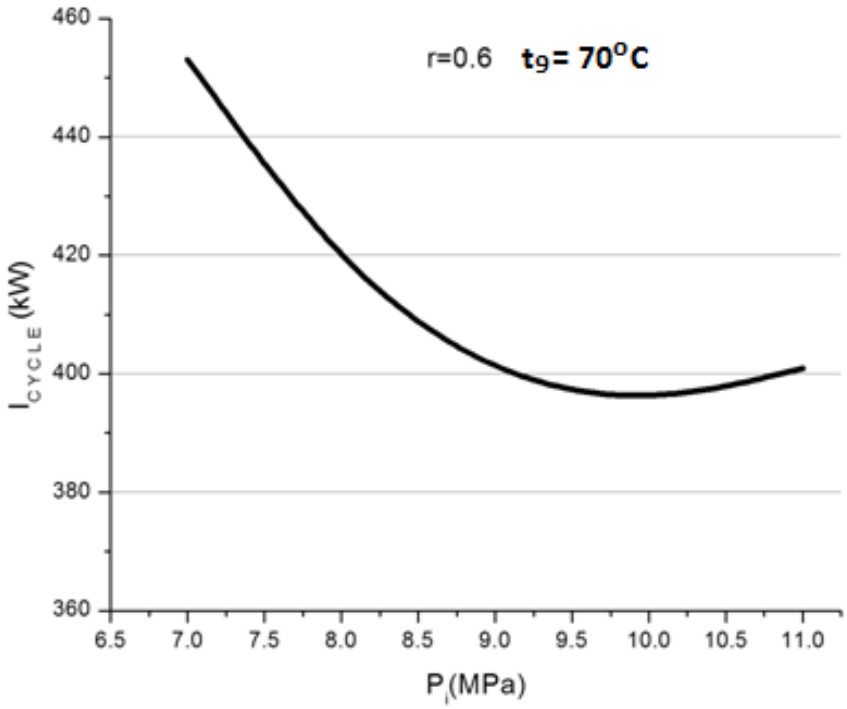

Fig. 2.14: Total cycle irreversibility vs. bleed pressure

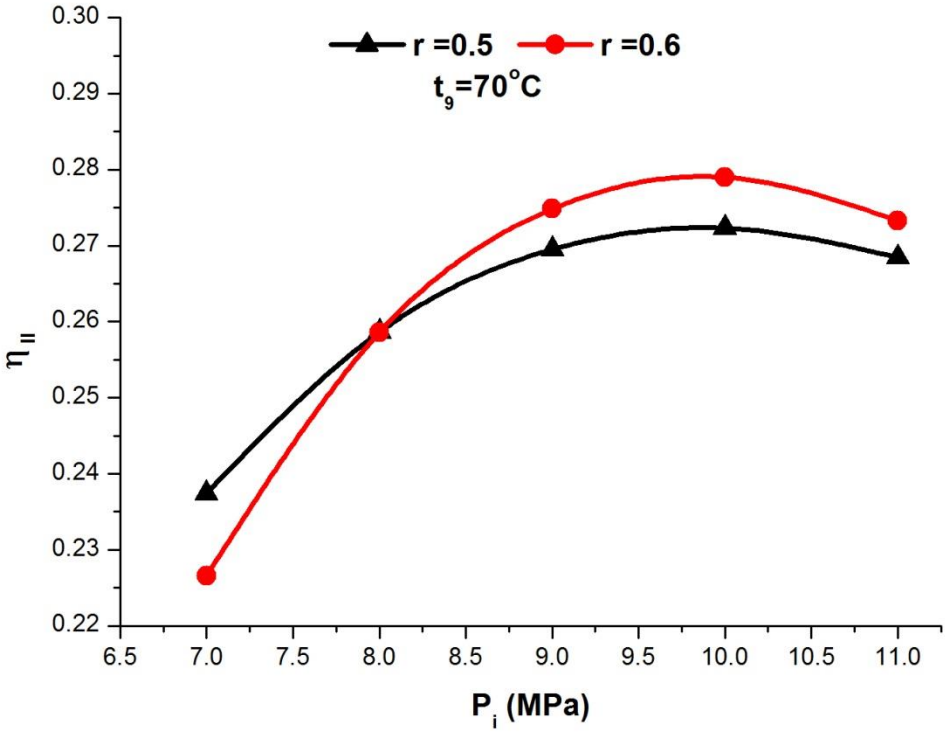

Fig. 2.15: 2nd law efficiency vs. bleed Pressure

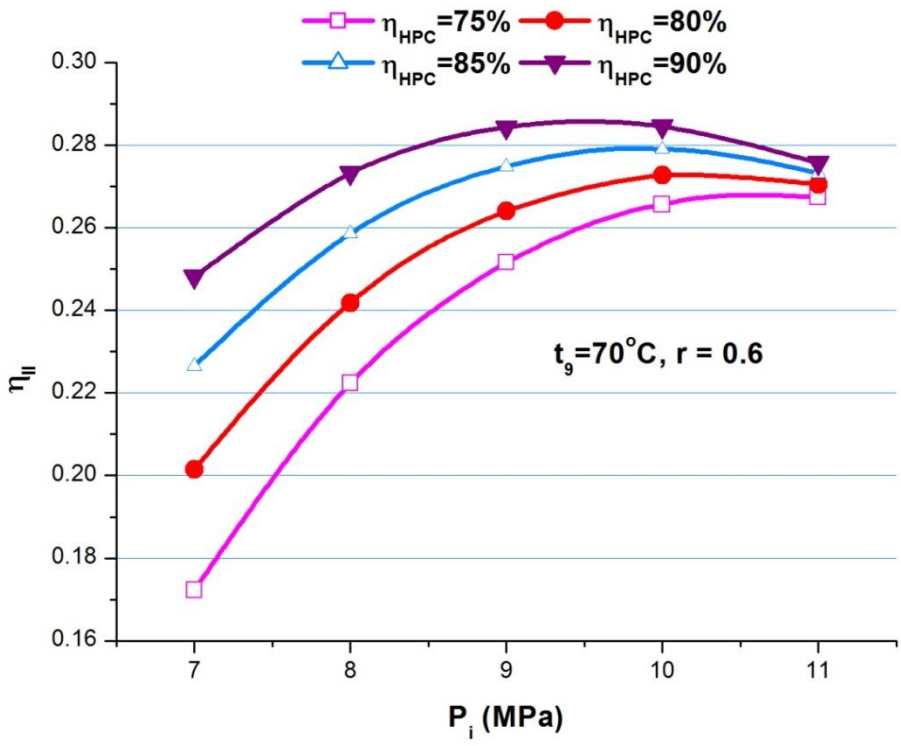

Fig. 2.16: 2nd law efficiency vs. bleed pressure for various compressor efficiencies

It is evident from Fig. 2.16 that higher HP compressor efficiency will help to improve 2nd law efficiency more significantly at lower bleed pressure. It is also observed that for specified bleed ratio as well as turbine inlet and exit conditions, it is possible to maximize 2nd law efficiency at comparatively lower bleed pressure for higher compressor efficiency.

2.5. Chapter Summary

In the present analysis, effects of regenerative heating using turbine bleed gas on a transcritical CO_2 power cycle have been explored. It is observed that there are three key parameters associated with regenerative heating that will influence cycle performance for specified rating of components (compressors, turbine and regenerators) and turbine inlet-outlet conditions.

The key findings of the analysis are summarised as follows:

- 1st law efficiency of the cycle shows an increasing trend as more and more CO_2 is extracted at any intermediate stage of turbine expansion. However, maximum limit of CO_2 extraction will be fixed by the overall size (NTU) of the high temperature (HT) regenerator.
- 1st law efficiency is improved to some extent compared to that of the base line cycle i.e. the cycle without turbine bleeding and single stage regeneration.
- With a specified value of other operating parameters, there is an optimum value of bleed pressure corresponding to which net power output as well as cycle 1st law efficiency achieves the maximum value.
- With turbine bleeding it is possible to achieve higher second law efficiency compared to that of baseline cycle without regeneration using bleed gas.
- An optimum bleed pressure exists corresponding to maximum second law efficiency.
- High pressure compressor efficiency affects cycle performance more significantly either for higher bleed ratio or for lower bleed pressure.

3. CO_2 power cycle with multi-stage compression and intercooling

3.1 Objective of the work

It is observed in the previous chapter that a regenerative transcritical CO_2 power cycle is capable of producing reasonably good power using low grade heat of flue gas. However, a transcritical CO_2 power cycle can be executed only if a low temperature heat sink is available. Efficiency of a low grade heat driven supercritical CO_2 power cycle is appreciably low as large power is consumed by the compressor. These disadvantages can be overcome by considering a CO_2 power cycle with multi-stage compression an intercooling. To get reasonably good power output (even with higher heat rejection temperature) SO_2 free flue gas at 180^{o}C is considered as the heat source. In the present study, assuming the minimum cycle temperature as 35^{o}C, a CO_2 power cycle with multi-stage compression and intercooling is evaluated. Proposed cycle is a CO_2 Brayton cycle for which turbine exit pressure varies on either side (above and below) of the critical pressure. Initially the study was done for two stages and then results are obtained for multi-stage compression also by introducing similar analysis.

3.2 System description and modelling:

The layout of the baseline CO_2 power cycle and corresponding Temperature-entropy diagrams are shown in Fig. 3.1 (a) and (b) respectively. This is a waste heat recovery CO_2 power cycle with single stage compression. The relative performance of two-stage and multi-stage compression CO_2 power cycles with respect to this baseline cycle has been reported in this chapter.

The layout of a CO_2 power cycle with two-stage compression and intercooling is shown in the Fig. 3.2 (a). Figure 3.2 (b) shows corresponding Temperature-entropy diagram. Supercritical CO_2 after expansion in the turbine undergoes a partial cooling process in the regenerator before it enters the low pressure (LP) cooler (state-3). In the LP cooler CO_2 is cooled to 35^{o}C (state-4) and then compressed from lowest cycle pressure P_L to intermediate pressure P_i (State-5). The CO_2 undergoes an isobaric cooling process (5-6) before it enters into the HP compressor at 35^{o}C. In the HP compressor, CO_2 is compressed from P_i to the highest cycle pressure P_H (state-7). Before entering the heat recovery unit (HRU), CO_2 is heated from state-7

to sate-8 by utilizing the heat of turbine exhaust gases. By utilizing industrial low temperature waste heat CO_2 is then heated up to turbine inlet temperature i.e. 150^oC.

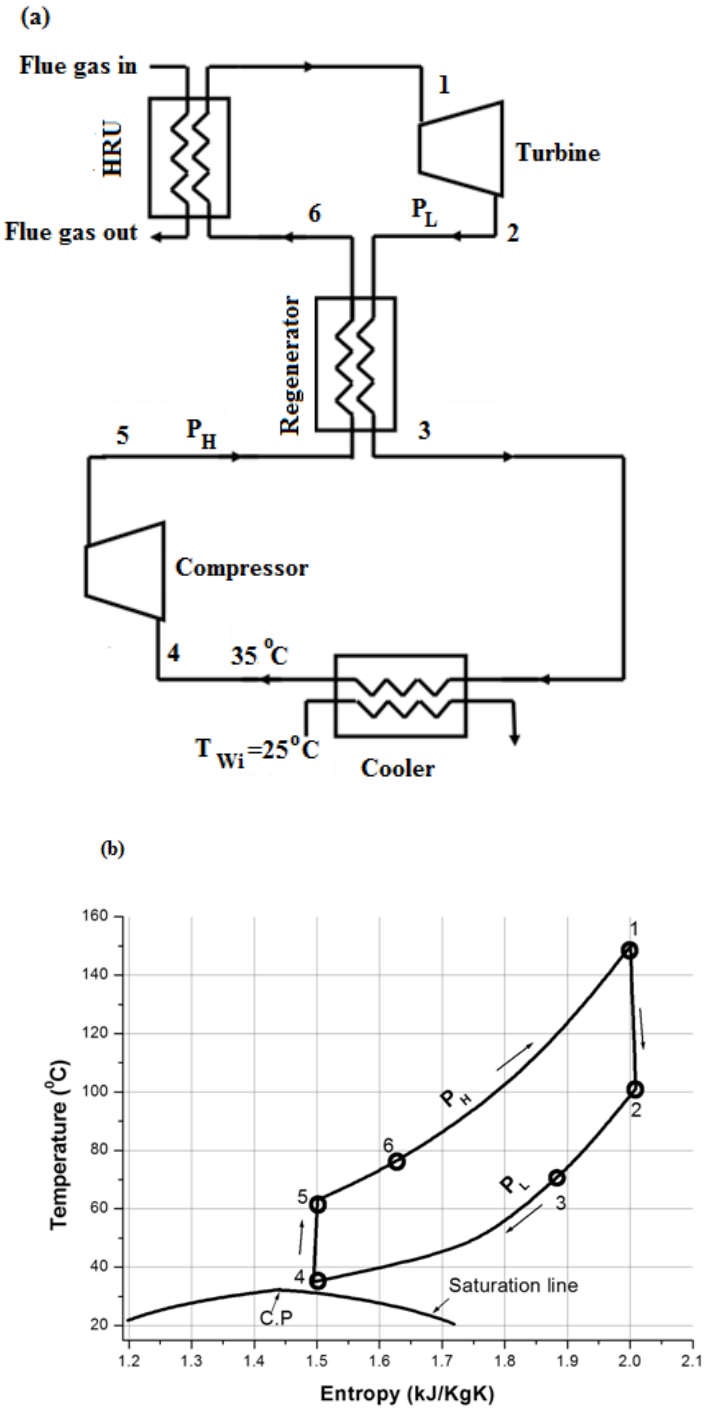

Fig. 3.1(a): Layout of the baseline CO_2 power cycle (b): Temperature-Entropy diagram of the baseline CO_2 power cycle

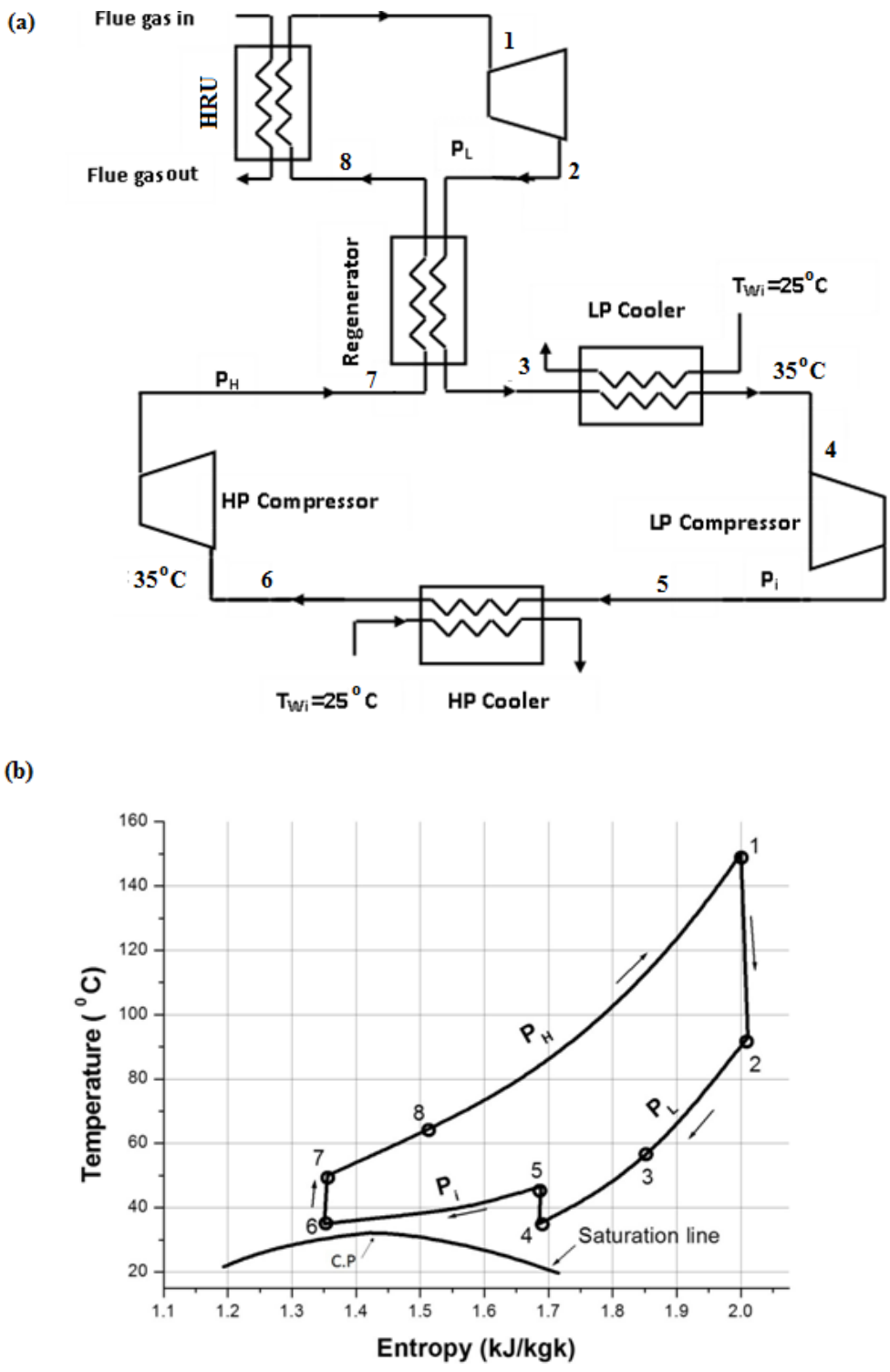

Fig. 3.2(a): Layout of the CO_2 power cycle with two-stage compression and intercooling. (b): Temperature-Entropy diagram of the CO_2 power cycle with two-stage compression and intercooling.

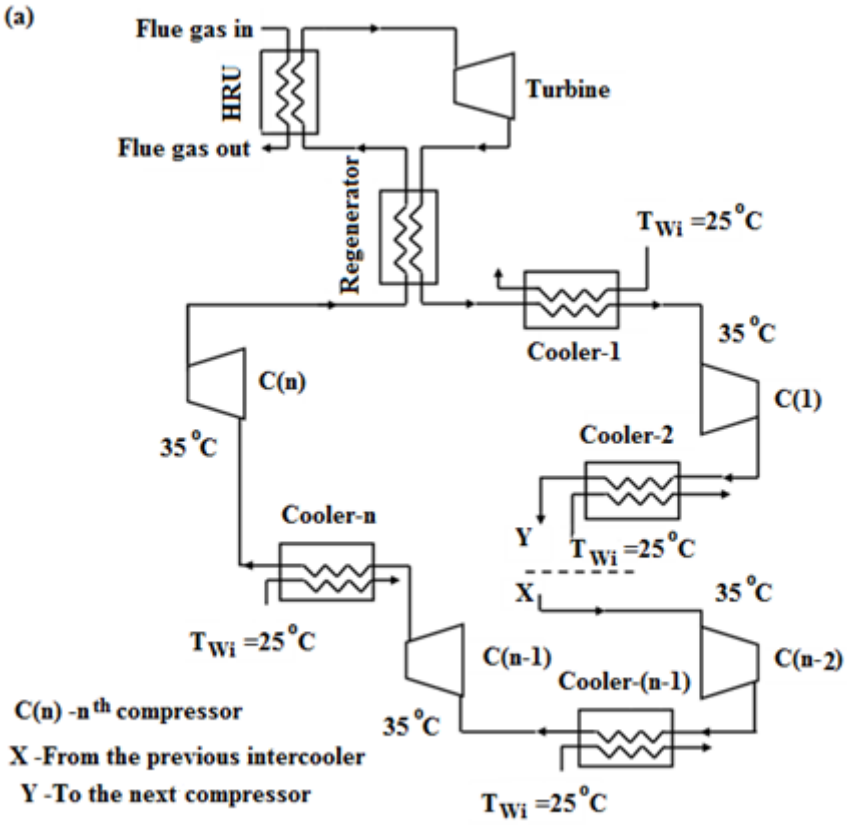

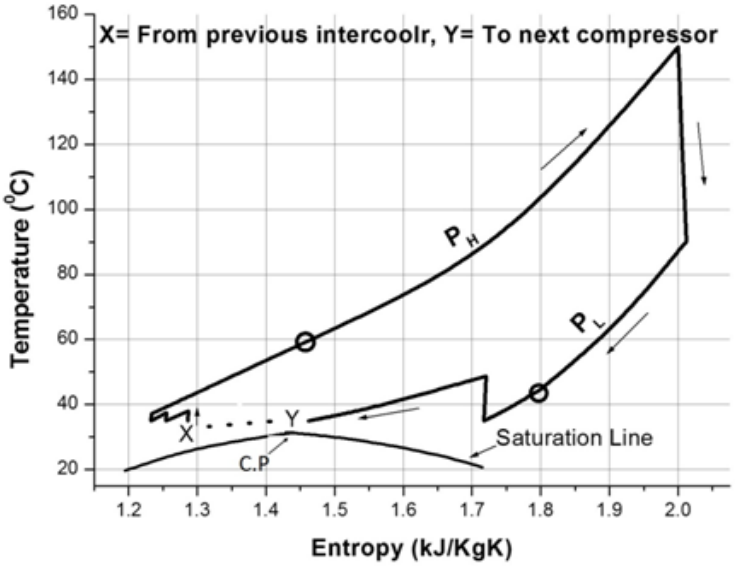

Fig. 3.3(a): Layout of the CO_2 power cycle with multi-stage compression and intercooling. (b): Temperature-Entropy diagram of the CO_2 power cycle with multi-stage compression and intercooling.

It should be noted that instead of two-stage compression and intercooling, multi-stage compression and intercooling can also be adopted. Figure 3.3(a) and (b) show the layout and corresponding Temperature-entropy diagrams respectively. For multi-stage compression arbitrary number of stages of compression is assumed. It has been shown by broken line. X is representing the stream of CO_2 coming out from previous stage of intercooler at 35^{o}C and Y is representing the stream of CO_2 entering to next compression stage. Equal pressure rise is assumed during each stage of compression.

Using energy balance, a thermodynamic model has been developed to demonstrate effects of various operating parameters on the performance of the CO_2 power cycle for two-stage and subsequently for multi-stage compression cycles with intercooling. REFPROP-7 (Lemmon et al. 2002) is utilized for evaluation of thermodynamic properties of CO_2 at various state points. While carrying on system modelling following assumptions are made:

i. Fluid pressure loss due to friction is negligible.

ii. Turbine and compressor efficiencies are assumed to be 90% and 85% respectably.

iii. Minimum terminal temperature difference in regenerator is 8°C.

iv. Ambient condition is specified as 1 bar and 25°C.

v. Depending on ambient condition the minimum cycle temperature is 35°C.

vi. Turbine inlet temperature is 150°C assuming low grade waste heat is available at 180°C.

vii. Pinch point temperature difference in the Heat recovery unit (HRU) is 15°C

viii. There is no extraneous heat loss except heat rejection in coolers.

ix. Flue gas is free from SO_2 and temperature of the flue gas at exit of the HRU is not restricted by the acid dew point temperature.

Values of operating parameters describing operating conditions of the cycle are summarised in table 3.1.

Table 3.1: Standard operating parameters

Parameter	value
Turbine inlet temperature of CO_2 (T_H)	150°C
Lowest cycle temperature (T_L)	35°C
Flue gas inlet temperature to HRGH (T_{gi})	180°C
Specific heat of flue gas (C_{Pg})	1.063 kJ kg^{-1} k
Pinch point temperature difference in HRGH ($\Delta T_{Pinch,HRGH}$)	15°C
Pinch point temperature difference in regenerator ($\Delta T_{Pinch,R}$)	8°C
Isentropic efficiency of turbine(η_T)	0.9
Isentropic efficiency of compressor (η_C)	0.85
Ambient temperature (T_0)	25°C

3.2.1 Energy analysis

Energy balance for various components of a CO_2 Brayton cycle with two stage compression and intercooling (Refer to Fig. 3.2 (b)) can be expressed by following equations, component wise.

- For the heat recovery unit (HRU):

The heat balance equation of the HRU is represented as:

$$q_{HRU} = (h_1 - h_8) = \dot{m}_g C_{Pg}(T_{gi} - T_{go}) \quad (3.1)$$

The mass flow rate of the flue gas in kg kg^{-1} of CO_2 can be expressed as

$$\dot{m}_g = \frac{h_1 - h_8}{c_{Pg}\,(T_{gi} - T_{go})} \quad (3.2)$$

Where, c_{Pg} is specific heat of the flue gas. It may be noted that the flue gas exit temperature from HRU can be expressed as

$$t_{go} = t_8 + \Delta t_{Pinch,HRU} \quad (3.3)$$

- For turbine:

Isentropic efficiency of the turbine may be expressed as

$$\eta_T = \frac{h_1 - h_2}{h_1 - h_{2s}} \quad (3.4)$$

In the above equation h_{2s} is the enthalpy of CO_2 at turbine exit condition if expansion is isentropic.

Specific work output for the turbine of CO_2 power cycle with 2-stage compression and intercooling is:

$$w_T = h_1 - h_2 \quad (3.5)$$

- For regenerator:

In regenerator, hot fluid (i.e. CO_2) exiting the turbine (state-2) has a smaller value of mean heat capacity compared to the colder stream coming out from the high pressure compressor (i.e., state-7). Hence, the HRU inlet enthalpy of CO_2 is

$$h_8 = h_7 + (h_2 - h_3) \quad (3.6)$$

Also the temperature corresponding to the state point-3 is

$$t_3 = t_7 + \Delta t_{Pinch,R} \quad (3.7)$$

- For cooler & intercoolers:

Heat duties of high pressure (HP) and low pressure (LP) coolers (i.e., intercoolers) are expressed as

$$q_{LPCO} = h_3 - h_4 \quad (3.8)$$

$$q_{HPCO} = h_5 - h_6 \quad (3.9)$$

- For compressors:

Isentropic efficiencies of low pressure and high pressure compressor are expressed by equations (3.10) and (3.11) respectively.

$$\eta_{LPC} = \frac{h_{5s} - h_4}{h_5 - h_4} \quad (3.10)$$

$$\eta_{HPC} = \frac{h_{7s} - h_6}{h_7 - h_6} \quad (3.11)$$

Where, h_{5S} and h_{7S} are enthalpy at compressor outlet for isentropic compression.

Equations (3.12) and (3.13) are representing compressors' specific work input:

$$w_{LPC} = (h_5 - h_4) \tag{3.12}$$

$$w_{HPC} = (h_7 - h_6) \tag{3.13}$$

Hence, for a 2-stage compression and intercooling, the specific work output of the cycle is

$$w_{SPECIFIC} = w_T - w_{HPC} - w_{LPC} \tag{3.14}$$

Specific work output for CO_2 power cycle with multi stage compression and intercooling

$$w_{SPECIFIC} = w_T - \sum_{i=1}^{n} w_{Ci} \tag{3.15}$$

Hence 1st law efficiency for the CO_2 power cycle for two or multi stage compression with intercooling as well as for the baseline cycle is:

$$\eta_I = \frac{w_{SPECIFIC}}{q_{HRU}} \tag{3.16}$$

3.2.2 Exergy analysis:

Exergy destructions (or irreversibilities) of components of the cycle for two-stage compression and intercooling are estimated by following equations:

- For heat recovery unit:

Irreversibility in the HRU is expressed as follows:

$$I_{HRU} = T_0(s_1 - s_8) + \dot{m}_g C_{Pg} T_0 \ln\frac{T_{go}}{T_{gi}} \tag{3.17}$$

- For the turbine:

$$I_T = T_0(s_2 - s_1) \tag{3.18}$$

- For regenerator:

$$I_R = T_0(s_3 - s_2) + T_0(s_8 - s_7) \quad (3.19)$$

- For intercoolers:

In intercoolers CO_2 is cooled by water available at ambient temperature. Hot water coming out from intercoolers attains the ambient temperature again by dissipating heat to local environment. Thus, as the change in entropy of cooling water is zero, irreversibilities associated with intercoolers are expressed as:

$$I_{LPCO} = (h_3 - h_4) - T_0(s_3 - s_4) \quad (3.20)$$

$$I_{HPCO} = (h_5 - h_6) - T_0(s_5 - s_6) \quad (3.21)$$

- For compressors:

$$I_{LPC} = T_0(s_5 - s_4) \quad (3.22)$$

$$I_{HPC} = T_0(s_7 - s_6) \quad (3.23)$$

Total cycle irreversibility for the cycle with 2-stage compression and intercooling is calculated by adding component irreversibilities as:

$$I_{CYCLE} = I_{HRU} + I_T + I_R + I_{LPCO} + I_{HPCO} + I_{LPC} + I_{HPC} \quad (3.24)$$

On the other hand, total cycle irreversibility for multi-stage compression and intercooling is estimated as:

$$I_{CYCLE} = I_{HRU} + I_T + I_R + \sum_{i=1}^{n} I_{COi} + \sum_{i=1}^{n} I_{Ci} \quad (3.25)$$

Hence 2nd law efficiency or Exergy efficiency of the cycle is:

$$\eta_{II} = \frac{E_{gi} - I_{CYCLE} - E_{go}}{E_{gi}} \quad (3.26)$$

In the equation (3.26) E_{gi} and E_{go} are exergies entering and leaving the HRU with the flue gas respectively. These are represented as follows:

$$E_{gi} = \dot{m}_g C_{Pg}(T_{gi} - T_0) - \dot{m}_g C_{Pg} T_0 \ln \frac{T_{gi}}{T_0} \quad (3.27)$$

$$E_{go} = \dot{m}_g C_{Pg}(T_{go} - T_0) - \dot{m}_g C_{Pg} T_0 \ln \frac{T_{go}}{T_0} \quad (3.28)$$

3.3 Results and discussion:

Results are obtained from the developed model. Initially, for specified highest pressure (12MPa) and temperature (150°C) the effect of varying lowest pressure and intermediate pressure on the performance of a CO_2 based power cycle with two stage compression and intercooling is reported. Optimum values of performance parameters (either for maximum specific work or for 2nd law efficiency) at different turbine inlet conditions for the cycle with two-stage compressions are compared with those of the baseline cycle. Finally, how cycle performance is getting affected by increasing number of compression stages and intercooling has also been described. During the entire analysis lowest cycle temperature is fixed at 35°C.

3.3.1 Energy analysis

For specified turbine inlet condition (i.e., P_H=12MPa, T_H=150°C), the simultaneous effects of varying lowest cycle pressure (P_L) and intermediate pressure (P_i) on specific work output ($w_{SPECIFIC}$) for two stage compression and intercooling is shown in a surface plot of Fig. 3.4(a). It is observed that for any specified value of intermediate pressure, initially specific work output increases with increase in lowest cycle pressure. However, it decreases beyond an optimum lowest cycle pressure for which specific work output is a maximum. Both work output from the turbine (w_T) and low pressure (LP) compressor work input (w_{LPC}) decreases with increasing lowest cycle pressure. From Fig. 3.4(b) it is observed that LP compressor work input initially decreases at a faster rate with an increase in lowest cycle pressure. However, above a certain value of lowest cycle pressure, it decreases at a slower rate compared to turbine work output. This may be also observed from P-h diagrams, i.e., Figs. 3.5(a) and 3.5(b).

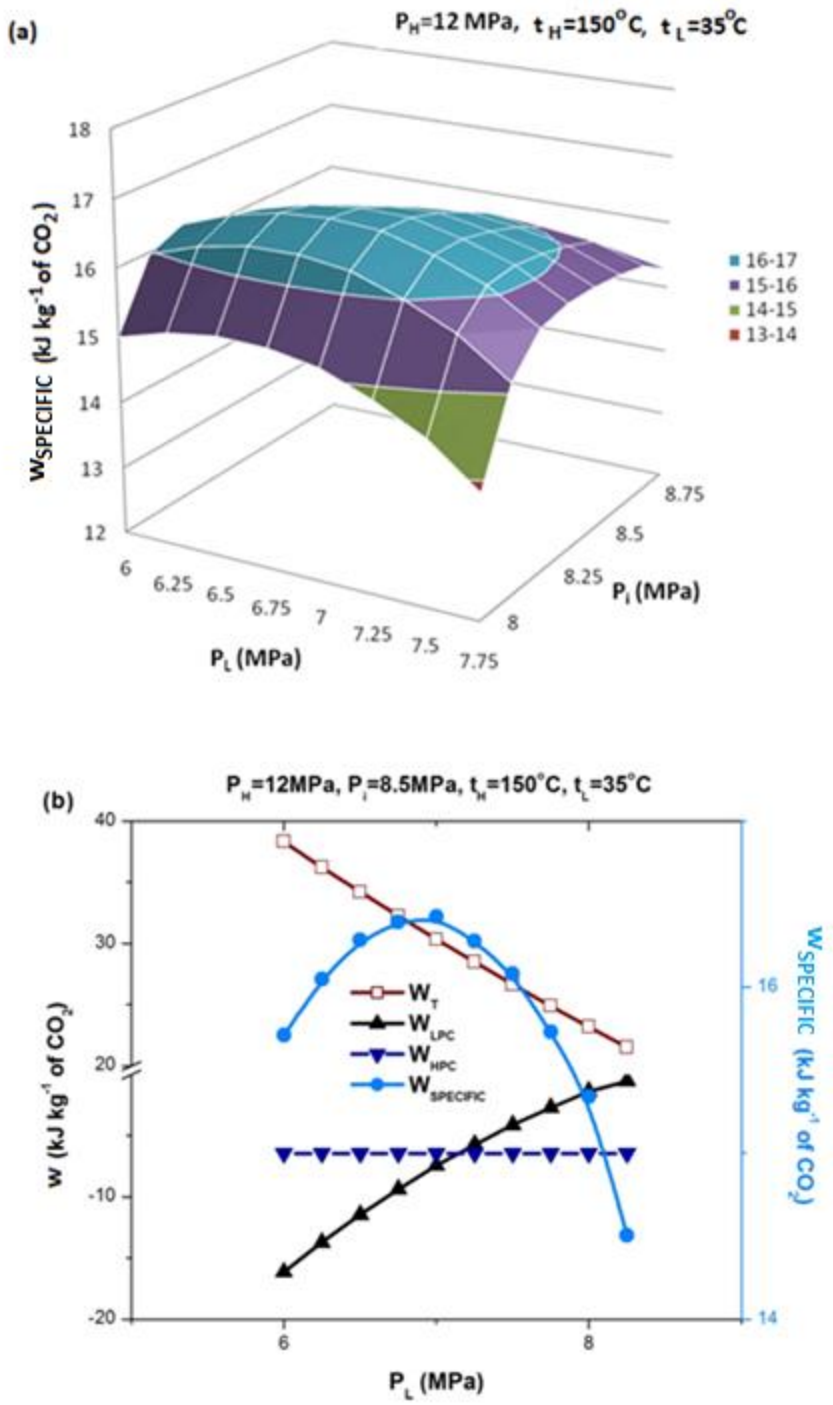

Fig. 3.4 (a): Effect of Lowest cycle pressure and Intermediate pressure on Specific Work output of the cycle with two-stage compression and Intercooling. (b): Effect of varying lowest cycle pressure on trend of different components of Specific work output.

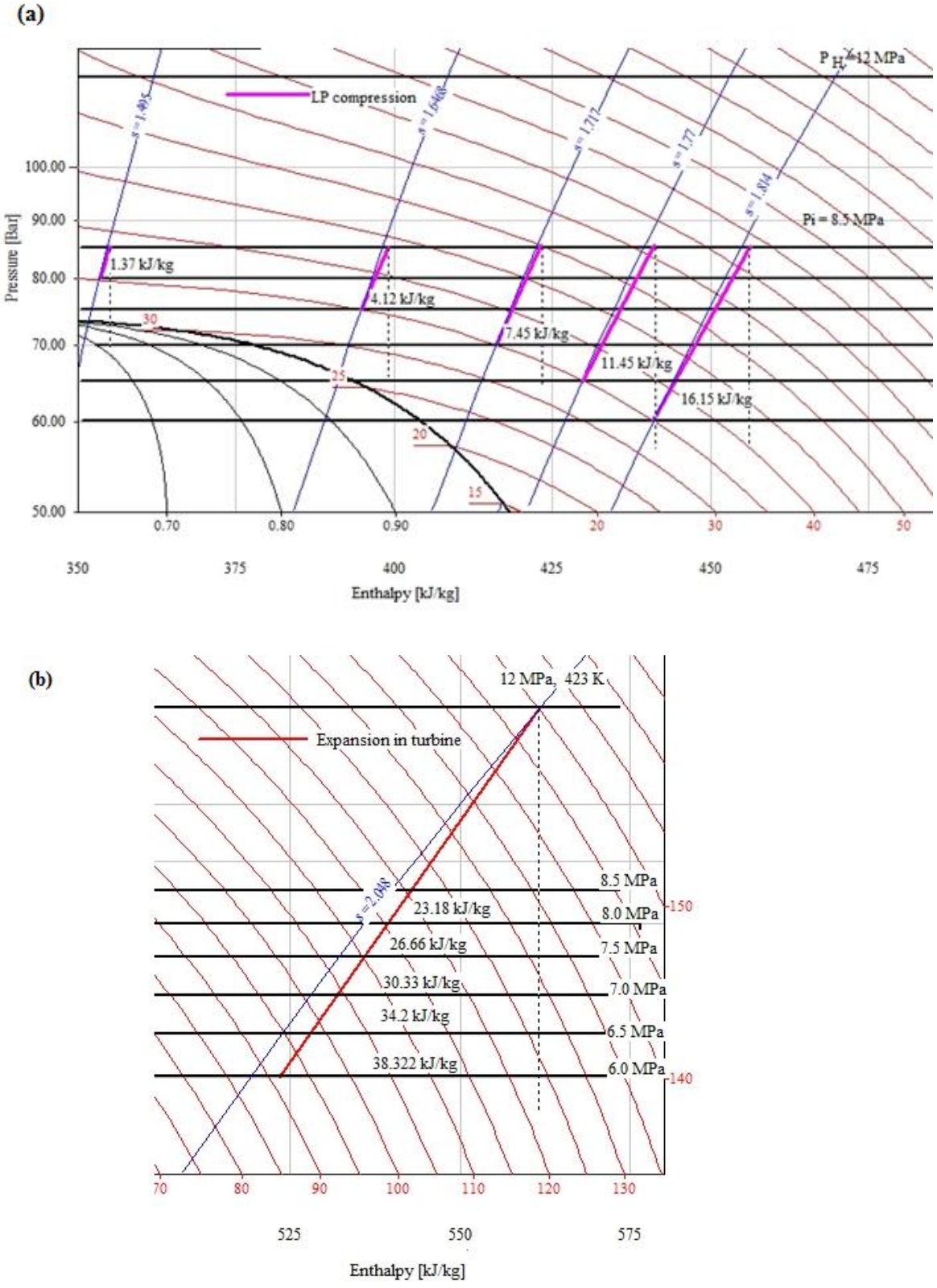

Fig. 3.5 (a): P-h diagram showing effects of lowest cycle pressures on LP compressor work input. (b): P-h diagram showing effects of lowest cycle pressures on turbine work output

(c)

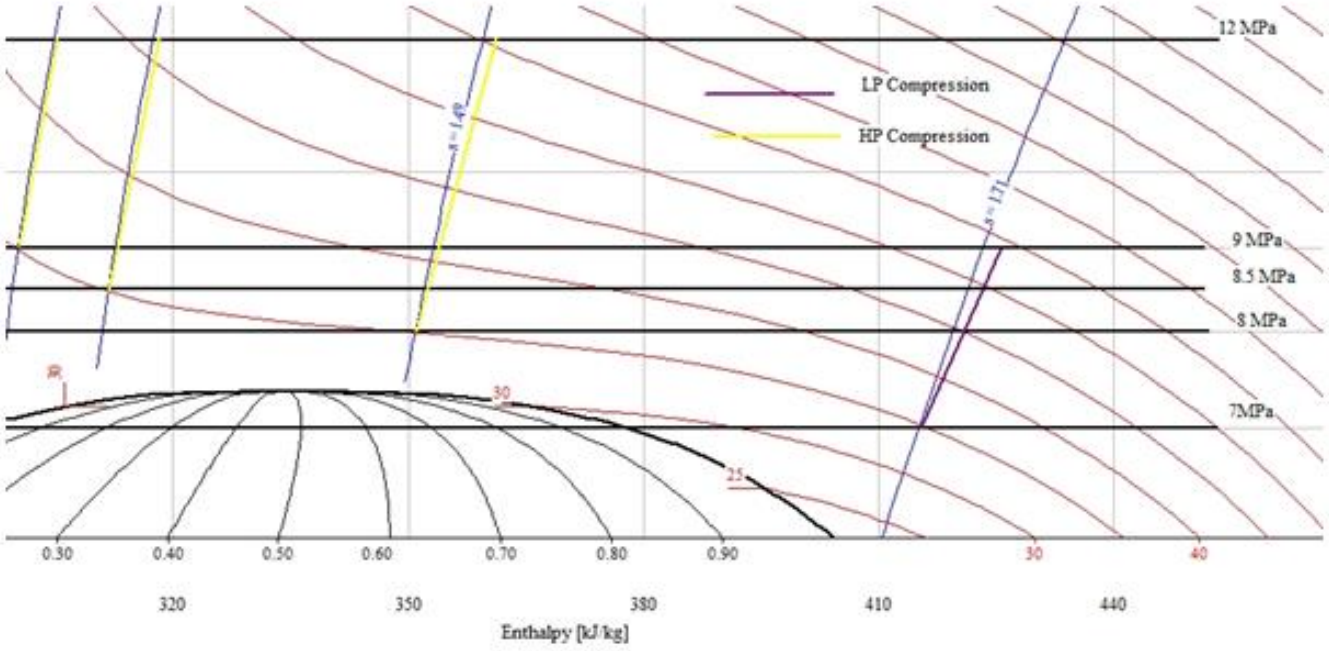

Fig. 3.5 (c): P-h diagram for intermediate pressures vs. LP and HP compressors work inputs

It is clear from the P-h diagram shown in Fig. 3.5 (a) that with increase in lowest cycle pressure, state points corresponding to inlet condition of the LP compressor get shifted towards left along the 35°C isothermal line. The slope of non-isentropic lines (η_C=0.85) along which actual compression takes place gradually increases towards the left of the P-h diagram. Thus the LP compressor power input decreases with increase in lowest cycle pressure due to reduction in change in enthalpy of CO_2 associated with the combined effect of upward movement of state point corresponding to LP compressor input and higher slope of non-isentropic lines of compression towards left of the P-h diagram. On the other hand, for specified intermediate pressure when lowest cycle pressure is varied, turbine power output decreases only due to reduction in change in enthalpy of CO_2 associated with the upward movement of state point at the turbine exit along the non-isentropic line (η_C=0.9) as shown in Fig. 3.5(b). Thus turbine work output decreases at a slower rate compared to work input to LP compressor. However, above a

certain value of lowest cycle pressure, turbine output becomes comparatively more sensitive to increment in lowest cycle pressure as the numerical value of change in enthalpy associated with a non isentropic line of LP compression undergoes smaller decrement. In this situation, specific work output decreases with increase in lowest cycle pressure. It should be noted that with increasing intermediate pressure LP compressor work input increases, whereas HP compressor work input decreases. Initially second parameter dominates the first parameter, i.e. HP compressor work input decreases at a faster rate than the corresponding increase in LP compressor work input. It is due to a large shift of state points corresponding to HP compressor inlet conditions towards the left of the P-h diagram as shown in Fig. 3.5(c). However, above a certain value of intermediate pressure this shifting becomes negligible due to very steep slope of the isotherm at t=35°C. Thus LP compressor work input is comparatively more sensitive to varying intermediate pressure. It is also possible to obtain a peak value of specific work output corresponding to an intermediate pressure if the lowest cycle pressure is specified. In other words, for any specified highest pressure, a combination of an intermediate pressure and the lowest cycle pressure exist for which specific work output is maximized as shown in the surface plot, i.e., Fig. 3.4 (a).

Figure 3.6 shows the simultaneous effect of varying lowest cycle pressure and intermediate pressure on the 1st law efficiency with two stage compression and intercooling for a specified turbine inlet condition. It is evident from the Fig. 3.6 that the 1st law efficiency of the proposed cycle decreases with an increase in intermediate pressure. This is because the heat duty appreciably increases with a higher value of intermediate pressure. On the other hand, 1st law efficiency increases with a higher value of the lowest cycle pressure due to corresponding increase in heat duty of the regenerator. Fig. 3.7 is the two-dimensional representation of Fig. 3.6 which helps to explore some extra information than 3-D surface plot. It is observed from the two-dimensional plots in Fig. 3.7 that after certain value of lowest cycle pressure, efficiency decreases due to reduction in specific work. Also 1st law efficiency increases with intermediate pressure initially, as increase in specific work output dominates over corresponding increment in heat duty. Thus, for the specified turbine inlet condition, it is possible to identify a maximum possible value of the 1st law efficiency.

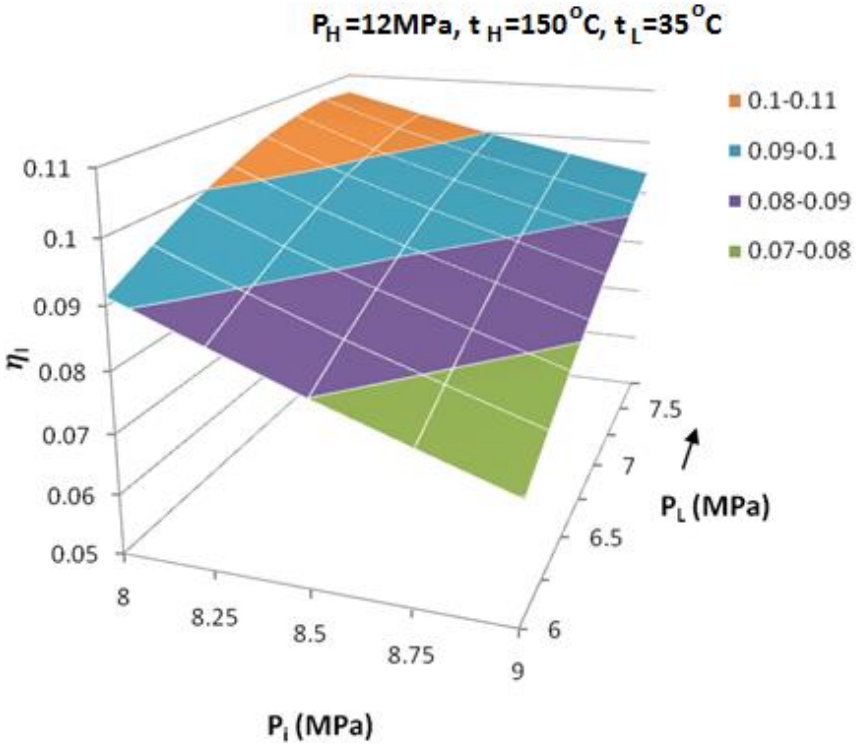

Fig. 3.6: Effect of lowest cycle pressure and intermediate pressure on 1st law efficiency of the cycle with two-stage compression and intercooling.

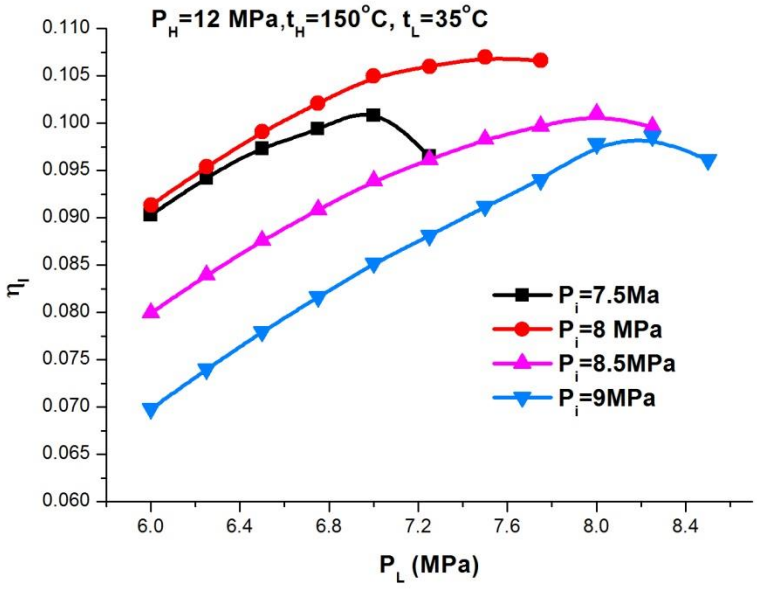

Fig. 3.7: Two-dimensional representation of Fig. 3.6

Effect of lowest cycle pressures on the specific work output of the base line cycle (with P_L-axis in reverse order) for different turbine inlet pressures are shown in Fig. 3.8. It is observed that for each specified turbine inlet condition, an optimum lowest cycle pressure exists for which specific work output of the baseline cycle is a maximum.

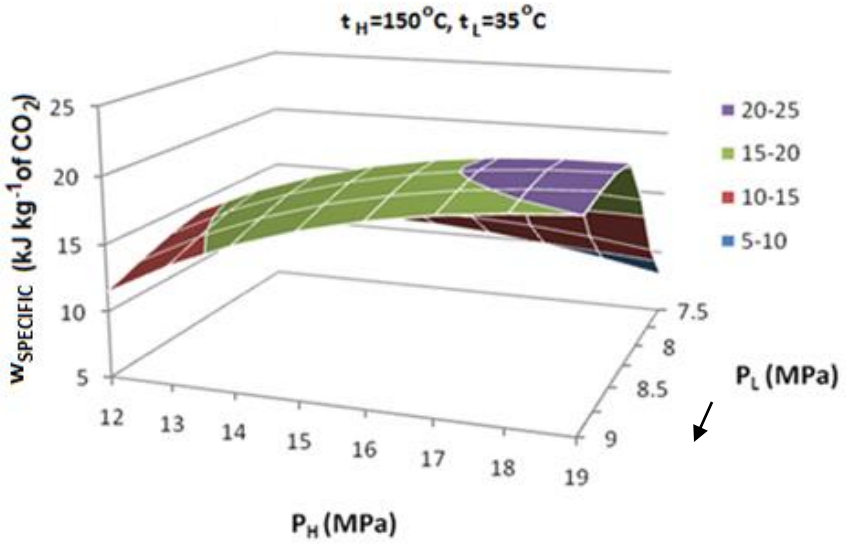

Fig. 3.8: Effect of Lowest cycle pressure and highest cycle pressure on specific work output of the baseline cycle.

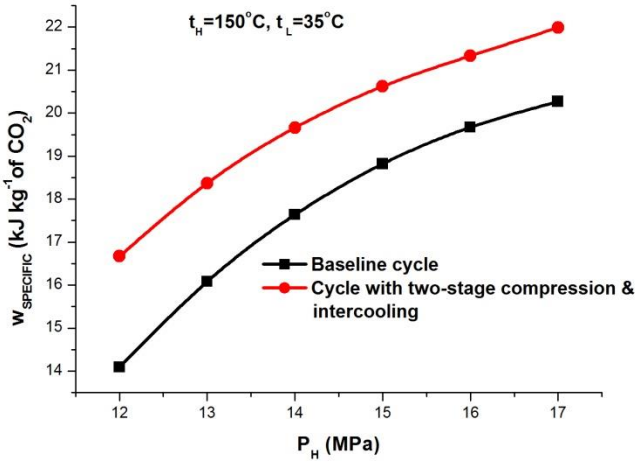

Fig. 3.9: Comparison of maximum possible specific work outputs of cycle with two-stage compression and intercooling and that of the baseline cycle.

For specified highest cycle pressures or turbine inlet pressures, maximum possible specific work outputs of the proposed cycle with two stage compression and intercooling are compared with those of the baseline cycle in Fig. 3.9. It is evident from the Fig. 3.9 that the proposed cycle is capable of producing higher specific work compared to baseline cycle if the turbine inlet condition and the lowest cycle temperature are specified. It should be noted that for the proposed cycle it is possible to select a zone for maximum specific work output from the surface plot of Fig. 3.4(a) for specified turbine inlet pressure (12 MPa). Further specific work outputs are calculated for very small intervals of pressures (0.05MPa) within this selected zone of the surface plot. The maximum possible value of specific work may be selected from this generated data set. Similar process is repeated to determine maximum possible specific work output at other turbine inlet pressures. For the baseline cycle, maximum specific work outputs at different turbine inlet pressures can be obtained by calculating specific work outputs for very small intervals of lowest cycle pressure within the selected zone for maximum specific work output in the surface plot of Fig. 3.8. Conditions of maximum specific work outputs for both proposed and base line cycles at different turbine inlet pressures are tabulated in Table 3.2.

Table 3.2: operating condition for maximum possible specific work output at different turbine inlet pressure (P_H).

Cycle with two-stage compression & intercooling				Baseline cycle		
P_H (MPa)	P_i(MPa)	P_L(MPa)	$w_{SPECIFIC}$ (kJ kg^{-1} of CO_2)	P_H (MPa)	P_L(MPa)	$w_{SPECIFIC}$ (kJ kg^{-1} of CO_2)
12.00	8.25	6.80	16.67	12.00	8.2	14.09
13.00	8.30	6.95	18.37	13.00	8.25	16.08
14.00	8.40	7.2	19.66	14.00	8.30	17.64
15.00	8.40	7.30	20.62	15.00	8.30	18.82
16.00	8.45	7.45	21.33	16.00	8.35	19.67
17.00	9.10	8.10	21.99	17.00	8.40	20.27

Simultaneous effects of varying lowest cycle pressure (i.e. turbine exit pressure) as well as highest cycle pressure (i.e. turbine inlet pressure) on 1st law efficiency of the baseline cycle under specified operating conditions are shown in the 3-D surface plot of Fig. 3.10. It is observed that for each turbine inlet pressure, an optimum lowest cycle pressure exists for which the 1st law efficiency is a maximum. With a smaller value of the lowest cycle pressure, the 1st law efficiency of the baseline cycle have multiple peak values with an increase in turbine inlet pressure (P_H) as

shown in Fig. 3.10. This is explained with simultaneous plots of regenerator heat duty, HRU heat duty and specific work output with P_H as shown in the Fig. 3.11.

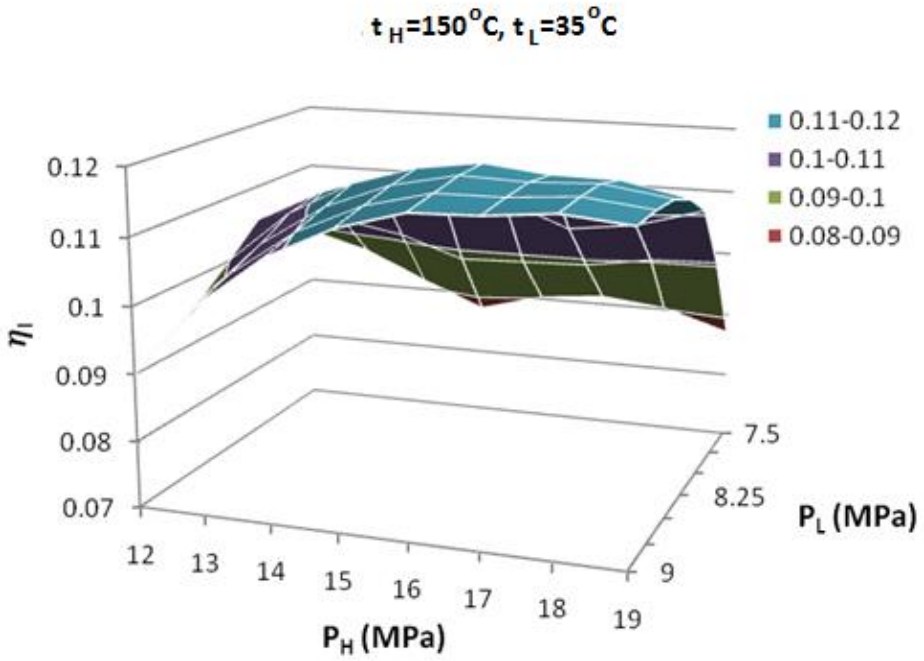

Fig. 3.10: Effect of lowest and highest cycle pressure on 1st law efficiency of the baseline cycle

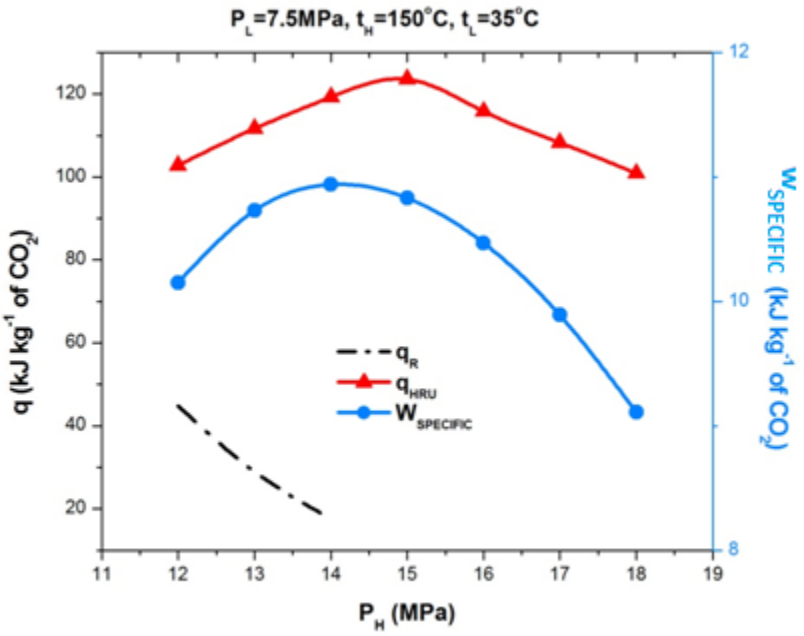

Fig. 3.11: Effect of highest cycle pressure on heat duty and specific work output of the baseline cycle

The first peak of 1st law efficiency is due to incremental specific work output and 2nd peak is due to reduced heat input with the incremental turbine inlet pressure.

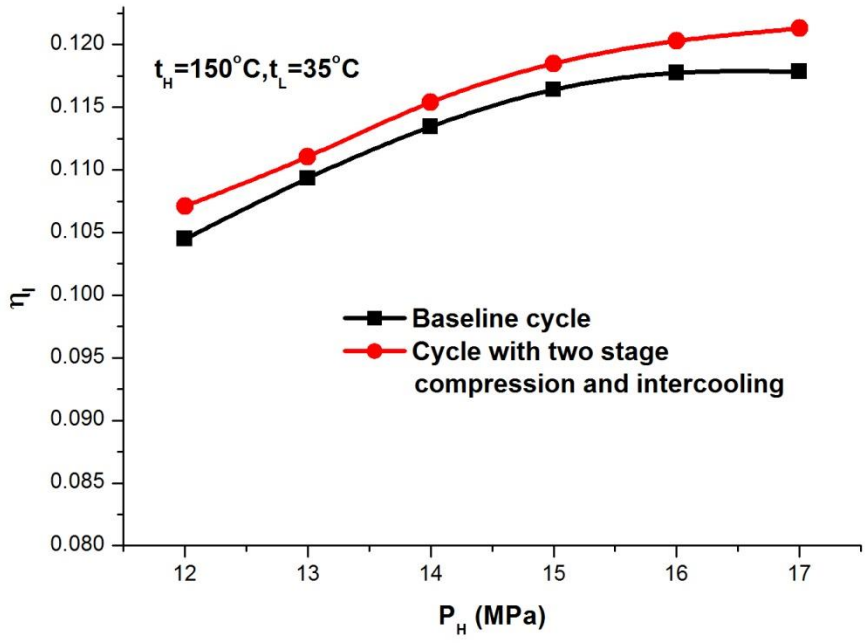

Fig. 3.12: Comparison of maximum possible 1st law efficiency of cycle with two-stage compression and intercooling and that of the baseline cycle.

Table 3.3: operating condition for maximum possible 1st law efficiency at different turbine inlet pressure

Cycle with two-stage compression & intercooling				Baseline cycle		
P_H (MPa)	P_i(MPa)	P_L(MPa)	η_I	P_H (MPa)	P_L(MPa)	η_I
12.00	8.00	7.60	0.1072	12	7.95	0.1045
13.00	8.05	7.60	0.1114	13	8.15	0.1096
14.00	8.50	8.10	0.1150	14	8.15	0.1139
15.00	8.80	8.20	0.1184	15	8.3	0.1164
16.00	9.25	8.30	0.1204	16	8.3	0.1179
17.00	9.4	8.30	0.1215	17	8.4	0.1184

The comparison between maximum possible 1st law efficiencies at different P_H of the proposed cycle (with two stage compression and intercooling) and that of the baseline cycle at different highest cycle pressures is shown in Fig. 3.12. It is also clear from Fig. 3.12 that it is possible to obtain a small improvement in 1st law efficiency for the proposed cycle compared to that of the baseline cycle. However, this improvement is not much significant. Conditions of maximum 1st law efficiency for both proposed and base line cycles at different turbine inlet pressures are tabulated in Table 3.3.

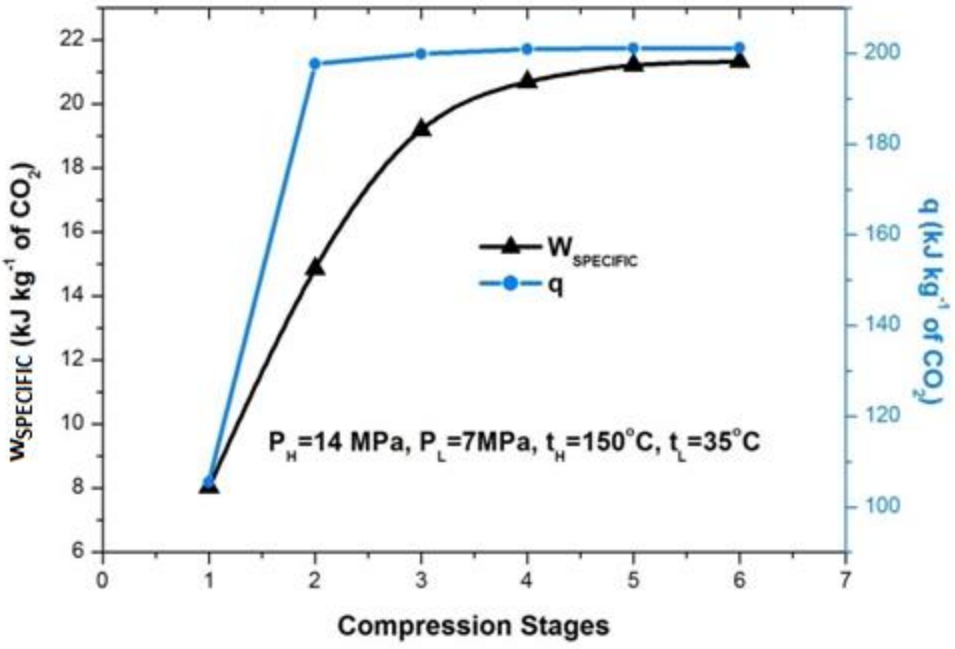

Fig. 3.13: Effect of varying compression stages on Specific work output and heat input.

Effects of compression stages on specific work output and specific heat input are shown in the Fig. 3.13. It should be noted that equal pressure rise during each compression stage is assumed. Specific work output increases with increase in number of compression stages. However, beyond a certain number of compression stages, specific work output poorly responses to increment in number of compression stages. It is also demonstrated in Fig. 3.13 that heat duty drastically increases as two stage compression is introduced instead of single stage.

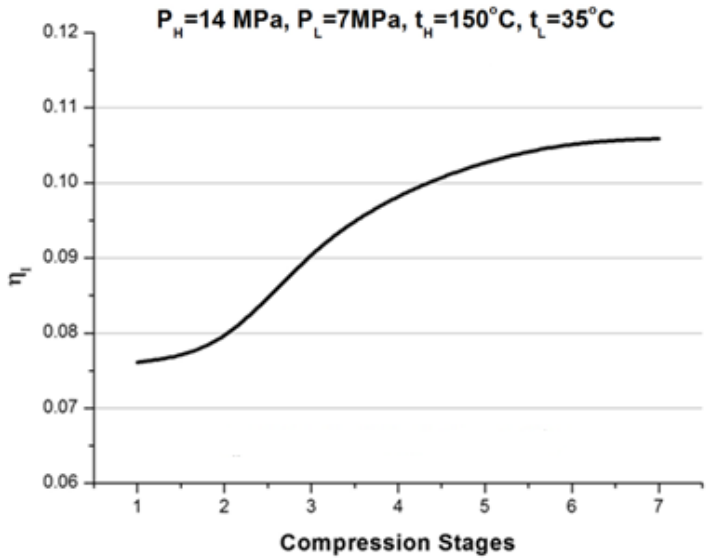

Fig.3.14: Effect of varying number of compression stages on 1st law efficiency

Figure 3.14 shows the variation of 1st law efficiency with no. of compression stages. 1st law efficiency gets improved with higher number of compression stages. Initially small improvement in 1st law efficiency is observed due to substantial increase in heat input per kg of CO_2. With further increase in number of compression stages appreciable improvements in 1st law efficiency are observed due to increase in specific work output. Then slower rate of increment is obtained for 1st law efficiency as specific work output increases at a slower rate with the increase in number of compressors.

3.3.2 Exergy analysis

Effect of lowest cycle pressure and intermediate pressure on the irreversibilities of different components of a CO_2 power cycle with two-stage compression and intercooling are presented in Fig. 3.15 and Fig. 3.16 respectively. It is observed that irreversibility variations of the HRU and the high pressure intercooler contribute to major part of total cycle irreversibility. Irreversibility of the HRU decreases with an increase in lowest cycle pressure as heat duty appreciably reduces without altering effective temperature difference between the flue gas and the supercritical CO_2 stream. With an increase in lowest cycle pressure, irreversibility of the high pressure intercooler decreases because of the lower inlet temperature of CO_2 stream entering to the device. On the other hand, irreversibility associated with the HRU and high pressure intercooler increase with higher intermediate pressure as shown in the Fig. 3.16. In this case, heat duty of the HRU

appreciably increases without altering effective temperature difference between hot and cold streams. Heat duty of high pressure intercooler also increases appreciably as inlet temperature of CO_2 increases.

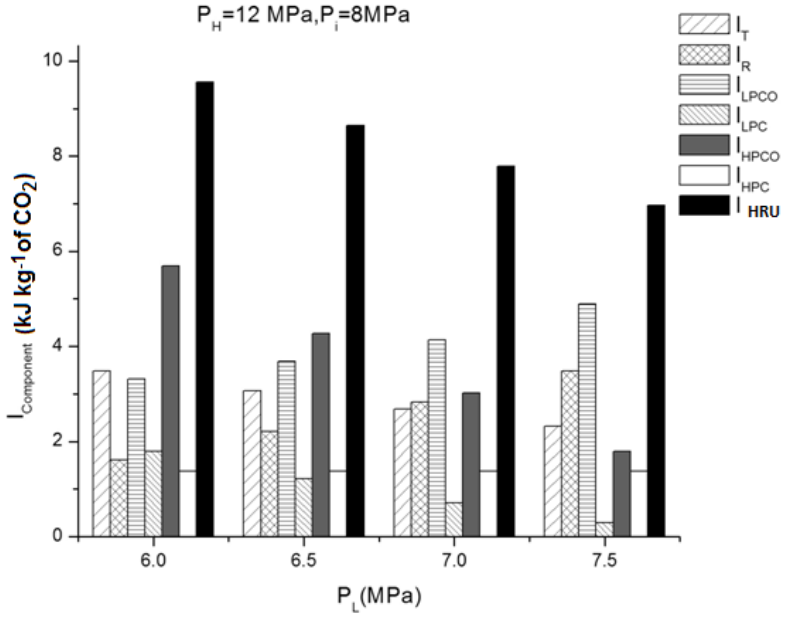

Fig. 3.15: Component irreversibility vs. lowest cycle pressure for the cycle with two-stage compression & Intercooling.

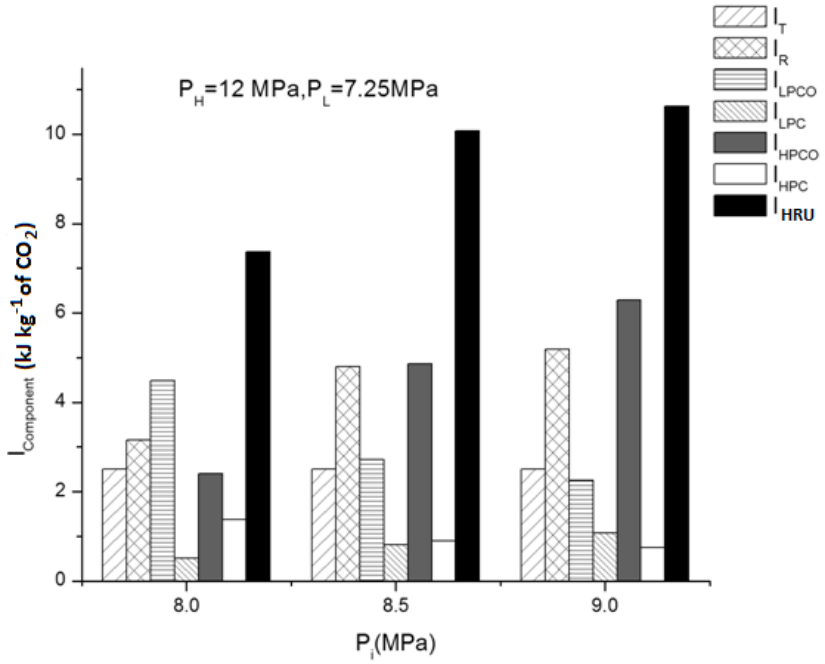

Fig. 3. 16: Component irreversibility vs. intermediate pressure for the cycle with two-stage compression & intercooling.

Due to above nature of irreversibility associated with the HRU and high pressure intercooler, total cycle irreversibility decreases with increasing lowest cycle pressure and increases with increasing intermediate pressure as shown in the surface plot in Fig. 3.17.

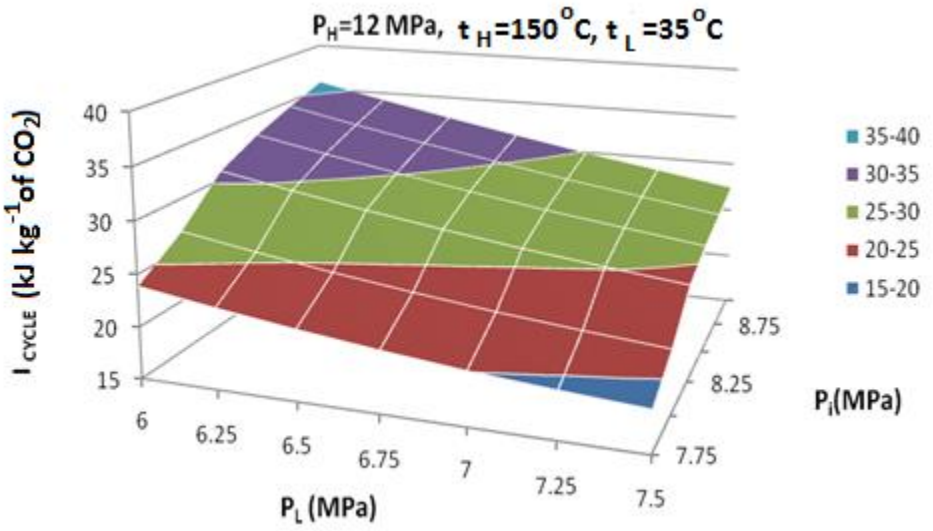

Fig. 3.17: Effect of Lowest cycle pressure and Intermediate pressure on irreversibility of the cycle with two-stage compression and Intercooling.

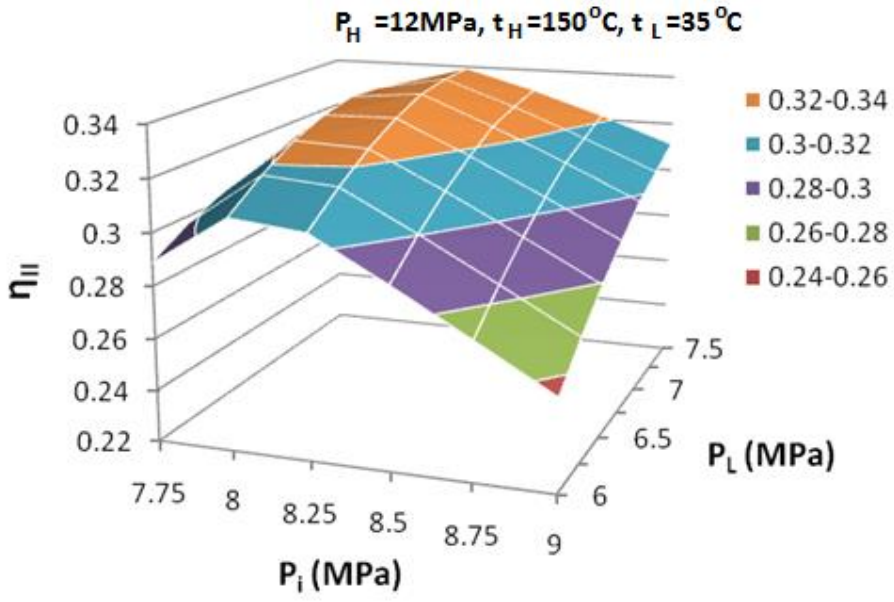

Fig. 3.18: Effect of Lowest cycle pressure and Intermediate pressure on 2nd law efficiency of the cycle with two-stage compression and Intercooling.

Simultaneous effects of lowest cycle pressure and intermediate pressure on 2nd law efficiency of a CO_2 power cycle with two-stage compression and intercooling are shown in Fig. 3.18. It is clear from this surface plot that for a specified turbine inlet condition, an optimum combination of lowest cycle pressure and intermediate pressure exists for which the 2nd law efficiency is a maximum. It should be noted that though total cycle irreversibility decreases with higher value of lowest cycle pressure this is also responsible for higher exergy content of the flue gas leaving the HRU. Thus an optimum lowest cycle pressure corresponding to maximum 2nd law efficiency exists if remaining operating parameters are specified. On the contrary, an optimum intermediate pressure for maximum 2nd law efficiency exists as exergy associated with the flue gas from the HRU decreases with higher values of intermediate pressures.

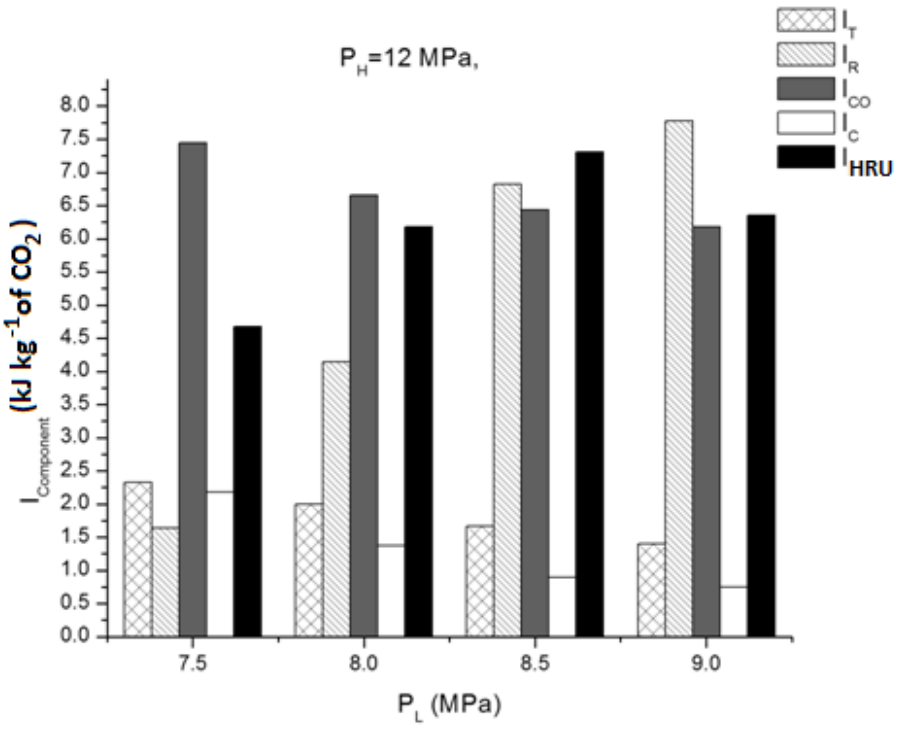

Fig. 3.19: Component irreversibility vs. lowest cycle pressure for the Baseline cycle

The effect of varying lowest cycle pressures on the component irreversibility of a base line cycle is demonstrated in Fig. 3.19. It is observed that irreversibility of the HRU initially increases with P_L. However, above a certain value of lowest cycle pressure, irreversibility of the

HRU decreases with an increase in P_L. This is because initially heat duty of the HRU increases with higher value of lowest cycle pressure due to the small heat duty of the regenerator. However, above a certain value of P_L, CO_2 is heated substantially by the process of regeneration before entering to the HRU. The mean temperature difference between working fluids remains constant during the process of waste heat recovery. Irreversibility associated with the cooler decreases substantially with higher values of P_L due to the smaller inlet temperature of CO_2 stream. Irreversibility associated with the regenerator increases substantially with an increase in lowest cycle pressure of the baseline cycle due to the higher inlet temperature of hot stream of CO_2.

It is shown in Fig. 3.20 that cycle irreversibility of the baseline cycle initially increases with P_L and above a certain value of P_L it decreases. The variation of exergy associated with the flue gas leaving the HRU with varying lowest cycle pressure is a mirror image of total irreversibility variation of the baseline cycle. Thus, an optimum lowest cycle pressure exists for the maximum 2nd law efficiency of the baseline cycle for specified highest cycle pressure or turbine inlet pressure as shown in Fig. 3.21.

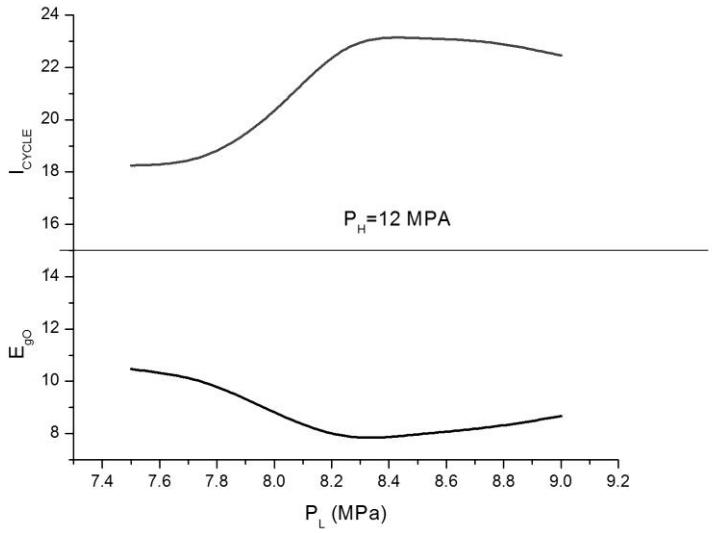

Fig. 3.20: Cycle irreversibility & exergy of flue gas at exit of HRU vs. lowest cycle pressure for the baseline cycle

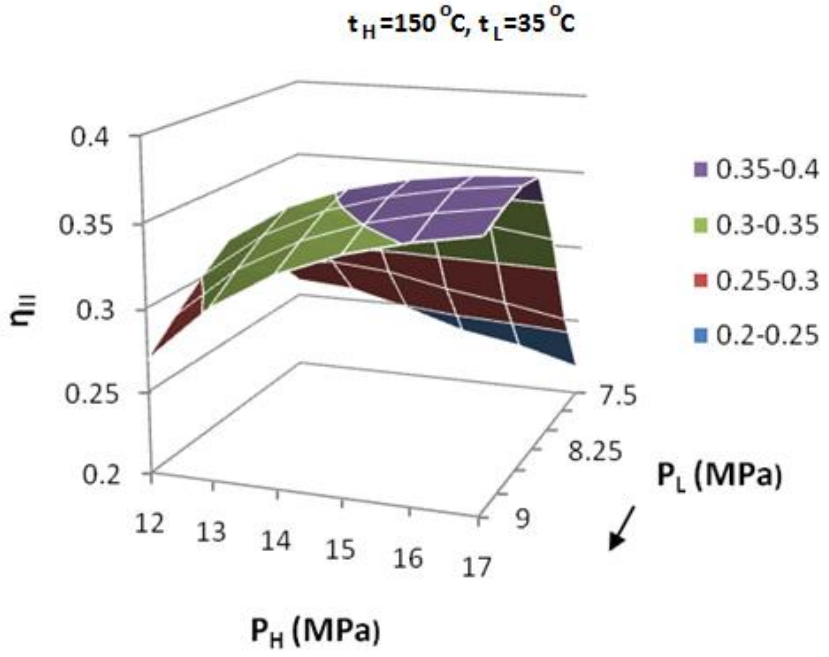

Fig. 3.21: Effect of highest and lowest cycle pressures on 2nd law efficiency of the baseline cycle

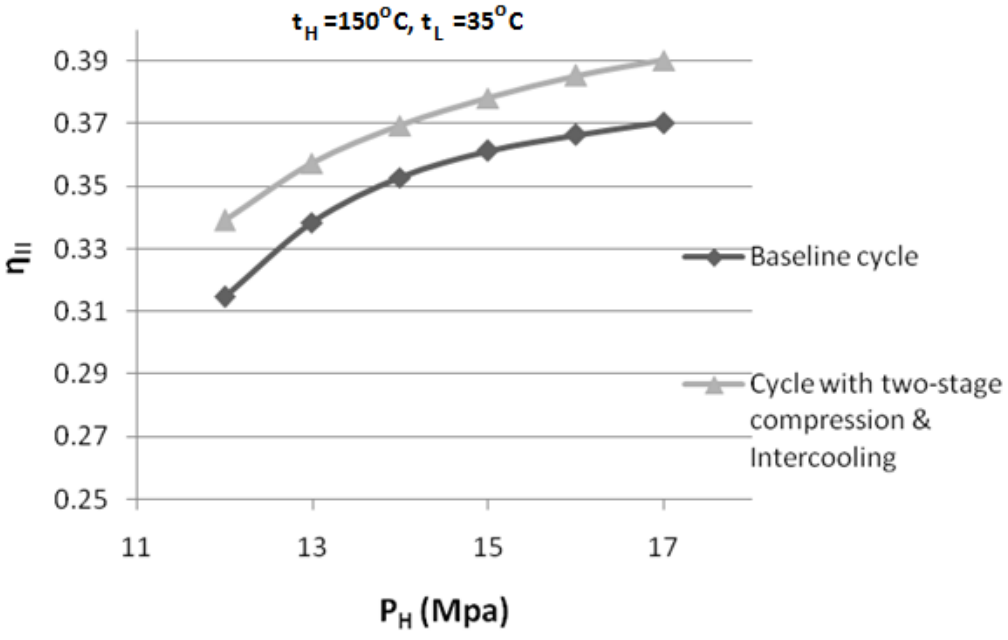

Fig. 3.22: Comparison between maximum possible 2nd law efficiency of cycle with two-stage compression and intercooling & that of the baseline cycle for specified turbine inlet condition.

In Fig. 3.22 maximum possible 2nd law efficiency of the CO_2 power cycle with two-stage compression and intercooling is compared with that of the baseline cycle when highest cycle pressure, highest cycle temperature and lowest cycle temperature are specified. It is observed that it is possible to obtain higher exergy efficiency by adopting two-stage compression with intercooling.

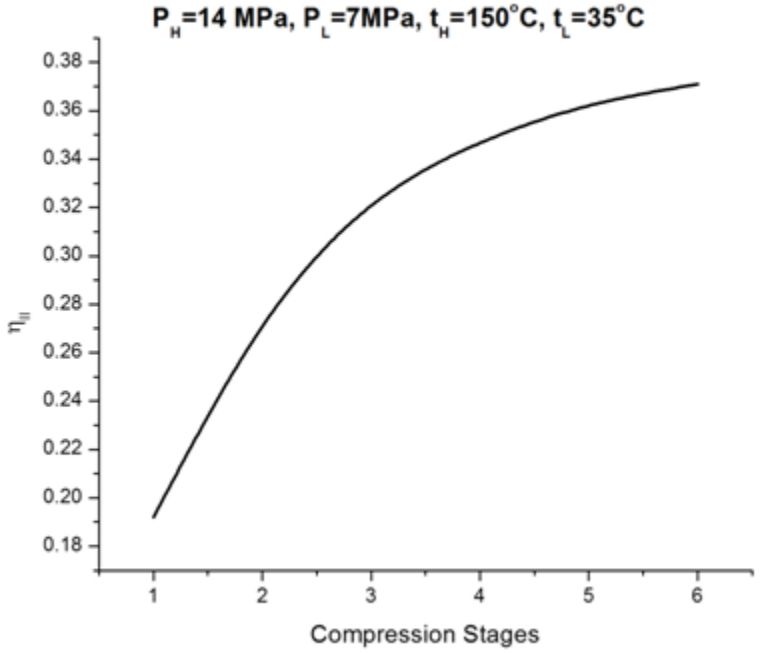

Fig. 3.23: Effect of varying number of compression stages on 2nd law efficiency

The effect of number of compression stages on 2nd law efficiency is shown in Fig. 3.23. As two-stage compression is adopted instead of single stage compression, cycle irreversibility distinctly increases due to higher irreversibility associated with the 2nd stage intercooling and higher heat duty of the HRU. However, significant improvement in 2nd law efficiency is observed due to larger exergy associated with the flue gas at the HRU inlet. Also exergy associated with the outgoing flue gas stream appreciably decreases due to the lower exit temperature of the flue gas from the HRU. Further increase in number of compression stages leads to an improvement in 2nd law efficiency due to reduction in total cycle irreversibility. Above a certain number of

compression stages, 2nd law efficiency does not increase appreciably with further increment in number of compression stages.

3.4 Chapter summary:

In present analysis a thermodynamic model has been developed for a CO_2 based power cycle to explore the effects of multi stage compression with intercooling assuming the lowest cycle temperature to be 35ºC. The outcome of the study can be summarized as follows:

- With the specified turbine inlet condition and lowest cycle temperature an optimum combination of lowest cycle pressure and intermediate pressure exists for which specific work output or 2nd law efficiency of the CO_2 power cycle with two-stage compression and intercooling is maximized.

- A CO_2 power cycle with two-stage compression and intercooling is capable of producing higher specific work output and 2nd law efficiency compared to baseline cycle if the turbine inlet condition and the lowest cycle temperature are specified.

- Maximum possible 1st law efficiency of the CO_2 power cycle with two-stage compression and intercooling is slightly higher compared to that of the baseline cycle for specified turbine inlet condition and lowest cycle temperature.

- Specific work output as well as the 1st law efficiency of the CO_2 power cycle substantially gets improved with multi stage compression and intercooling. However, this improvement becomes insignificant above a certain number of compression stages.

- 2nd law efficiency can be improved by adopting higher number of compression stages. However, above certain number of compression stages this improvement is negligible.

4. T-CO_2 Power cycle vs. Organic flash cycle (OFC): A comparative study

4.1 Objective of the work

Transcritical CO_2 power cycle is capable of producing reasonably good power output using waste heat of flue gas, free from SO_2. Due to the absence of pinch limitation, a Transcritical CO_2 power cycle can recover a greater amount of heat by cooling the flue gas closer to the ambient temperature. However, very high operating pressure in the HRU is obviously a disadvantage of the T-CO_2 power cycle.

Organic flash cycle is another possible option that eliminates pinch limitation of the conventional ORC and can recover maximum heat by cooling the SO_2 free flue gas closer to the ambient temperature. Operating pressure in HRU of the OFC is appreciably smaller compared to that of the T-CO_2 power cycle. However, a comparative study between the T-CO_2 power cycle and the OFC should be conducted to explore the suitability of the OFC as one of the possible replacements of the T-CO_2 power cycle.

In the present chapter, thermodynamic and economic performance of T-CO_2 power cycle is compared with that of the OFC while utilizing low grade heat of waste flue gas produced due to combustion of sulphur free fuel. Hence, during thermodynamic analysis, extraction of maximum possible power from a given flow rate of flue gas is the basic objective instead of thermal efficiency as the flue gas exit temperature of a heat recovery unit is not bounded by the phenomena like sulphuric acid condensation. For the OFC, R245fa and R600 are selected as the working fluids as their saturation vapour lines are having positive slopes and their critical temperatures (154.05°C and151.98°C respectively) are close to the inlet temperature of the selected flue gas (i.e. 150°C). Thus, both working fluids can be heated to the highest possible cycle temperature, i.e. 140°C, to obtain significant amount of saturated vapour at comparatively higher value of specified flash pressure. This also produces a higher specific enthalpy drop during expansion in the turbine and also allows a higher mass of vapour to enter into the turbine. Moreover, R245fa is having zero ozone depletion potential. However corresponding GWP is significantly high. On the other hand, R600 is having zero ODP and corresponding GWP is ~20. R600 is a highly flammable hydrocarbon too.

4.2 System descriptions and assumptions.

4.2.1 Organic Flash Cycle (OFC)

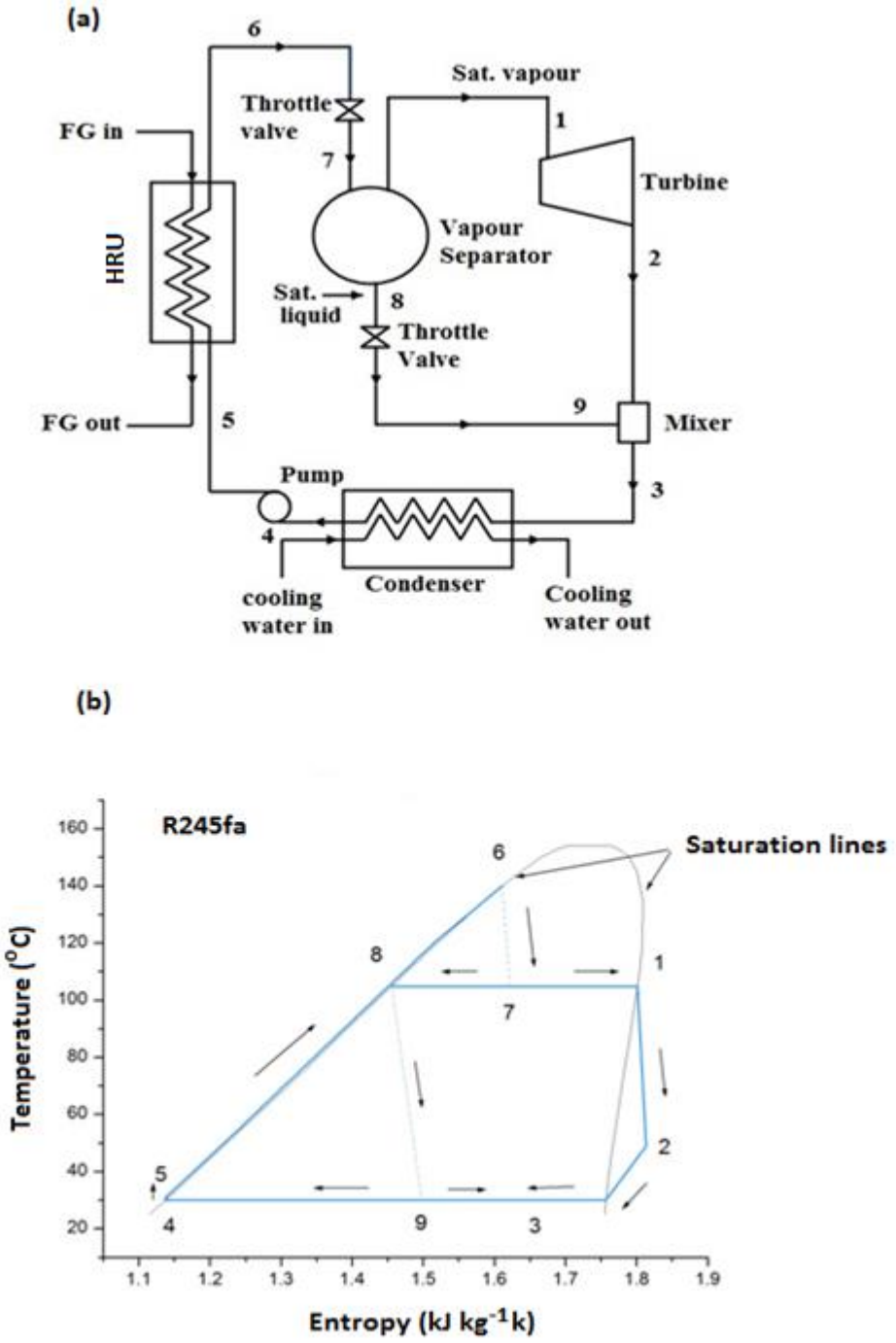

Fig. 4.1 (a): Layout of an OFC (b) Temperature-entropy diagram of OFC

System layout and Temperature-entropy diagram of an OFC are presented in Figs. 4.1(a) and 4.1(b) respectively. Sub-cooled R245fa or R600 coming out from the pump is heated to a saturated liquid state at 140°C (state-6) by using waste heat of flue gas produced

due to burning of sulphur free fuel. This saturated liquid is throttled to the turbine inlet pressure (state-7) and allowed to enter the flash drum or vapour separator. Saturated vapour coming out from the vapour separator expands (state change 1-2) in the turbine to produce power output. Exhaust stream coming out from the turbine (state-2) mixes with stream coming out of the LP throttle valve (state-9). Then the total mass of working fluid condensed to saturated liquid state (state-4) at condenser pressure and finally it is pressurized to gas heater pressure (state-5) using a pump.

4.2.2 T-CO_2 Power Cycle

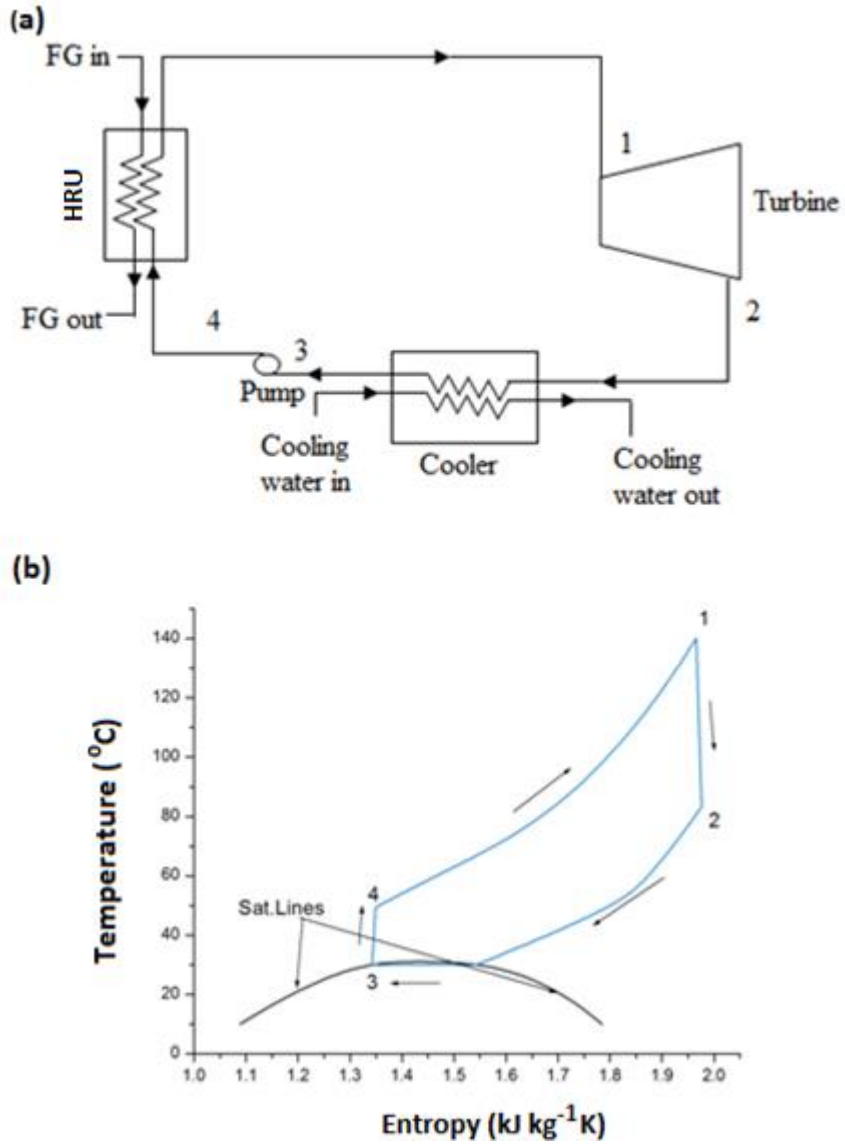

Fig. 4.2 (a): Layout of a T-CO_2 power cycle (b): Temperature -entropy diagram of a T-CO_2 power cycle.

Figures 4.2 (a) and 4.2 (b) are representing system layout and T-s diagram of a T-CO_2 power cycle. Here regeneration is not considered as this allows the flue gas to leave the gas heater at a comparatively higher temperature with sufficiently higher work potential. Also, this adds to an additional equipment cost. Supercritical CO_2 stream after being heated (i.e., state change 4-1) in the heat recovery unit, expands (i.e., state change 1-2) in the turbine. Subsequent exhaust CO_2 stream is cooled (i.e., state change 2-3) to saturated liquid state and is pressurised to turbine inlet pressure (i.e., state-4) using a compressor.

4.2.3 Assumptions

1. Turbine efficiency is assumed to be 90%.
2. Compressor and pump efficiencies both are assumed to be 85%.
3. Flue gas inlet temperature is 150°C.
4. Terminal temperature difference in the high temperature side of the gas heaters for both cycles is 10°C.
5. Ambient condition is specified by 100kPa and 15°C.
6. Cooling water is available at 15°C.
7. Pinch point temperature difference at condenser is assumed to be 5°C.
8. Tube side mass flux of CO_2 is assumed to be 350 kg m^{-2} s^{-1} to keep pressure drop below 30kPa. Corresponding R245fa and R600 mass flux are assumed to be 550 kg m^{-2} s^{-1} and 350 kg $m^{-2}s^{-1}$ respectively for a maximum permissible pressure drop of 50kPa.
9. Maximum permissible flue gas velocity is 15 m s^{-1}.
10. Flue gas thermo-physical properties are assumed to be same as atmospheric air. Thus, the effect of steam condensation from the flue gas in HRU is not considered.
11. Flue gas does not contain any SO_2.
12. Configurations of all heat exchangers are assumed to be of shell and tube type with fixed tube sheet arrangement.
13. Due to low capacity of proposed heat recovery system radial flow turbine is used.
14. Flash drum is modelled as a vertical process vessel (Al-Zuhair et al. 2011)
15. The steady flow operating condition is assumed.

4.3. Mathematical Modelling:

4.3.1 Thermodynamic analysis

In thermodynamic analysis, two performance parameters are considered i.e. Work output per unit mass of flue gas (FG) flow and 2nd law efficiency (η_{II}).

Specific work outputs for OFC and T-CO_2 power cycle are expressed by equations 4.1(a) and 4.1(b) respectively.

$$w_{Specific} = w_T - w_P \qquad 4.1(a)$$

$$w_{Specific} = w_T - w_C \qquad 4.1(b)$$

Where for OFC, $w_T = x(h_1 - h_2)$, $w_P = h_5 - h_4$ (refer to Fig. 4.1(b)) and for T-CO_2 power cycle $w_T = h_1 - h_2$, $w_C = h_4 - h_3$ (refer to Fig. 4.2(b))

Work output per kg of flue gas is

$$W\ kg^{-1} of\ FG = m_f . w_{specific} \qquad (4.2)$$

Also, in equation (4.2)

$$m_f = \frac{c_{Pg}(T_{gi} - T_{go})}{q} \qquad (4.3)$$

Where, $q = h_6 - h_5$ for OFC (refer to Fig. 4.1 (b)) and $q = h_1 - h_4$ for T-CO_2 power cycle (refer to Fig. 4.2 (b)).

2nd law efficiency of both cycles calculated using equation (4.4) is as shown below:

$$\eta_{II} = \frac{E_{gi} - \sum I_{Component} - E_{go} - E_{wo}}{E_{gi}} = \frac{W\ kg^{-1} of\ FG}{E_{gi}} \qquad (4.4)$$

Where

$$E_{gi} = c_{Pg}\left(T_{gi} - T_0\right) - c_{Pg} T_0 \ln \frac{T_{gi}}{T_0} \qquad (4.5)$$

$$E_{go} = c_{Pg}\left(T_{go} - T_0\right) - c_{Pg} T_0 \ln \frac{T_{go}}{T_0} \qquad (4.6)$$

$$E_{wo} = m_w\{(h_{wo} - h_{wi}) - T_0(s_{wo} - s_{wi})\} \quad (4.7)$$

In equation (4.7), m_w is the cooling water flow rate in kg kg^{-1} of flue gas, h_{wo} & s_{wo} are specific enthalpy and entropy of water stream leaving the condenser/cooler. h_{wi} & s_{wi} are corresponding values at condenser inlet or at dead state. It should be noted that cooling water at condenser inlet is in dead state as it enters at ambient condition.

Irreversibilities of individual components of the OFC (refer to Fig. 4.1 (b)) are expressed as follows:

$$I_T = m_f x T_0\,(s_2 - s_1) \quad (4.8)$$

$$I_m = m_f T_0\{s_3 - x s_2 - (1-x)s_9\} \quad (4.9)$$

$$I_{HPTH} = m_f T_0(s_7 - s_6) \quad (4.10)$$

$$I_{LPTH} = m_f T_0(1-x)(s_9 - s_8) \quad (4.11)$$

$$I_P = m_f T_0(s_5 - s_4) \quad (4.12)$$

$$I_{Condenser} = m_f T_0(s_4 - s_3) + m_w T_0(s_{wo} - s_{wi}) \quad (4.13)$$

$$I_{HRU} = c_{Pg} T_0 \ln\frac{T_{g0}}{T_{gi}} + m_f T_0(s_6 - s_5) \quad (4.14)$$

Irreversibilities of different components of the T-CO_2 power cycle (refer to Fig. 4.2 (b)) are also as follows:

$$I_T = m_f T_0\,(s_2 - s_1) \quad (4.15)$$

$$I_{Cooler} = m_f T_0(s_3 - s_2) + m_w T_0(s_{wo} - s_{wi}) \quad (4.16)$$

$$I_C = m_f T_0(s_4 - s_3) \quad (4.17)$$

$$I_{HRU} = c_{Pg} T_0 \ln\frac{T_{g0}}{T_{gi}} + m_f T_0(s_1 - s_4) \quad (4.18)$$

4.3.2 Economic analysis

As operating pressure of the heat recovery unit (HRU) is relatively higher for the T-CO_2 power cycle than that of the OFC, only thermodynamic performance comparison of these two

cycles will be misleading. It is therefore necessary to compare costing of these two cycles also to select a better option.

4.3.2.1 Heat exchanger area calculation

For the modelling of the heat transfer inside the heat exchanger, each heat exchanger is considered as consisting of 20 numbers of subsections with an equal enthalpy drop of the working fluid within each of these subsections. Working fluids are always assumed to flow through the tube of the shell and tube heat exchanger. Overall heat transfer coefficient of each subsection can be presented as

$$U_i = \frac{1}{\frac{1}{\alpha_{si}} + \frac{1}{\alpha_{ti}}} \tag{4.19}$$

Area of each subsection of heat exchangers

$$A_i = \frac{m_f \Delta h_{fi}}{U_i LMTD_i} \tag{4.20}$$

The total area for heat transfer of the heat exchanger is obtained by adding the area of all these individual subsections. Kern's method (1950) is employed for the determination of shell side heat transfer coefficient. For different operating conditions, tube side convective heat transfer coefficient is obtained from following correlations.

- For subcritical flow, Gnielinski correlation (Gnielinski. 1976) is employed
- For super critical flow of CO_2 in heat recovery gas heater, Krasnoschekov-Protopov correlation (Pioro et al. 2004) is employed.
- For condensing CO_2, R245fa and R600 Cavallini and Zecchin correlation (Cavallini and Zecchin, 1974) is used.

4.3.2.2 Equipment Bare Module cost estimation

Equation used for the purchased cost of individual equipment (C_P^0) at ambient operating pressure and using carbon steel (CS) construction is as follows (Turton et al. 2009):

$$\log_{10} C_P^0 = K_1 + K_2 \log_{10} Z + K_3 (\log_{10} Z)^2 \tag{4.21}$$

Where, Z is the parameter for capacity and size of the equipment as provided in the Table.4.1. To take care of elevated operating pressure and material other than CS, basic cost is modified to obtain the bare module cost as expressed by following equation (Turton et al. 2009):

$$C_{BM} = C_P^0(B_1 + B_2 F_P F_M) = C_P^0 F_{BM} \quad (4.22)$$

In this equation $F_{P,}$ F_m and F_{BM} are pressure factor, material factor and bare module factor respectively. F_P for flash drum is assumed to be 1 and bare module factor for equipment like compressor and turbine can be obtained directly from the Fig A.19 (Turton et al. 2009). The expression for pressure factor for remaining equipments is as shown below (Turton et al. 2009):

$$\log_{10} F_P = C_1 + C_2 \log_{10} P + C_3 (\log_{10} P)^2 \quad (4.23)$$

Where, P is the operating pressure in bar gauge. The values of constants of equations (4.21), (4.22) and (4.23) are also provided in table 4.1 (Turton et al. 2009).

Table 4.1: Constants for BMC analysis (Turton et al. 2009)

	CO_2 HRU	OFC HRU	CO_2 cooler/ condenser	OFC Condenser	Turbine	Compressor	Pump	Vapour separator
Z→	Heat transfer area (m^2)				W_T (kW)	W_C (kW)	W_P (kW)	V ($m^{3)}$
K_1	4.3247				2.2476	5.0355	3.3892	3.4974
K_2	-0.303				1.4965	-1.8002	0.0536	0.4485
K_3	0.1634				-0.1618	0.8253	0.1538	0.1074
C_1	-0.00164			0	-	-	-0.3935	-
C_2	-0.00627			0	-	-	0.3957	-
C_3	0.0123			0	-	-	-0.00226	-
B_1	1.63				-	-	1.89	2.25
B_2	1.66				-	-	1.35	1.82
F_M	1				-	-	1	
F_P	-				-		-	1
F_{BM}	-	-	-	-	3.5	2.7	-	-

It should also be noted that equation (4.22) is a representation of equipment bare module cost in $ according to price level of the year 2001. Thus, the same for current financial year can be determined by following equation to take care of the time value of money:

$$C_{BM} = \frac{CEPCI_{Current\ year}}{CEPCI_{2001}} C_{BM2001} \qquad (4.24)$$

In equation (24) CEPCI is Chemical engineering plant cost index. CEPCI is 574.6 in equation 4.24.

4.4. Result and discussion

Objective of the present work is to explore the better option out of T-CO_2 power cycle and OFC for low temperature waste heat recovery to generate power from a sulphur free flue gas. Comparisons are made between performance of these two cycles, i.e. OFC and T-CO_2 power cycle. Performance comparison includes both thermodynamic and economic aspects as operating pressures of these two cycles being different, bare module cost of equipment are also different. Hence performance comparison should include economic implications also.

In the present study, three performance parameters (i.e. work output per unit mass of flue gas, 2nd law efficiency and equipment BMC per unit power output) are considered for conducting a comparison between OFC and T-CO_2 power cycles. During the analysis, working fluids for both cycles are assumed to be heated up to 140°C by using waste heat of flue gas that enters at 150°C to the heat recovery unit. Also, the condenser temperature is assumed to be 30°C for all cycles.

In this analysis 1st law efficiency and specific work output are not considered as performance parameters as higher value of specific work output and 1st law efficiency does not exclusively represent the effectiveness of the waste heat recovery scheme. How effectively waste heat of the flue gas is utilized is better estimated by the work output per unit mass of the flue gas and the 2nd law efficiency. It is because effectiveness of any waste heat recovery power cycle depends on how much network is finally obtained irrespective of the 1st law efficiency as the heat input is only through waste heat recovery and not by fuel input.

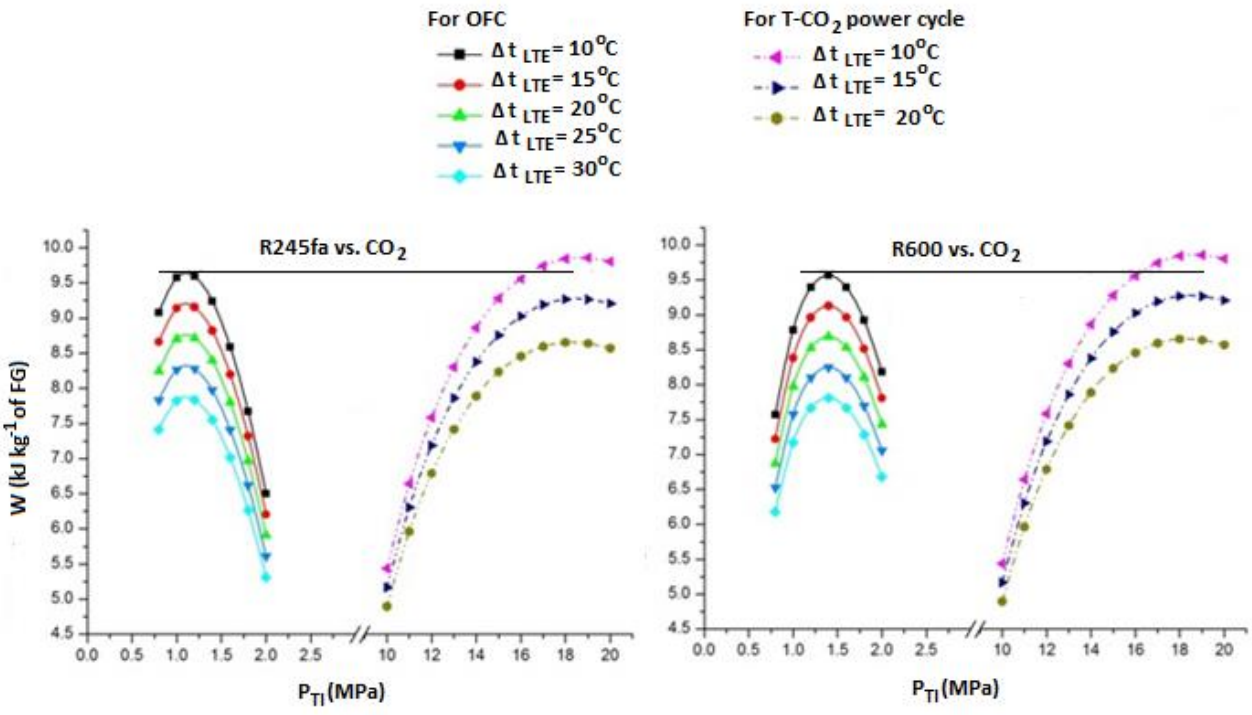

Fig. 4.3: Comparison between work output per kg of flue gas of OFCs and that of T-CO_2 power cycles

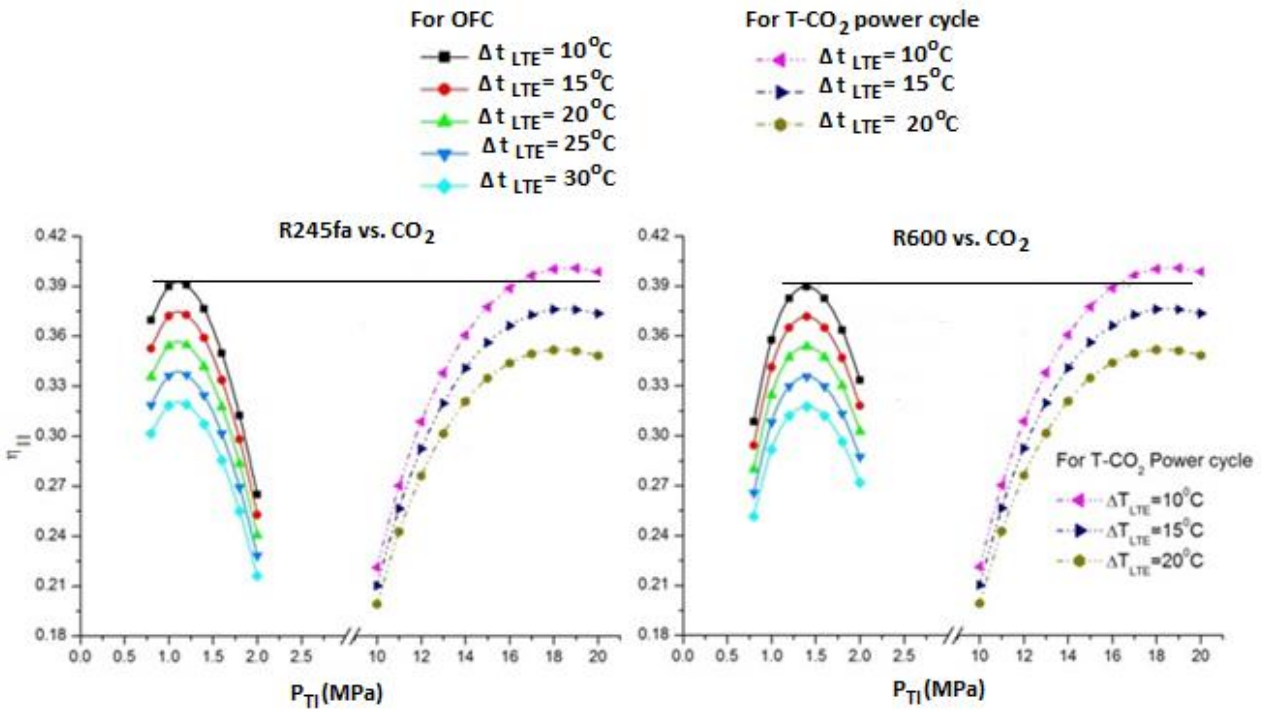

Fig. 4.4: Comparison between 2nd law efficiencies of OFCs and that of T-CO_2 power cycles.

Variations of work output per unit mass of flue gas and 2nd law efficiency for OFCs and T-CO_2 power cycles are shown in Figs. 4.3 and 4.4 respectively. It is observed that there exist optimum turbine inlet pressures for OFCs and T-CO_2 power cycle corresponding to which both work output per kg of flue gas and 2nd law efficiency become maximum. Both increasing turbine work output and compressor work input with increasing turbine inlet pressure results to a maximum work output per unit mass of FG for T-CO_2 power cycle at an optimum turbine inlet pressure. On the other hand, specific enthalpy drop during expansion in the OFC turbine increases with an increase in turbine inlet pressure. However, a lesser fraction of mass of R245fa or R600 enters the turbine with elevated turbine inlet pressure due to degraded vapour quality. Thus an optimum turbine inlet pressure exists for which turbine work output as well as work per unit mass of FG for the OFC is a maximum. According to equation 4.4, at same turbine inlet pressure, 2nd law efficincy will also be a maximum.

It is also observed that T-CO_2 power cycle is capable of producing slightly higher 2nd law efficiency and work output for each kg flow of flue gas when flue gas is cooled to the lowest practical temperature (i.e. 10^0C terminal temperature difference is maintained at the low temperature end of the heat recovery gas heater). However, corresponding turbine inlet pressure for T-CO_2 power cycle is appreciably higher compared to that of OFCs. Also work output per unit mass of FG and 2nd law efficiency of T-CO_2 power cycle is more sensitive to increment in terminal temperature difference at the low temperature end of the HRU due to corresponding higher 1st law efficiency.

Component irreversibility variations with varying turbine inlet pressure for OFC with R600 and T-CO_2 power cycle are presented in Fig. 4.5 (a) and 4.5 (b) respectively. It is observed in Fig.4.5 (a) that irreversibilities of LP and HP throttle valves are the major contributors to the total cycle irreversibility of the OFC. Irreversibility associated with the HP throttle valve decreases with an increase in turbine inlet pressure. On the other hand, irreversibility of the LP throttle valve increases with an increase in turbine inlet pressure. It is observed in Fig. 4.5 (b) that for T-CO_2 power cycle, irreversibilities associated with the turbine and the compressor increase with an increase in the turbine inlet pressure. However, irreversibilities associated with the HRU and the cooler decrease appreciably with an increase in turbine inlet pressure.

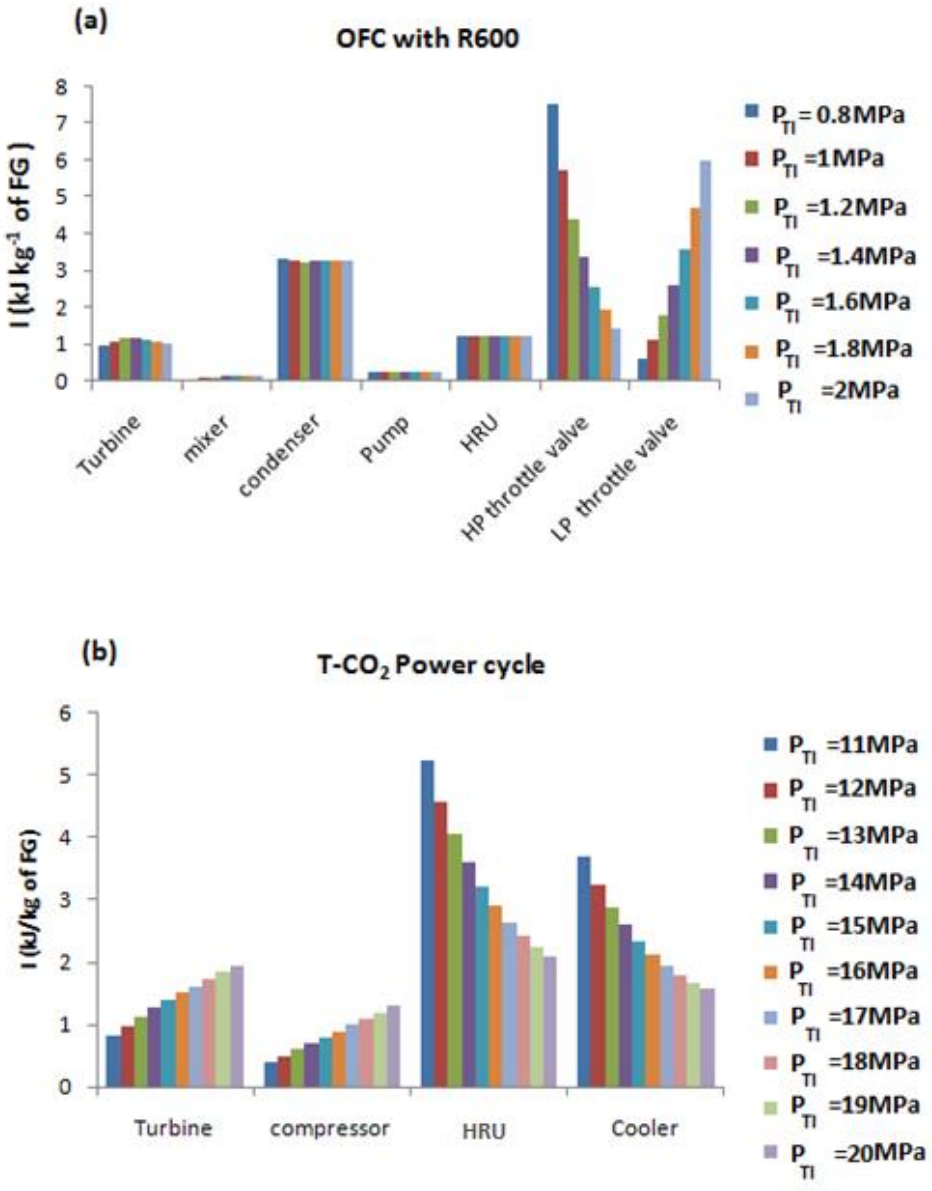

Fig. 4.5 (a): Variation of Component irreversibility of OFC with varying turbine inlet pressure. (b): Variation of Component irreversibility of T-CO2 power cycle with varying turbine inlet pressure.

It is observed from Fig. 4.6 (a) and 4.6 (b) that heat transfer area of the Heat Recovery units for unit power output is much higher for both OFCs compared to that of the T-CO_2 cycle when flue gas is allowed to cool to the lowest possible practical temperature. Corresponding value for the HRU of the T-CO_2 power cycle is significantly lower due to concave temperature profile of the supercritical CO_2 as shown in Fig. 4.7. It should be noted that the total heat transfer area of OFCs do not vary with turbine inlet pressure as HRU

operating condition is independent of the turbine inlet pressure. However, area of the HRU per unit power output becomes minimum at turbine inlet pressure corresponding to which work output per kg of flue gas is a maximum. On the other hand, total HRU area of T-CO_2 power cycle slowly increases with an increase of turbine inlet pressure as temperature profiles of CO_2 and flue gas come closer to each other. However, HRU area per unit power output shows a decreasing trend due to increment in work output with elevated turbine inlet pressure of the T-CO_2 power cycle.

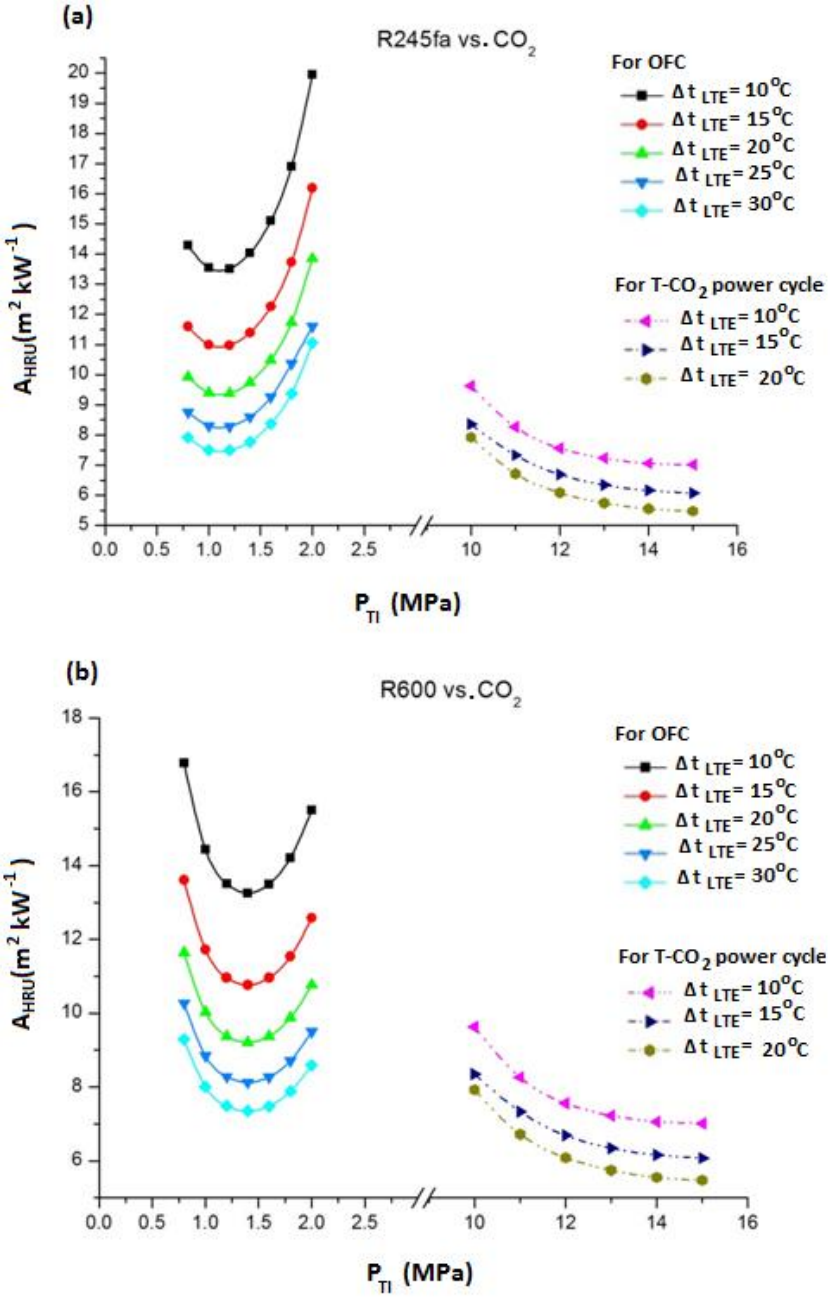

Fig. 4.6 (a): Comparison between HRU area per unit power output of OFC with R245fa and that of T-CO_2 power cycle (b): Comparison between HRU area per unit power output of OFC with R600 and that of T-CO_2 power cycle.

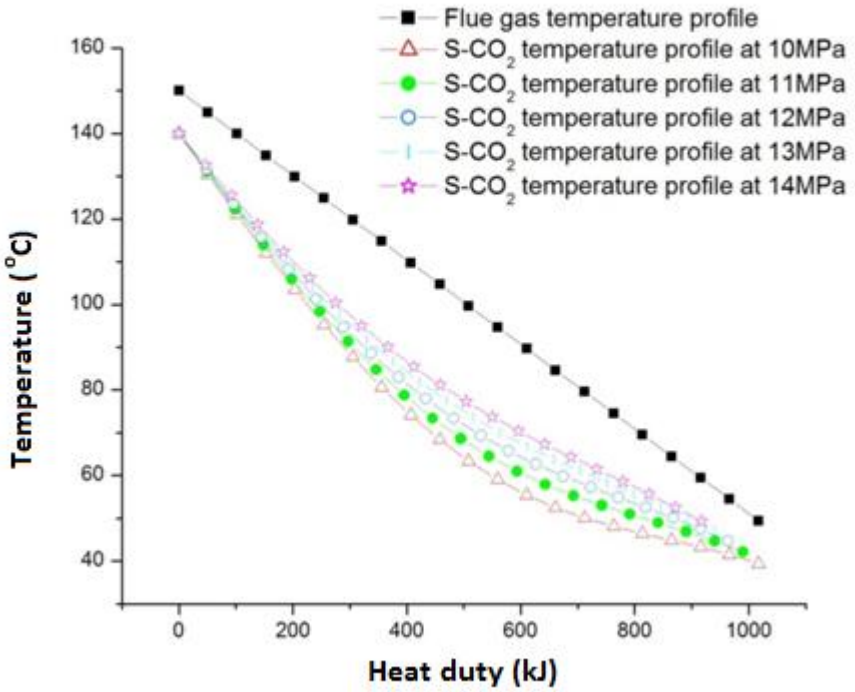

Fig. 4.7: T-Q diagram for T-CO_2 power cycle

In this situation, it is necessary to conduct economic analysis as HRU operating pressure (i.e. turbine inlet pressure) of the T-$_{CO2}$ power cycle corresponding to maximum work output per kg of flue gas and maximum 2nd law efficiency is much higher compared to HRU operating pressure of the OFCs. From Fig. 4.8 (a) and 4.8(b) it is clear that total bare module costs (BMCs) per unit power for OFCS are somewhat higher compared to that of the T-CO_2 power cycle when maximum possible heat is recovered from a given mass of the flue gas. It should be noted that though larger heat recovery area leads to higher BMCs of the HRU of the OFCs, total BMCs become competitive to that of T-CO_2 power cycle due to relatively lower BMCs of turbine and Pump of the OFCs. It is also observed in Table.4.2 that work outputs per kg of FG corresponding to these minimum BMCs per unit power output are almost equal for OFCs and T-CO_2 power cycle. It is observed from Fig. 4.8 (a) and 4.8(b) that total BMCs per unit power output can be appreciably reduced for both OFCs (using R245fa and R600 as working fluid respectively) by increasing terminal temperature difference at the low temperature end of the HRU. Though, corresponding improvement for the T-CO_2 power cycle is negligible due to rapid drop of work output for a given mass flow rate of the flue gas.

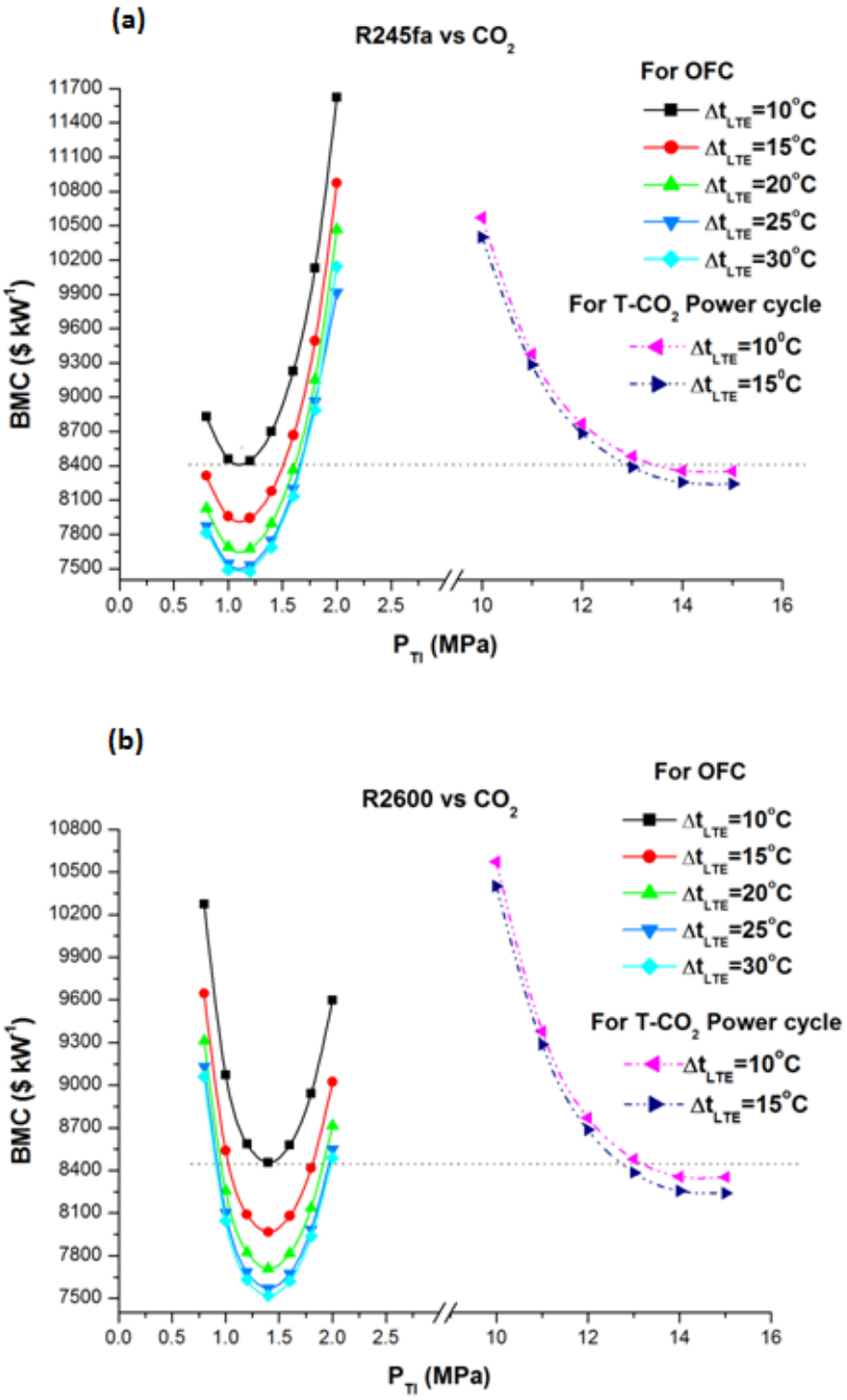

Fig. 4.8 (a): Comparison between BMC per unit power of OFC with R245fa and that of the T-CO_2 power cycle (b): Comparison between BMC per unit power of OFC with R600 and that of the T-CO_2 power cycle.

4.5. Chapter summary

In the present study, comparative thermodynamic as well as economic analyses are performed for OFCs and T-CO_2 power cycle while producing power utilizing low grade waste heat of a sulphur free flue gas. In this study, work output per kg of flue gas and the 2^{nd} law efficiency are considered as the performance parameters, as these provide better estimations of effectiveness of a heat recovery scheme.

It is observed that T-CO_2 power cycle can produce slightly higher work output per kg of flue gas as well as 2^{nd} law efficiency compared to that of OFCs using R245fa and R600 as working fluids if the flue gas is allowed to leave the heat recovery gas heater at the lowest possible practical temperature. With maximum possible cooling of flue gas, minimum possible BMC per unit power output of the T-CO_2 power cycle is somewhat lower compared to that of both OFCs. However, work outputs per kg of FG corresponding to these minimum BMCs are almost equal for all three cycles. BMCs per unit power for both OFCs can be reduced substantially by increasing terminal temperature difference at the low temperature end of the HRU. However, BMC per unit power output of T-CO_2 power cycle is less sensitive to this reduction in terminal temperature difference.

Finally, T-CO_2 power cycle is a better option if maximum work potential of flue gas is to be exploited with maximum safety and minimum environmental impact. OFCs can provide economically better solution if smaller work output per unit mass of flue gas is acceptable. However, R245fa may lead to some environmental impact due to its higher GWP and there is the chance of explosion with R600 OFC.

5. Ejector assisted organic flash cycle (OFC)

5.1 Objective of the work

Though OFC is preferred for low grade waste heat recovery due to the absence of pinch limitation in the HRU, unutilized energy of the fluid stream entering into the LP throttle valve is obviously a limitation of an OFC. In the present study, primary objective is to utilize this energy in an ejector to entrain the exiting working fluid from the turbine at a pressure which is lower than the operating pressure of the condenser. This improves turbine power output. Lowest possible operating pressure of the condenser will depend on ambient temperature. It should be noted that the condenser pressure is the saturation pressure corresponding to a temperature which is 15 to 20°C higher than the ambient temperature. The turbine exit pressure should be such that total working fluid exiting the diffuser of the ejector be at condenser pressure. Initially, waste heat of SO_2 free flue gas available at 150°C is utilized to run the cycle. The scheme is demonstrated by using butane (i.e. R600) as the working fluid as ODP and GWP of butane are zero and close to 20 respectively. However, at the later stage of the study, the maximum achievable first law efficiency and work output for each of the cycles are evaluated and presented using four different working fluids (i.e. Butane, Isopentane, R245fa and R245ca). It should be noted that all selected working fluids are dry working fluids with zero ODP and GWP<1050.

5.2. System description

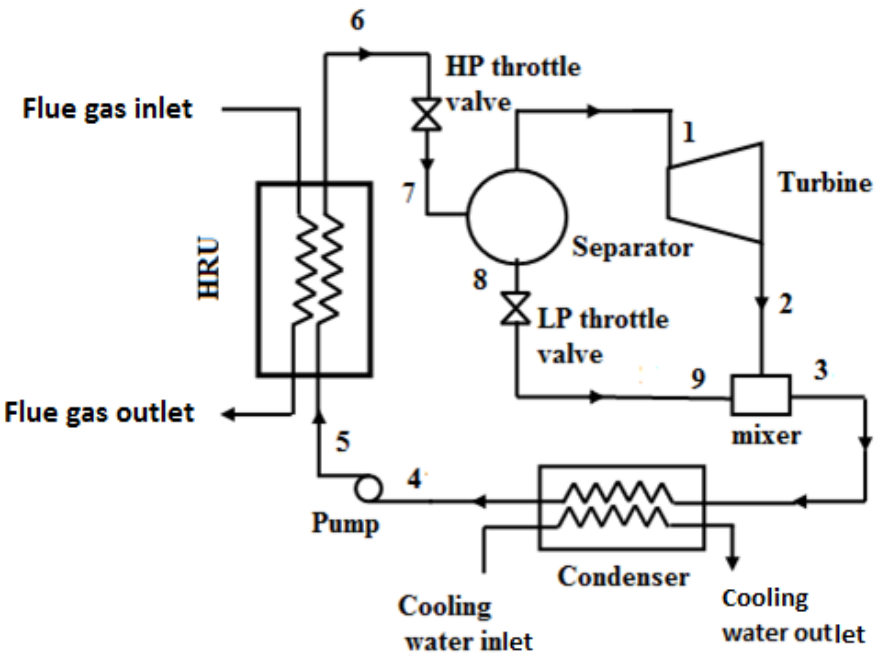

Fig. 5.1 (a): Layout of a basic OFC

(b)

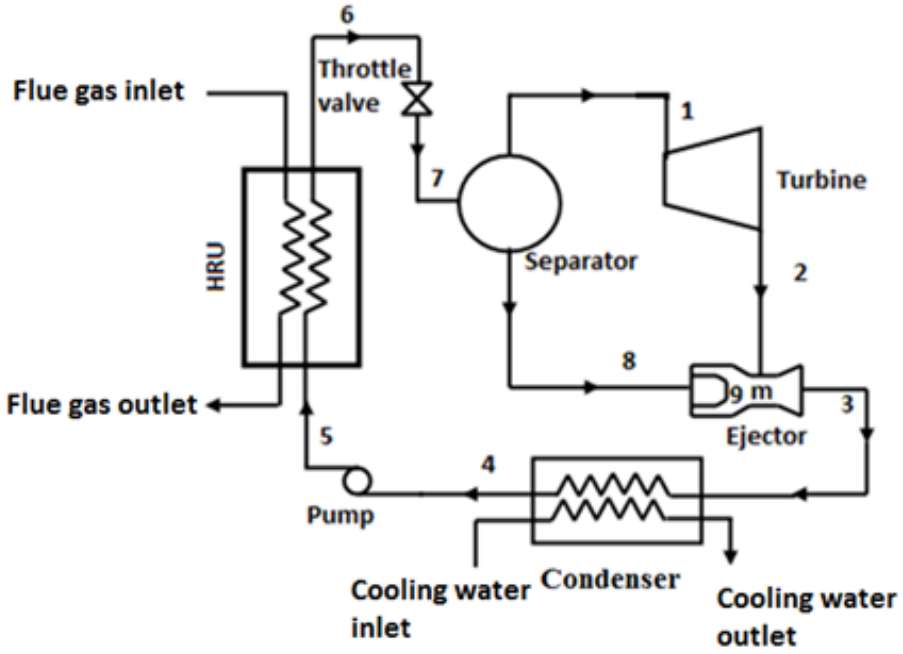

(c)

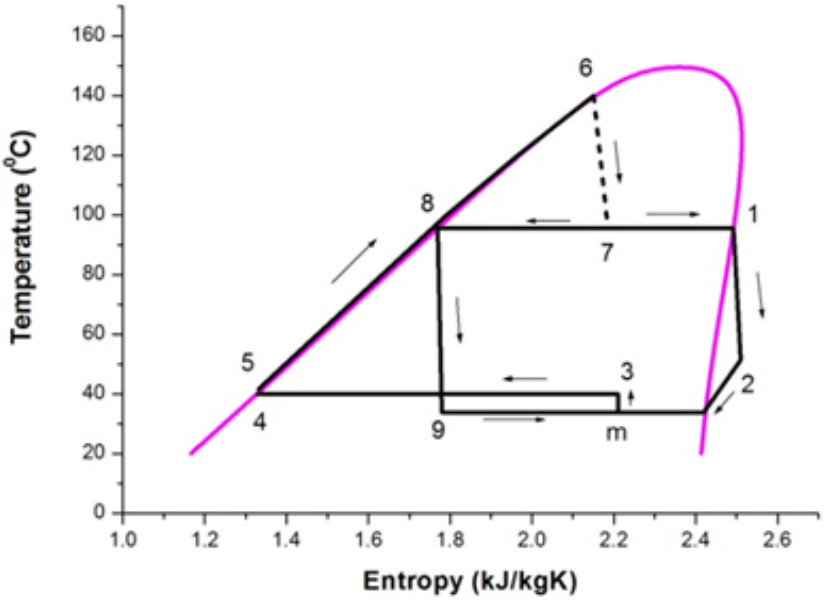

Fig. 5.1 (b): Layout of an OFC with ejector. (c): Temperature-entropy diagram of the OFC with ejector

The layout of an OFC is shown in Fig. 5.1(a). In this OFC, saturated liquid stream exiting the vapour separator (at state-8) is throttled to condenser pressure (i.e. state-9) and allowed to mix with the exhaust stream coming out from the turbine (at state-2).

In the present study, the basic OFC is modified by replacing its low pressure throttle valve with an ejector as shown in Fig. 5.1(b). T-s diagram of this modified OFC with the ejector is presented in Fig. 5.1(c). The fluid stream coming out of the HRU at saturated liquid state (i.e. state-6) after undergoing a throttling process (6-7) enters into the vapour separator. Dry saturated vapour exiting the vapour separator (at state-1) enters into the turbine and expands up to a pressure (i.e. state-2) which is lower than the operating pressure of the condenser. The saturated liquid mass leaving the vapour separator (at state-8) enters into the ejector as the primary flow to entrain the fluid mass exiting the turbine (at state-2). The turbine exit pressure is such that the mass of the working fluid at the exit of the diffuser is at the condenser pressure (i.e. state-3). After undergoing a condensation process (i.e. process 3-4) total mass of the working fluid is pressurized to HRU pressure (i.e. state-5) and finally heated to a saturated liquid state (i.e. state-6) by using waste heat of SO_2 free flue gas.

5.3. Mathematical modelling

Fluid properties at different state points are estimated using REFPROP7 (Lemmon et al. 2002). The model is developed based on following assumptions:

I. Steady flow operating condition is applicable for each of the equipments.
II. Flue gas is free from SO_2.
III. Turbine and pump isentropic efficiencies are assumed to be 90% and 85% respectively.
IV. Initially, the performance of the OFC with ejector is evaluated assuming nozzle and diffuser efficiencies as 85% each and the mixer efficiency is 95% (Yu and Li 2007, Erosy et al. 2007). However, at the end of the result and discussion, effects of varying ejector component efficiencies on first law efficiency of the ejector assisted OFC are presented.
V. The mixing pressure in the ejector should be lower than the secondary flow to entrain the secondary mass (Chen et al. 2014). Initially, for the simplicity of calculation, it is assumed that the pressure at the mixing

section is the same as that of the secondary flow (Bai et al. 2015a, Yu et al. 2013, Bai and Yu 2015, Bai et al. 2015b, Yu et al. 2007). However, effects of the varying pressure drop (say ΔP) in the suction nozzle are presented in section 5.4.2.

VI. For the analysis of the mixing section the homogeneous equilibrium model of two-phase flow is considered (Kornhauser 1990). This implies properties and velocities of working fluids are remaining constant except during the mixing process and at all time they are in thermodynamic quasi equilibrium.

VII. Velocity of secondary flow is assumed to be negligible compared to that of the primary flow (Yu et al. 2007).

VIII. The velocities at the inlet and outlet of the ejector are negligible.

IX. Extraneous heat loss is negligible except outflow of the flue gas.

Mathematical modelling may be divided into two parts – ejector modelling and thermodynamic modelling

5.3.1 Ejector modelling

The objective of ejector modelling in this study is to estimate the turbine exit pressure for the ejector assisted OFC (refer to Fig. 5.1(b) and 5.1(c)). Based on one-dimensional constant pressure mixing model, proposed by Kenan et al. (1950) ejector modelling is conducted as follows:

As working fluid mass exiting the turbine is entrained as the secondary flow of the ejector, entrainment ratio of ejector can be calculated by Eqn-5.1 as follows:

$$\mu = \frac{x}{1-x} \tag{5.1}$$

In Eqn-5.1, x represents quality of the working fluid at the exit of the throttle valve.
With an assumed value of turbine exit pressure velocities at nozzle exit is determined using Eqn-5.2.

$$u_9 = \sqrt{2\eta_N(h_8 - h_{9s})1000} \tag{5.2}$$

By neglecting the velocity of secondary flow momentum conservation equation can be presented as

$$(1-x)u_9 = u_{mi} \tag{5.3}$$

Now the-average velocity of mixed flow is

$$u_m = \frac{u_9\sqrt{\eta_m}}{1+\mu} \tag{5.4}$$

In above equation η_m is the mixing efficiency that includes frictional losses in mixing section. The expression of this mixing efficiency is presented below (Yu et al. 2007).

$$\eta_m = \frac{u_m^2}{u_{mi}^2} \tag{5.5}$$

Enthalpy after the mixing is estimated as follows.

$$h_m = \frac{h_8 + \mu h_2}{1+\mu} - \frac{u_m^2}{2000} \tag{5.6}$$

Entropy after mixing can be obtained as a function of the mixing section pressure andh_m, i.e.:

$$s_m = f(P_m, h_m) \tag{5.7}$$

Enthalpy at the exit of the diffuser is:

$$h_3 = h_m + \frac{u_m^2}{2000} \tag{5.8}$$

If the diffuser is an isentropic device then enthalpy at the exit of the diffuser will be

$$h_{3s} = h_m + \eta_D(h_3 - h_m) \tag{5.9}$$

Now, entropy can be estimated as a function of condenser pressure and h_{3s} , i.e.:

$$s_{3s} = f(P_C, h_{3s}) \tag{5.10}$$

When $s_{3s} = s_{m,}$, the initially assumed turbine exit pressure represents the final turbine exit pressure. Otherwise assumed value of turbine exit pressure is to be modified through iteration as shown in Fig. 5.2.

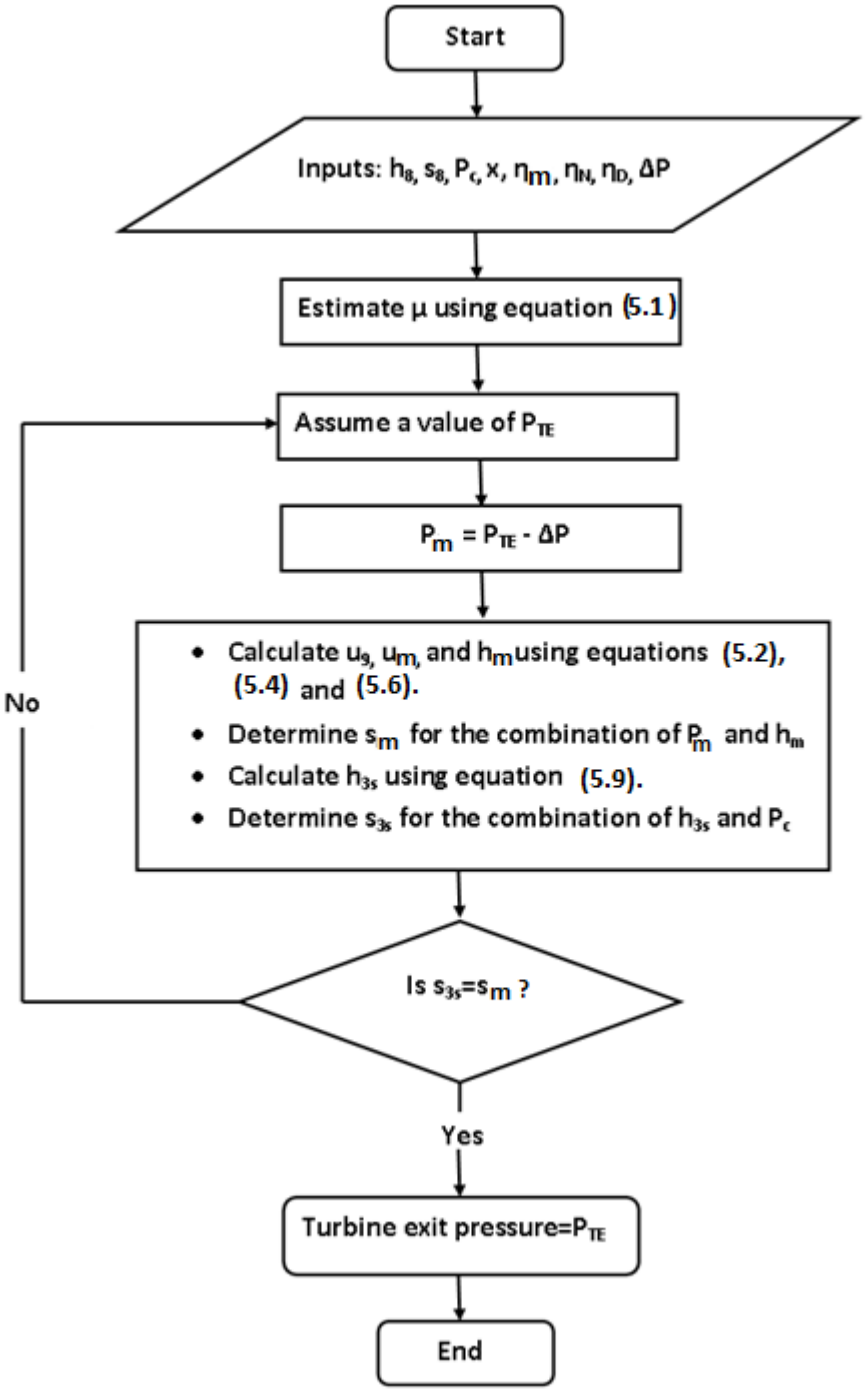

Fig. 5.2: Flow chart for turbine exit pressure estimation

5.3.2 Thermodynamic modelling

Mass of butane is heated by the waste heat of the flue gas (of one kg). This mass is estimated from energy balance of the HRU as shown in Eqn-5.11 (refer to Fig. 5.1(a), 5.1(b) and (c)).

$$m_f = \frac{c_{Pg}(T_{gi} - T_{go})}{(h_6 - h_5)} \qquad (5.11)$$

Cycle power output per unit mass of flue gas is

$$W_{NET} = W_T - W_P \tag{5.12}$$

Where W_T and W_P represent turbine work output and pump work input per unit mass of flue gas. These are as expressed in equations (5.13) and (5.14) respectively.

$$W_T = m_f x\,(h_1 - h_2) \tag{5.13}$$

$$W_P = m_f(h_5 - h_4) \tag{5.14}$$

It should be noted that h_2 for OFC with ejector is smaller compared to h_2 for OFC without ejector as turbine exit pressure of the OFC with ejector is less than the condenser pressure as shown in the T-s diagram of Fig. 5.1(c).

Now first law efficiency is expressed as

$$\eta_I = \frac{x\,(h_1 - h_2) - (h_5 - h_4)}{(h_6 - h_5)} \tag{5.15}$$

It is observed from Fig. 5.1(a) and 5.1(b) that operating conditions of the HP throttle valve and the HRU of the basic OFC remain unaffected after the insertion of the ejector into the system. Irreversibilities in the HP throttle valve (throttle valve in case of the ejector assisted cycle) and the HRU can be estimated using equation (5.16) and (5.17) respectively.

$$I_{HPTV} = m_f T_0(s_7 - s_6) \tag{5.16}$$

$$I_{HRU} = c_{Pg} T_0 \ln\left(\frac{T_{go}}{T_{gi}}\right) + m_f T_0(s_6 - s_5) \tag{5.17}$$

Inlet and outlet states of the turbine, condenser and pump for the OFC with ejector as well as those for the OFC without ejector are represented by identical numbers (i.e. 1 and 2 for the turbine, 4 and 5 for the pump, 3 and 4 for the condenser) as shown in Fig. 5.1(a) and 5.1(b). Hence, irreversibilities of these components for both of the cycles are presented generically by following equations:

$$I_T = m_f\, x\, T_0(s_2 - s_1) \quad (5.18)$$

$$I_P = m_f T_0(s_5 - s_4) \quad (5.19)$$

$$I_C = m_f T_0(s_4 - s_3) + m_w T_0(s_{wo-} s_{wi}) \quad (5.20)$$

Now irreversibilities of LP throttle valve and mixer of the basic OFC (refer to Fig. 5.1(a)) are as follows:

$$I_{LPTV} = m_f T_0(s_9 - s_8) \quad (5.21)$$

$$I_M = m_f T_0\{s_3 - xs_2 - (1-x)s_9\} \quad (5.22)$$

Irreversibility of the ejector (refer to Fig. 5.1(b)) is estimated by Eqn-5.23

$$I_{Ej} = m_f T_0\{s_3 - xs_2 - (1-x)s_8\} \quad (5.23)$$

Waste heat recovery increases with greater surface area of heat transfer and hence with increased capital cost. Effective utilization of this waste heat recovery is measured by the net work output. As a result, a compromise between better effectiveness of utilization of waste heat and required cost has to be made. For this purpose, a parameter 'area utilization temperature indicator (AUTI) is defined as

$$AUTI = \frac{W_{NET}}{UA} \quad (5.24)$$

AUTI is having a dimension of temperature and it indicates relative effect of utilization of available waste heat through its recovery and conversion to work against heat recovery unit area, representing capital cost.

5.4. Results and discussion

In the present study for specified flue gas inlet temperature, the temperature of the working fluid exiting the HRU is a fixed quantity as working fluid is heated close to the flue gas inlet temperature. 10°C pinch is assumed in the HRU. In this situation, the flash pressure is the parameter whose variation will have a significant effect on the cycle performance. Flash pressure is the pressure at which dry saturated vapour gets separated from the saturated liquid after the high pressure throttling process and it enters into the turbine.

Effects of varying flash pressure and terminal temperature difference in the low temperature end of the HRU on the performance of a low grade waste heat driven OFC with ejector are discussed in this section. These are studied considering a basic OFC as the baseline cycle. Initially, results are presented using butane as the working fluid and flue gas inlet temperature as 150°C. Cycle performances in terms of first law efficiency and work output per unit mass of flue gas are also compared for four different working fluids having zero ODP and GWP less than 1050.Then effects of varying flue gas temperature on cycle work output are also presented. Finally, a sensitivity analysis is conducted for varying ejector component efficiencies and varying differential pressure between the secondary flow inlet and the mixing section.

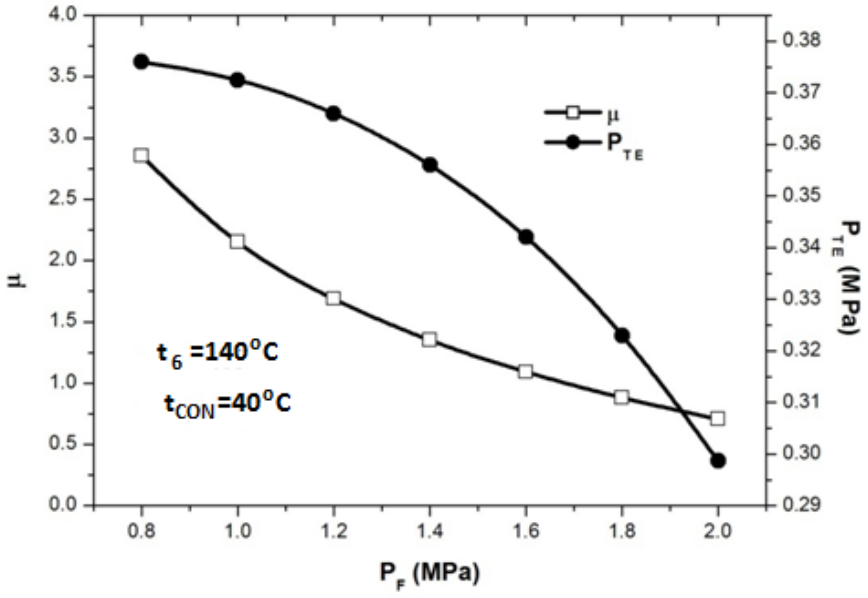

Fig. 5.3: Effects of varying flash pressure on entrainment ratio and turbine exit pressure.

5.4.1 Discussion with fixed values of ejector component efficiencies and negligible pressure drop in suction nozzle:

Effects of varying flash pressure(P_F) on ejector entrainment ratio (μ) and turbine exit pressure (P_{TE}) of the OFC with ejector are demonstrated in Fig. 5.3. It is observed from Fig. 5.3 that the ejector entrainment ratio decreases with increasing flash pressure. It is due to the degrading vapour quality (x) of working fluid at the exit of the HP throttle valve. As mass of working fluid to be entrained in the ejector gradually decreases with an increase in flash pressure, smaller turbine exit pressure is ensured by increasing the flash pressure.

Due to the smaller turbine exit pressure, specific enthalpy change of the working fluid in the turbine is more for the OFC with ejector compared to that of the basic OFC as shown in the P-h diagrams of Fig. 5.4. This results in increasing turbine power output for the OFC with ejector. For a better understanding of this fact, specific turbine power outputs along with thermodynamic properties corresponding to relevant state points of the OFC as well as the OFC with ejector are listed in table 5.1.

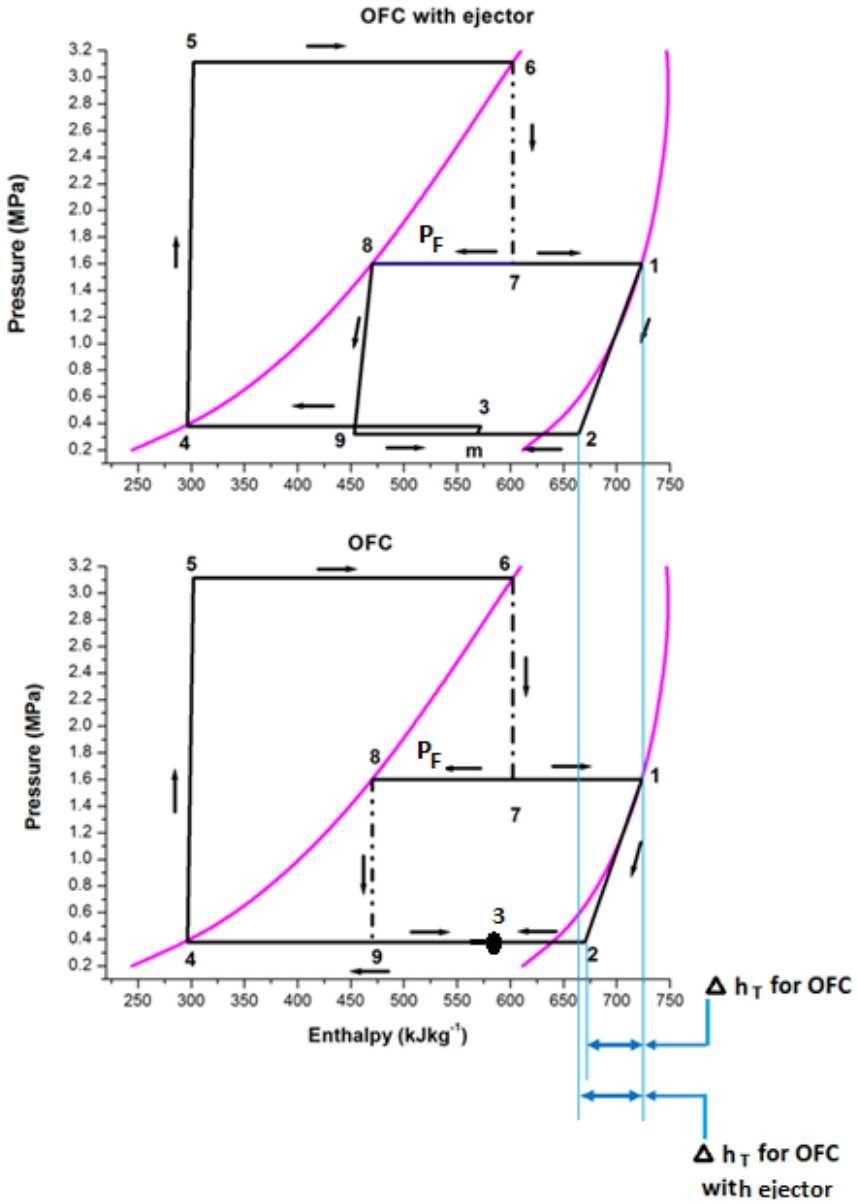

Fig. 5.4: P-h diagrams for the OFC and OFC with ejector

Table 5.1: comparison of specific turbine work outputs and relevant state points of the OFC and the OFC with ejector

For Butane									
T_6 (K)	P_F (MPa)	x	h1 (kJ kg^{-1})	OFC			OFC with ejector		
				P_{TE} (MPa)	h2 (kJ kg^{-1})	w_T (kJ kg^{-1})	P_{TE} (MPa)	h2 (kJ kg^{-1})	w_T (kJ kg^{-1})
140	1.2	0.628	706.55	0.379	663.638	26.949	0.366	662.324	27.774
	1.4	0.575	715.79	0.379	667.064	28.017	0.356	664.697	29.378
	1.6	0.522	723.63	0.379	669.918	28.038	0.342	666.012	30.077
	1.8	0.469	730.28	0.379	672.248	27.217	0.323	666.155	30.075
	2	0.414	735.85	0.379	674.038	25.590	0.299	664.939	29.357

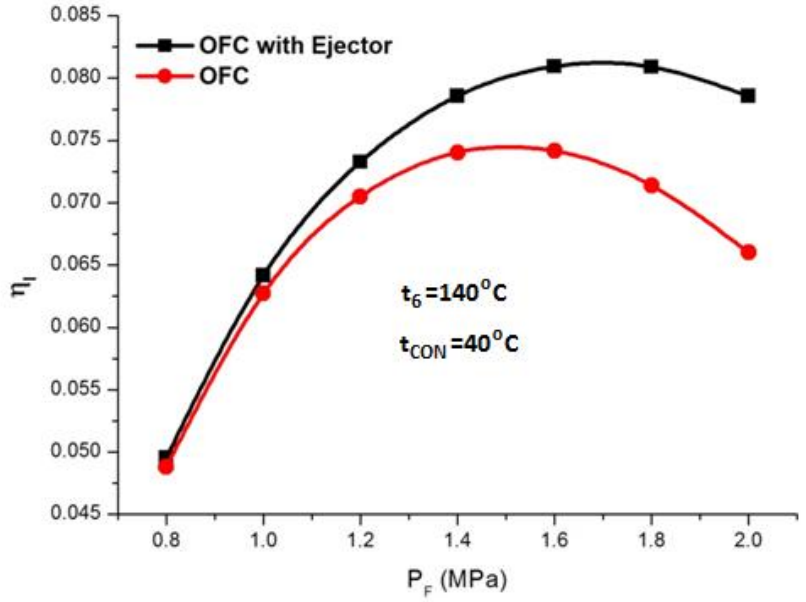

Fig. 5.5: Effects of varying flash pressure on 1st law efficiency

As the presence of the ejector results in higher turbine power output by reducing the turbine exit pressure, the OFC with ejector yields higher 1st law efficiency (η_I) compared to the baseline OFC as shown in Fig. 5.5. Though improvement of the 1st law efficiency achieved by introducing an ejector in an OFC configuration is insignificant at lower flash pressure, noticeable improvement is observed as flash pressure becomes more than 1.2 MPa.

It is further noted from Fig. 5.5 that for OFC with ejector as well as for basic OFC there exist optimum flash pressures corresponding to their maximum 1st law efficiencies. For each of the cycles, with an increment in flash pressure, mass flow rate of working fluid entering into the turbine decreases due to degrading vapour quality. However, this ensures a

larger drop in specific enthalpy during expansion of working fluid in the turbine. These two counteracting phenomena result in an optimum flash pressure corresponding to the maximum first law efficiency for each of the cycles.

As for the OFC with ejector, turbine exit pressure reduces with an increment in flash pressure; incremental change in specific enthalpy of working fluid during expansion in the turbine dominates the trend of 1st law efficiency even when flash pressure is higher compared to the optimum flash pressure of the cycle without ejector. Thus, the optimum flash pressure corresponding to the maximum 1st law efficiency of the cycle with ejector is higher compared to that of the cycle without ejector.

Work output per unit mass of flue gas is a measure of effective waste heat utilization if flue gas does not contain SO_2. Effects of varying flash pressure on work output per unit mass of flue gas for each of the cycles are presented in Fig. 5.6 assuming flue gas inlet temperature as 150°C. For specified terminal temperature difference at the low-temperature end of the HRU, these variations are similar to the variations of first law efficiencies.

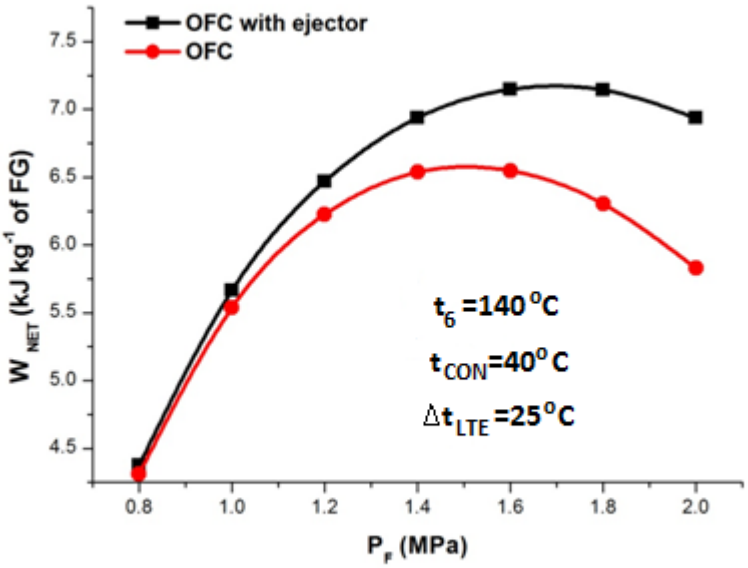

Fig. 5.6: Effects of varying flash pressure on work output per unit mass of flue gas

It is further observed in Fig. 5.7 (a) that difference between maximum possible work output per unit mass of flue gas (W_{NETMAX}) for the cycle with ejector and that of the cycle without ejector gradually increases as terminal temperature difference at the low-temperature end of the HRU (Δt_{LTE}) reduces. However, the reduction of terminal temperature difference at the low-temperature end of the HRU results in a reduced value of AUTI as shown in Fig. 5.7 (b).

This is an indication that larger sized HRU is required to produce unit power output if the flue gas is cooled to lower temperature. It should be noted that for a similar operating condition, OFC with ejector will have higher value of AUTI.

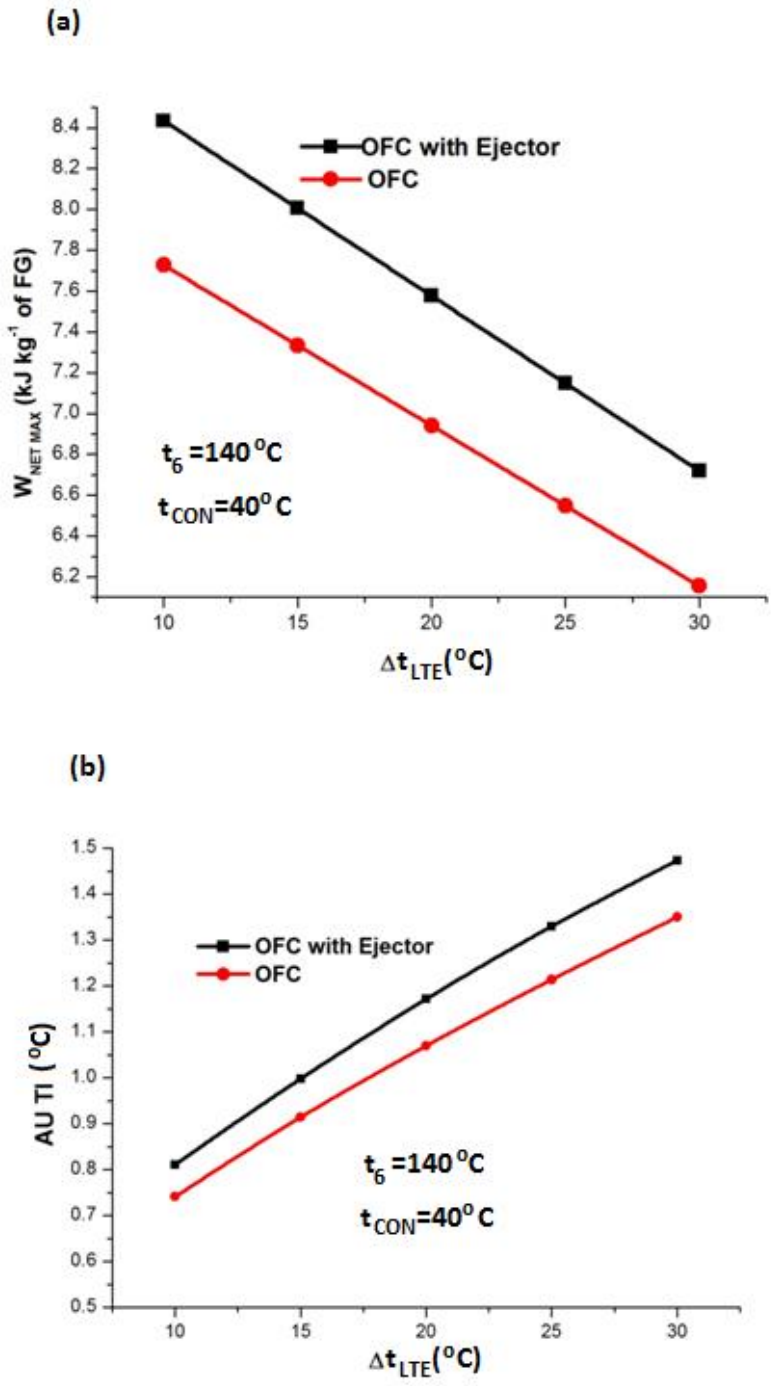

Fig. 5.7 (a): Maximum possible work output per unit mass of FG vs. terminal temperature difference at the low temperature end of the HRU. (b): AUTI vs. terminal temperature difference at the low temperature end of the HRU.

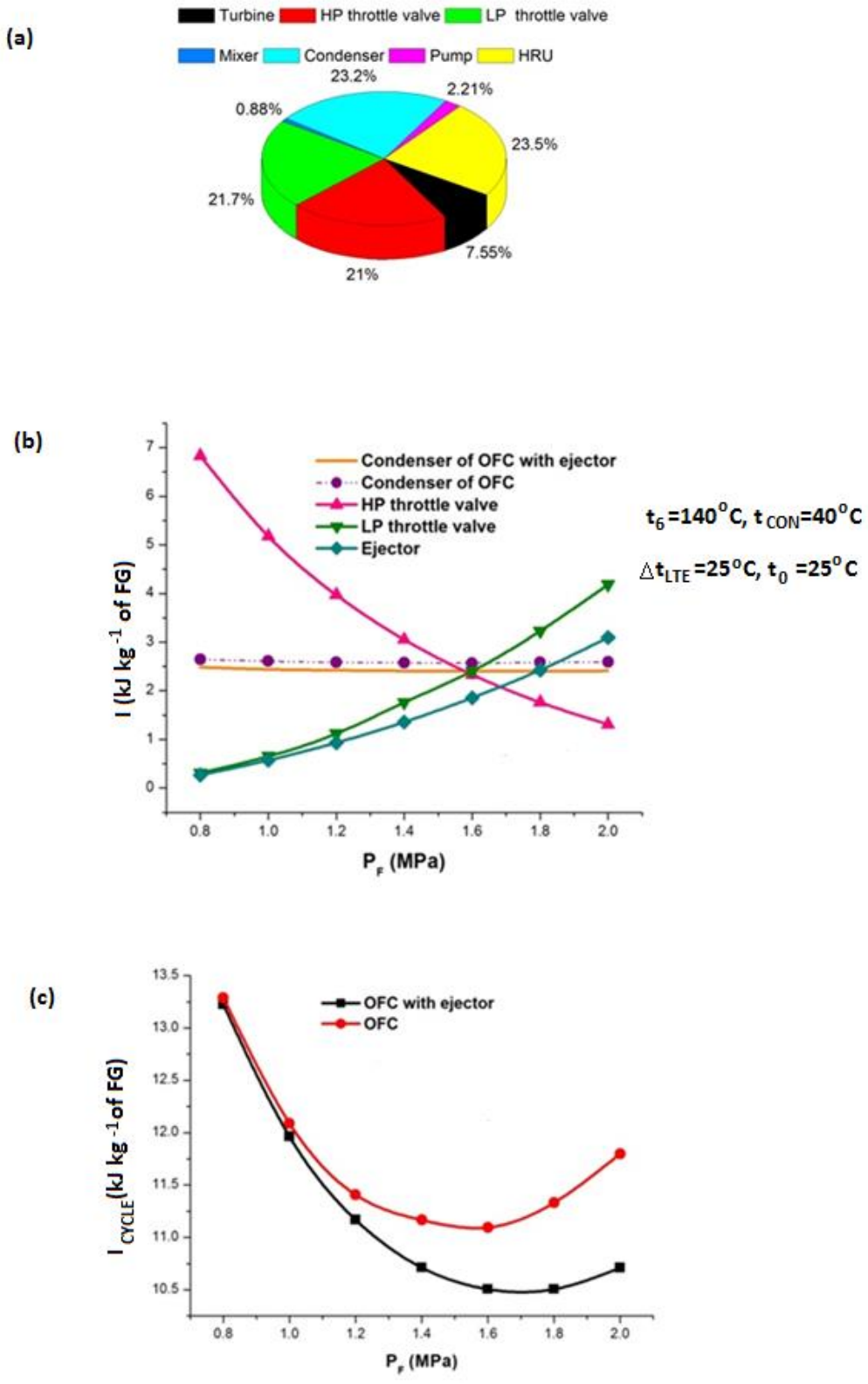

Fig. 5.8 (a): Component wise irreversibility distribution for the OFC. (b): Effects of varying flash pressure on irreversibilities of major components. (c): Effects of varying flash pressure on cycle irreversibility.

Irreversibility in each major component is estimated as shown in Fig. 5.8 (a). It is observed in Fig. 5.8(a) that the HRU, HP throttle valve, LP throttle valve and condenser are the major

contributors to cycle irreversibility of an OFC. Incorporation of an ejector in an OFC layout does not affect the operating condition of the HRU and HP throttle valve. In this situation effects of varying flash pressure on irreversibilities of LP throttle valve, ejector and condenser should be discussed.

It is observed in Fig. 5.8 (b) that irreversibility of the condenser of an OFC slightly reduces after the incorporation of an ejector into the system. It is further observed in Fig. 5.8 (b) that irreversibilities associated with the LP throttle valve as well as the ejector increase with an increase in flash pressure. However, as with an increment in flash pressure irreversibility of the ejector increases at a slower rate compared to that of the LP throttle valve, irreversibility of the ejector becomes comparatively smaller above certain flash pressure. Thus, above a certain flash pressure, a significant reduction in cycle irreversibility can be achieved by replacing the LP throttle valve of the OFC by an ejector as presented in Fig. 5.8 (c).

It is also observed in Fig. 5.8 (c) that for both of the cycles there are optimum flash pressures corresponding to minimum cycle irreversibilities. Counteracting effects of flash pressure variation on irreversibilities of HP and LP throttle valve result in optimum flash pressure corresponding to minimum cycle irreversibility of the OFC. After the incorporation of an ejector in the system, the optimum flash pressure corresponding to minimum cycle irreversibility occurs due to counteracting effects of flash pressure variations on irreversibility variations of the throttle valve and the ejector.

Table 5.2: Performance summary of the OFC and OFC with ejector with different working fluids

Working Fluid	t_{Cr} (°C)	ODP	GWP in 100 years	ASHRAE Safety category	t_{gi}=150°C, t_6 =140°C, t_{CON} =40°C Δt_{LTE} =25°C					
					OFC			OFC with ejector		
					P_F (MPa)	η_{IMax}	$W_{NET\ Max}$ (kJ kg^{-1} of FG)	P_F (MPa)	η_{IMax}	$W_{NET\ Max}$ (kJ kg^{-1} of FG)
Butane	152.98	0	20	A3	1.52	0.074	6.54	1.70	0.081	7.16
Isopentane	187.20	0	20	A3	0.66	0.073	6.53	0.73	0.080	7.16
R245fa	154.05	0	1030	B1	1.25	0.075	6.67	1.41	0.082	7.29
R245ca	174.42	0	726	-	0.88	0.073	6.52	0.96	0.080	7.15

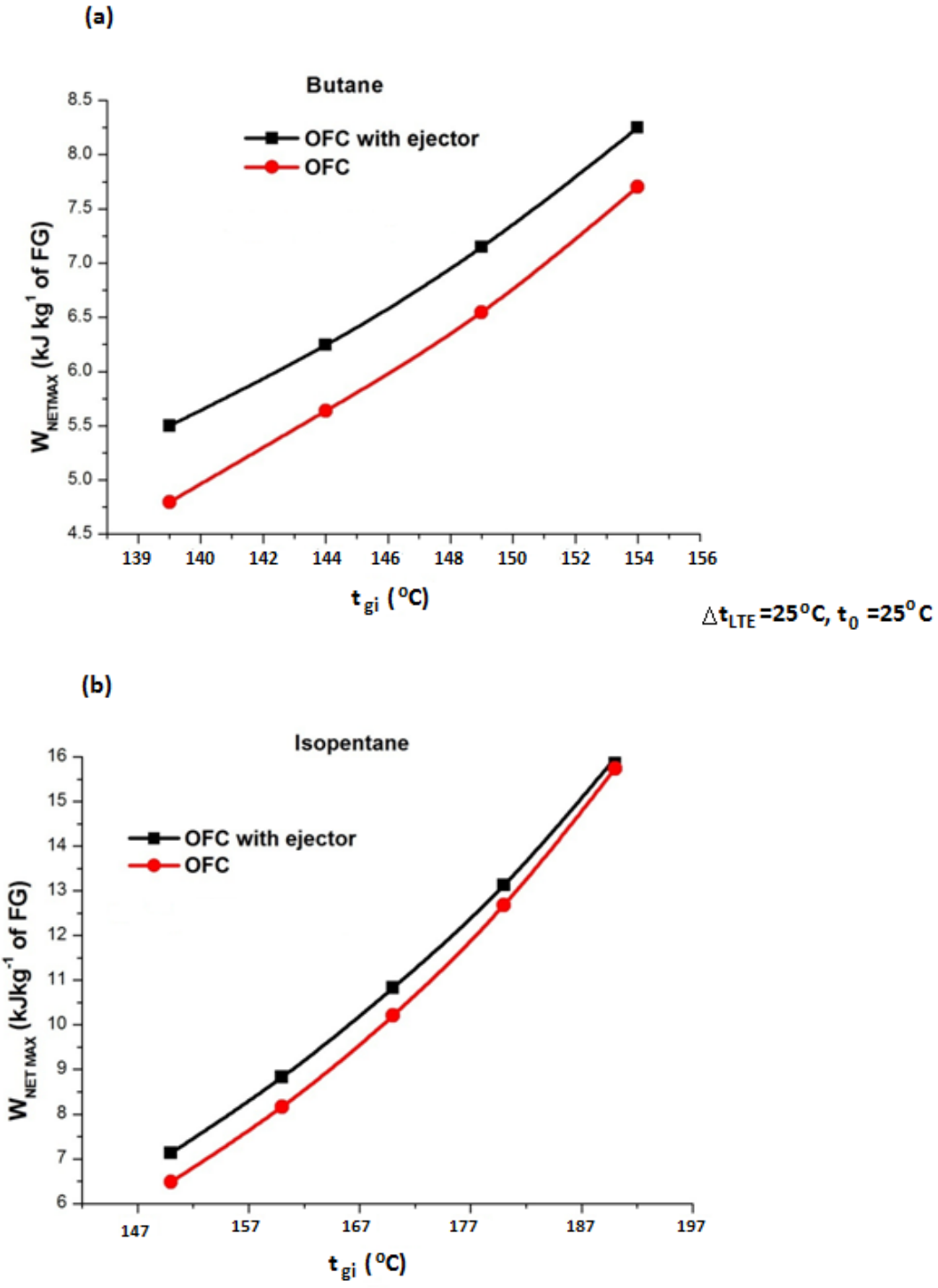

Fig. 5.9 (a): Effects of varying flue gas inlet temperature on work output per unit mass of FG with Butane. (b): Effects of varying flue gas inlet temperature on work output per unit mass of FG with Isopentane.

Performance of any thermodynamic cycle is greatly influenced by the selection of working fluids (Uusitalo et al. 2018, Bao and Zhao 2013, Besagni et al. 2015). In the table-5.2 comparative performance of the OFC and OFC with ejector using four different working fluids are presented. All selected working fluids are having zero ODP and GWP less than 1050 in 100years as shown in table-2. It is observed in table-5.2 that for all of the selected working fluids, OFCs with ejector yield higher first law efficiencies and work outputs per unit mass of flue gas compared to those of the basic OFC. It is also observed in table-5.2, that slightly higher first law efficiency and work output can be achieved by using R245fa compared to remaining three working fluids.

Effects of varying flue gas inlet temperature on maximum achievable work output per unit mass of flue gas are presented in Figs 5.9 (a) and 5.9 (b). In Fig. 5.9 (a), butane is the working fluid and flue gas temperature is varied from 140°C to 155°C. In Fig. 5.9 (b) Isopentane is the working fluid and flue gas temperature is varied from 150°C to 190°C. Working fluid exit temperature from the HRU (i.e. t_6) is kept 10°C below the flue gas inlet temperature for both cases. In fig 5.9 (a) and 5.9 (b) it is observed that improvement achieved in work output by the incorporation of an ejector into an OFC layout becomes less significant as working fluid exit temperature from the HRU comes closer to the critical temperature of working fluid. This is due to the higher entrained mass of secondary flow resulted from improved vapour quality in the separator exit with an exit temperature of the working fluid from the HRU closer to the critical temperature.

5. 4. 2 Sensitivity analysis for varying ejector component efficiencies and pressure drop in the suction nozzle:

Though in the previous section results are presented with constant values of ejector component efficiencies, it is necessary to conduct a sensitivity analysis of varying ejector component efficiencies on cycle performance as ejector component efficiencies would affect cycle performance appreciably (Besagni et al. 2015, Besagni et al. 2017). Ejector efficiency also varies appreciably with variation of operating conditions and ejector geometries (Liu and Groll 2013, Zheng and Deng 2017). Effects of varying ejector component efficiencies on cycle performance are discussed in this section considering butane as the working fluid.

Effects of variation of the efficiency of either the nozzle or the diffuser on the first law efficiency are presented in Fig. 5.10 (a). While describing the effects of varying any one of the ejector component efficiency, efficiencies of remaining ejector components are

assumed to have theoretically maximum values (i.e. 100%). It is observed that cycle first law efficiency reduces sharply as the efficiency of either the nozzle or the diffuser deviates from this maximum value. Cycle first law efficiency is sensitive to the efficiency variation of both diffuser and nozzle though it is slightly more sensitive for diffuser.

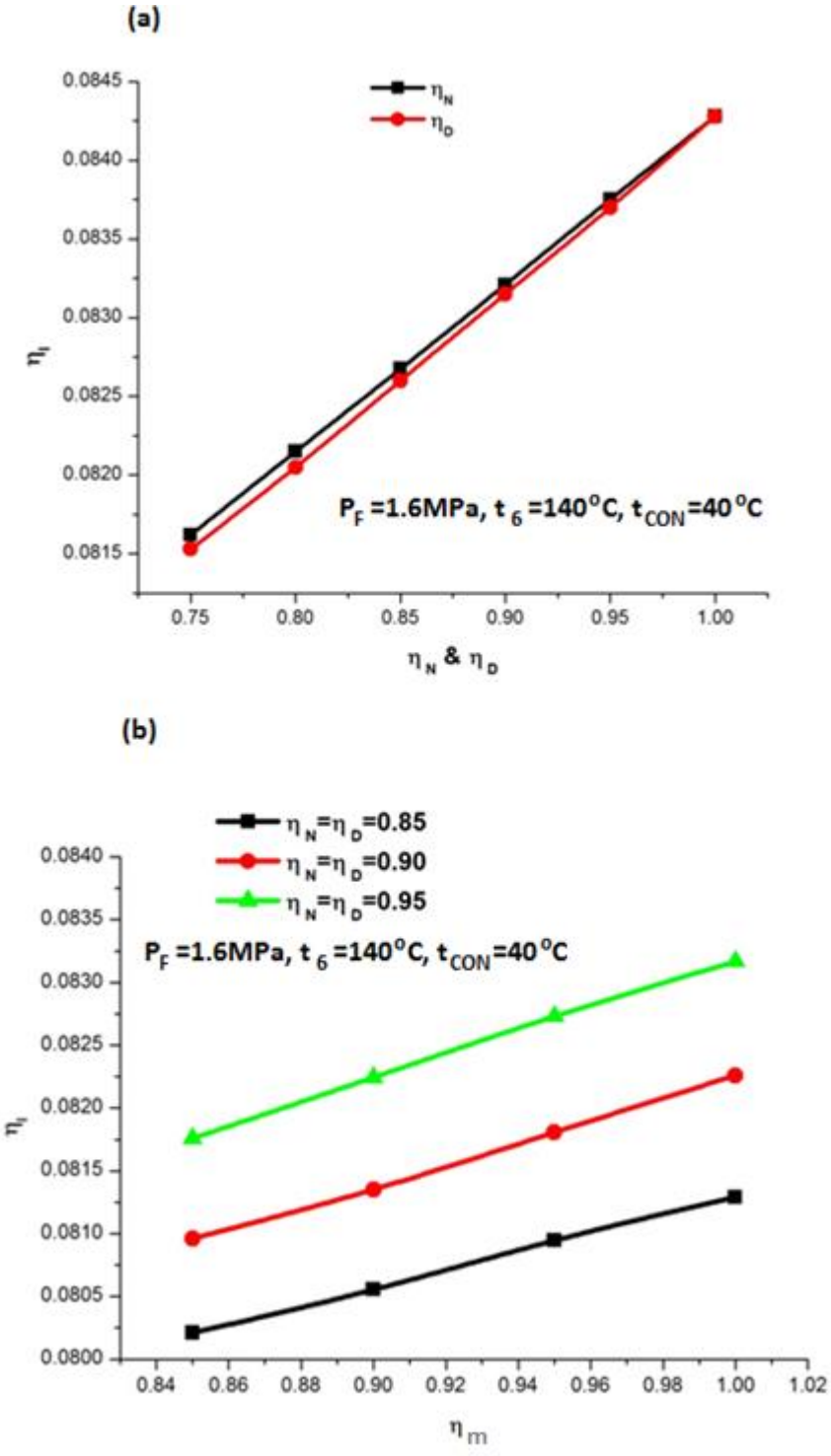

Fig. 5.10 (a): Effects of varying nozzle or diffuser efficiency on first law efficiency of the OFC with ejector. (b): Effects of mixing efficiency on first lay efficiency of the OFC with ejector

Effects of varying mixing efficiency on first law efficiency of the OFC with ejector for three different combinations of nozzle and diffuser efficiencies are shown in Fig. 5.10 (b). It is observed that first law efficiency variation is less sensitive to varying mixing efficiency compared to the varying nozzle and diffuser efficiency. For the nozzle and the diffuser efficiencies of 85%, first law efficiency increases from 8.02% to 8.13% as mixing efficiency is enhanced from 85% to100%. For 95% nozzle and diffuser efficiencies, as mixing efficiency is varied from 85% to 100%, first law efficiency is enhanced from 8.18% to 8.32%.

It is observed in Fig. 5.11 that the achievable turbine exit pressure gradually increases as larger pressure drop is considered in the suction nozzle. For any specified flash pressure, entrainment ratio is a fixed quantity for this study. Condenser pressure (i.e. diffuser exit pressure) is also constant as heat rejection always occurs at 40°C. In this situation turbine exit pressure (i.e. inlet pressure of the suction nozzle also) is expected to increase if there is a pressure drop in the suction nozzle. The higher turbine exit pressure leads to a lower turbine power output and first law efficiency. Thus during the designing of ejector, effort should be made to keep the pressure drop in the suction nozzle as minimum as possible.

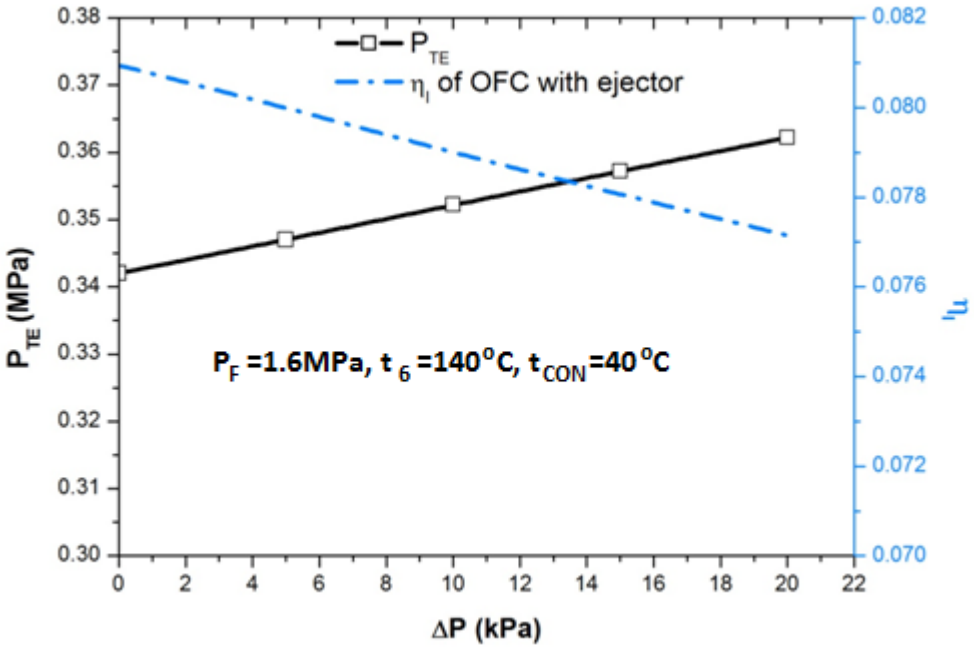

Fig. 5.11: Effects of varying pressure drop in suction nozzle on turbine exit pressure and First law efficiency.

5.5. Chapter summary

Due to the absence of pinch limitation in the HRU, an OFC is preferred for waste heat recovery from SO_2 free flue gas. However, this advantage is counteracted by the presence of two throttling process. In the present study, the LP throttle valve is replaced by an ejector. This ensures the expansion of the working fluid in the turbine to a pressure which is lower than the condenser pressure. The scheme is demonstrated initially by using butane as the working fluid irrespective of its high flammability as the use of HFCs are to be phased out by the year 2047. However, analysis is extended using four different working fluids. The major findings of this study can be summarised as follows:

- An OFC with ejector can produce higher first law efficiency and work output per unit mass of flue gas compared to a basic OFC, especially at higher flash pressure. An ejector based system is relatively more advantageous if temperature of exiting working fluid from the HRU is lower compared to the critical temperature of the working fluid.
- Smaller AUTI means larger HRU will be required for producing unit power output from the given mass of the flue gas. An OFC with Ejector is having a higher value of AUTI than that of the OFC without ejector if a similar operating condition is considered.
- Above a certain flash pressure, noticeable reduction of cycle irreversibility can be achieved by replacing the LP throttle valve and the mixer of an OFC by an ejector.
- Though cycles with R245fa are producing slightly higher power output using heat of the flue gas available at 150°C, butane and isopentane are preferable options to run the cycle due to lower value of GWP.

6. Ejector based organic flash combined power and refrigeration cycle (EBOFCP&RC)

6.1 Objective of the work

Organic flash cycles are preferred for low grade heat recovery from SO_2 free flue gas due to the absence of pinch limitation in the heat recovery unit. However, the saturated liquid stream leaving the vapour separator of an OFC carries an appreciable amount of heat energy. This heat is ultimately lost to cooling water during the process of condensation. In this chapter, an attempt has been made to utilize this heat energy for producing additional refrigeration effects along with power.

To produce additional refrigeration effect a conventional waste heat driven organic flash power cycle (OFC) utilizing R245fa as working fluid is modified by replacing its low pressure throttle valve with an ejector. R245fa coming out from the vapour separator at saturated liquid state is accelerated in the nozzle of the ejector to ensure that saturated vapour from evaporator can enter to the ejector as secondary flow and total mass of R245fa at the exit of the diffuser of the ejector be at condenser pressure. The modified cycle is designated as Ejector based organic flash combined power and refrigeration cycle (EBOFCP&RC).

It should be noted that the condenser temperature depends on the ambient temperature. For a higher condenser temperature (say 40°C) a compressor is to be introduced between the evaporator and the ejector to maintain appreciable refrigeration effect. This cycle is designated as compressor assisted ejector based organic flash combined power and refrigeration cycle (CAEBOFCP&RC).

In this chapter R245fa is selected as the working fluid mainly due to its non-flammable characteristics. R245fa is also having saturated vapour line with positive slope. R245fa is a Zero ODP working fluid with a GWP value of 1050. Always heating of the working fluid to the highest possible temperature is desirable due to the higher mean temperature of heat addition. For an OFC this highest possible temperature should be nearer to its critical temperature for achieving improved vapour quality after throttling. As the critical temperature of R245fa (i.e. 154.4 ° C) nearer to the selected flue gas inlet temperature (i.e. 170°C), above requirements can be satisfied using R245fa as the working fluid.

6.2 System description:

Layout of a conventional waste heat driven organic flash cycle using R245fa as the working fluid is shown in Fig. 6.1. Saturated liquid coming out from the heat recovery unit (i.e., state-6) enters the vapour separator after undergoing a throttling process (i.e., 6-7). Dry saturated vapour leaving the vapour separator expands (i.e., 1-2) in a turbine. R245fa leaving the vapour separator at saturated liquid state undergoes another throttling process (i.e., 8-9) and finally mixes with the exhaust stream coming out from the turbine. Total mass of R245fa coming out from the mixer (i.e., state-3) after being condensed (i.e., 3-4) to saturated liquid sate enters the pump. The pump pressurizes total mass of R245fa up to the HRU pressure (i.e., state-5). In the HRU, R245fa is heated (i.e., 5-6) to saturated liquid state using waste heat of the flue gas free from sulphur.

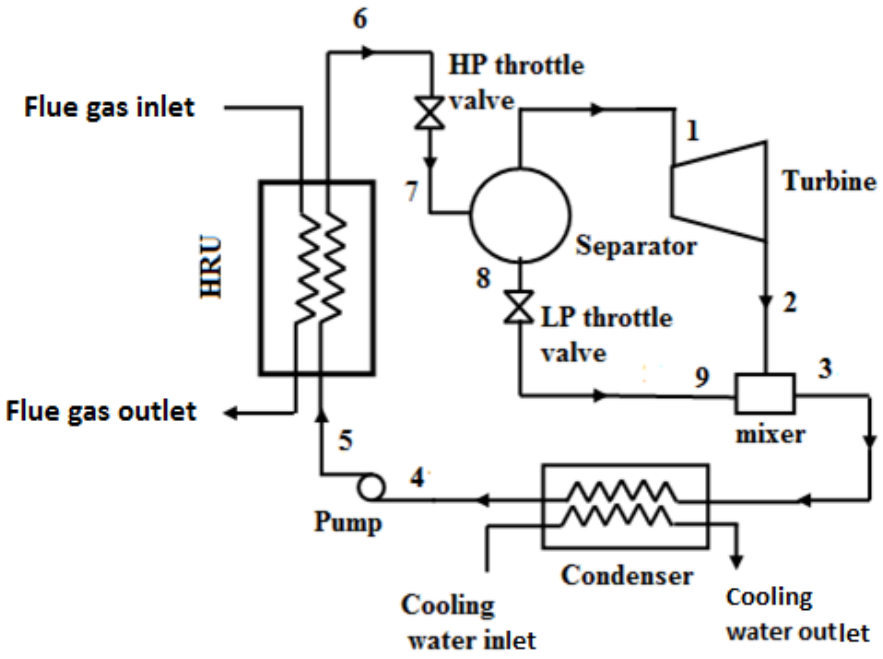

Fig. 6.1: Layout of an organic flash cycle (OFC)

Figures 2(a) and 2(b) are showing the layout and the corresponding T-s diagram of an ejector based organic flash combined power and refrigeration (EBOFCP&RC) cycle. This cycle is basically a modified conventional organic flash power cycle. In this cycle, saturated liquid coming out from the vapour separator is accelerated (i.e., 7-a) in the nozzle of the ejector as the primary flow. Dry saturated vapour leaving the evaporator (i.e., state-9) enters the ejector as the secondary flow. Entrainment ratio (i.e., ratio of mass of secondary flow to that of primary flow) of the ejector is such that the total mass of R245fa at the exit of the ejector

(i.e., state-n) be at the condenser pressure. Mass of R245fa leaving the ejector (State-n) mixes with the exhaust stream coming out from the turbine (i.e., state-2). Then total mass flow coming out from the mixer (i.e., state-10) enters the condenser. At the exit of the condenser (i.e., state-3), saturated liquid mass is split in two streams. One stream is pressurized (i.e., 3-4) to HRU pressure by a pump and another stream is throttled (i.e., 3-8) to the evaporator pressure.

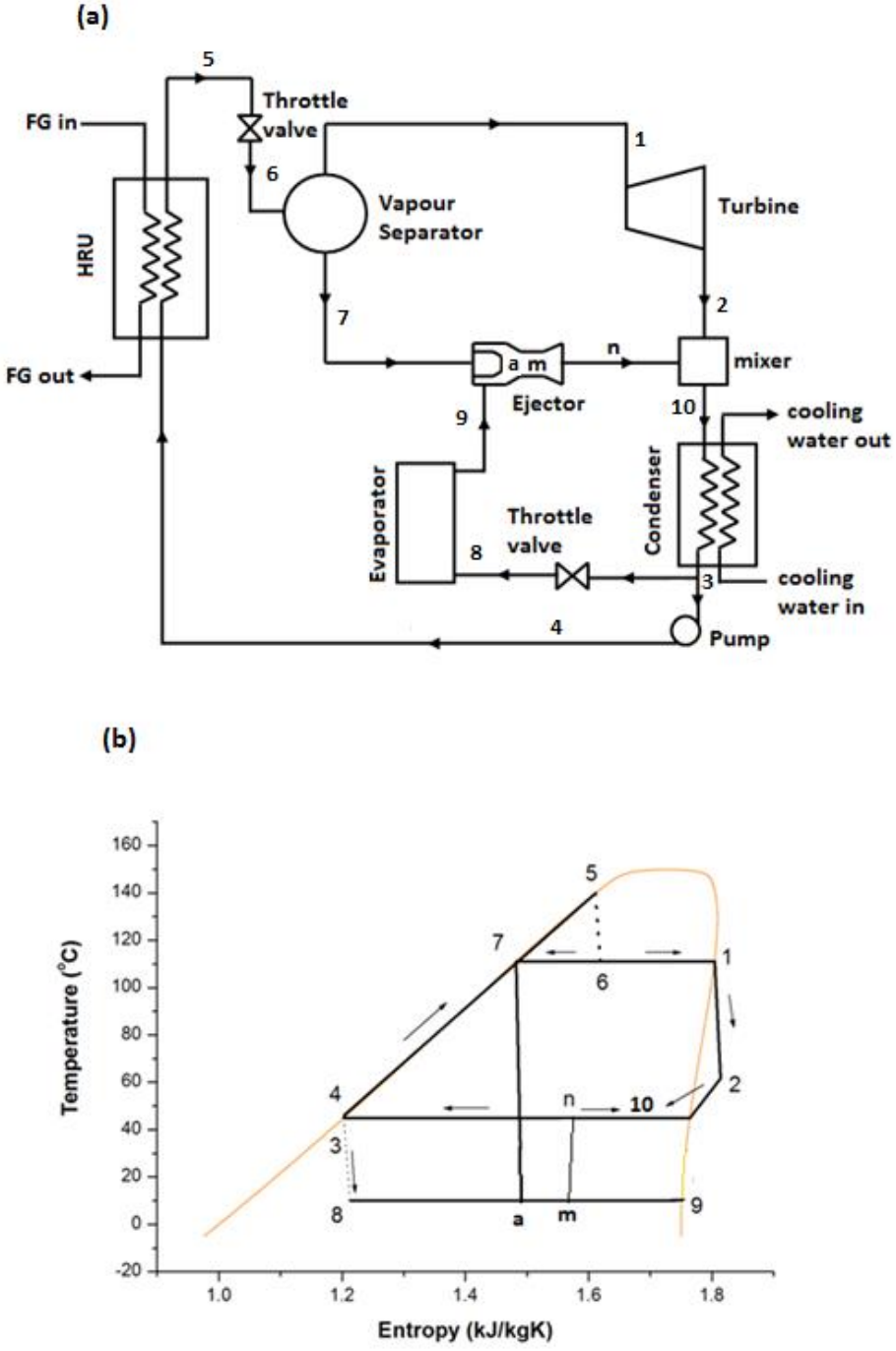

Fig. 6.2 (a): Layout of an EBOFCP&RC. (b): Temperature-entropy diagram of an EBOFCP&RC

Figures 6.3(a) and 6.3(b) are the layout and the T-s diagram of a compressor assisted ejector based organic flash combined power and refrigeration cycle (CAEBOFCP&RC). In this cycle, an additional compression (i.e., 9-10) is incorporated between the evaporator and the ejector to match the elevated condenser pressure.

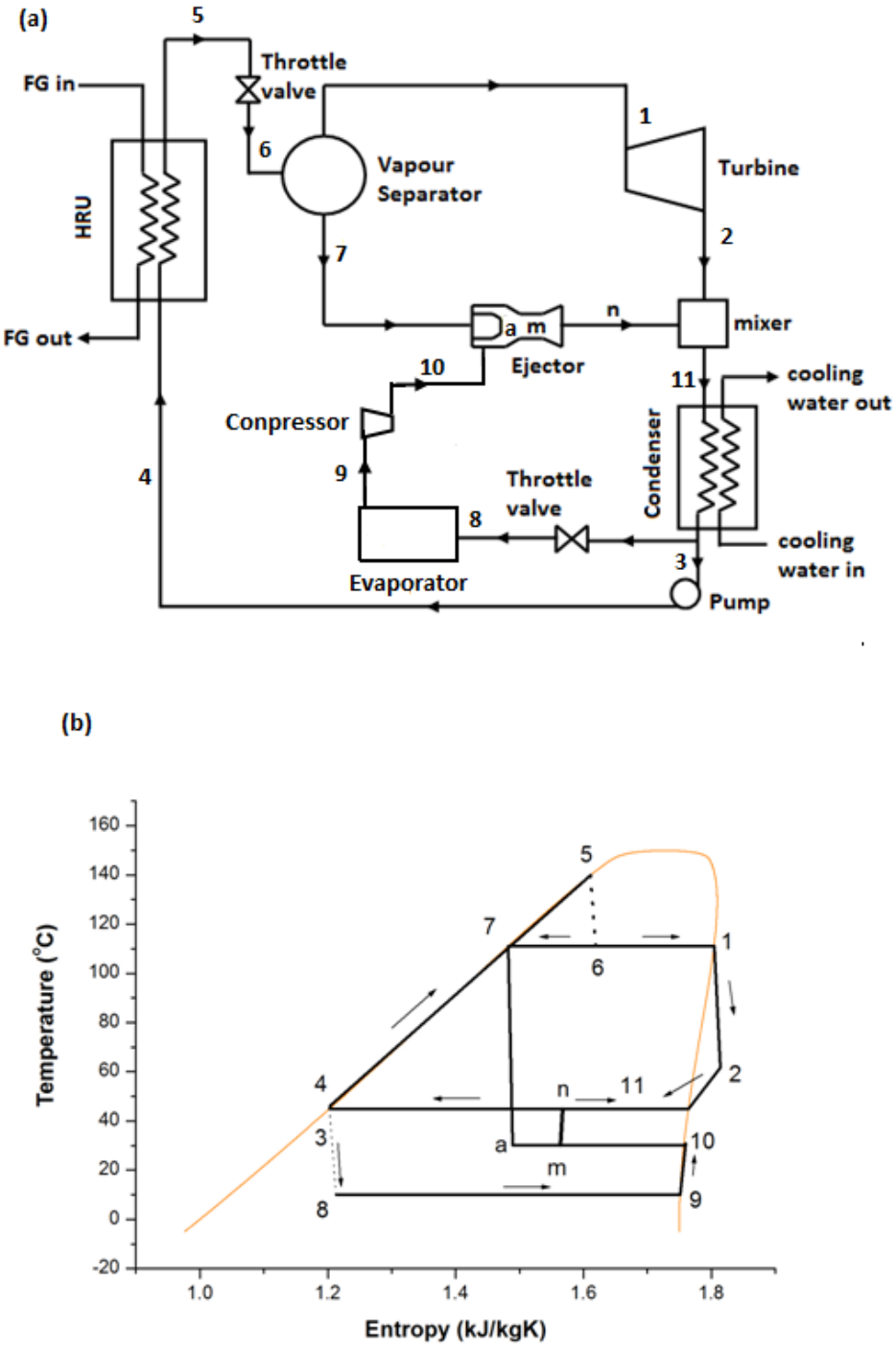

Fig. 6.3 (a): Layout of a CAEBOFCP&RC (b): Temperature-entropy diagram of a CAEBOFCP&RC

6.3. Mathematical Modelling:

During the mathematical modelling state point properties of R245fa are estimated using Refprop7 (Lemmon et al. 2002). The thermodynamic model is developed for the proposed cycles based on the following assumptions:

i. All flows are steady.
ii. It is assumed that 20kg s^{-1} of the flue gas is available at a temperature of 170 ^{0}C as the heat source.
iii. Pinch point temperature difference in HRU is 10^0C
iv. Flue gas is free from SO_2.
v. Isentropic efficiency of the turbine is 90%. Pump and compressor efficiencies are assumed to be 85%.
vi. For ejector, nozzle and diffuser efficiencies are 85% each and the mixer efficiency is 95%.
vii. Mixing in the mixing section of the ejector occurs at a constant pressure.
viii. The pressure drop of the secondary flow is neglected during ejector modelling (Bai et al. 2015, Yu et al. 2013).
ix. The velocities at the inlet and outlet of the ejector are negligible.
x. Extraneous heat loss is negligible.

6.3.1 Ejector modelling

For modelling of the ejector, the one dimensional mixing theory developed by Kenan et al. (1950) is applied.

The velocity of the primary flow coming out from the nozzle of the ejector may be expressed as

$$u_a = \sqrt{2\eta_N(h_7 - h_{as})10^3} \qquad (6.1)$$

Where h_7 is the enthalpy of the saturated liquid at the exit of the vapour separator or the nozzle inlet in kJ kg^{-1} and h_{as} is the enthalpy at the exit of the nozzle assuming the flow is isentropic.

The average velocity of the mixed flow is,

$$u_m = \frac{u_a\sqrt{\eta_m}}{1+\mu} \tag{6.2}$$

Corresponding value of the enthalpy of the mixed flow may be calculated from the following equation

$$h_m = \frac{h_7 + \mu h_{secondary}}{1+\mu} - \frac{u_m^2}{2000} \tag{6.3}$$

Where $h_{secondary} = h_9$ for the ejector based OFCP&RC (refer to Fig. 6.2) and $h_{secondary} = h_{10}$ for the compressor assisted ejector based OFCP&RC (refer to Fig. 6.3).

Now s_m is a function of h_m and P_m. It should be noted that in this study, $P_m = P_E$ and P_{COM} for the cycle without and with compressor respectively. At the exit of the diffuser, enthalpy is:

$$h_n = h_m + \frac{u_m^2}{2000} \tag{6.4}$$

Assuming isentropic process, ideal enthalpy at the exit of the diffuser is:

$$h_{ns} = h_m + \eta_D(h_n - h_m) \tag{6.5}$$

Now if exit pressure of the diffuser is equal to condenser pressure, entropy for the combination of h_{ns} and condenser pressure will be equal tos_m.

Initial calculation starts with an assumed value of entrainment ratio (μ) and its value is to be adjusted through iterations so that the diffuser exit pressure (P_n) becomes equal to the condenser pressure. Detail solution methodology for ejector modelling is presented in the flow chart of Fig. 6.4.

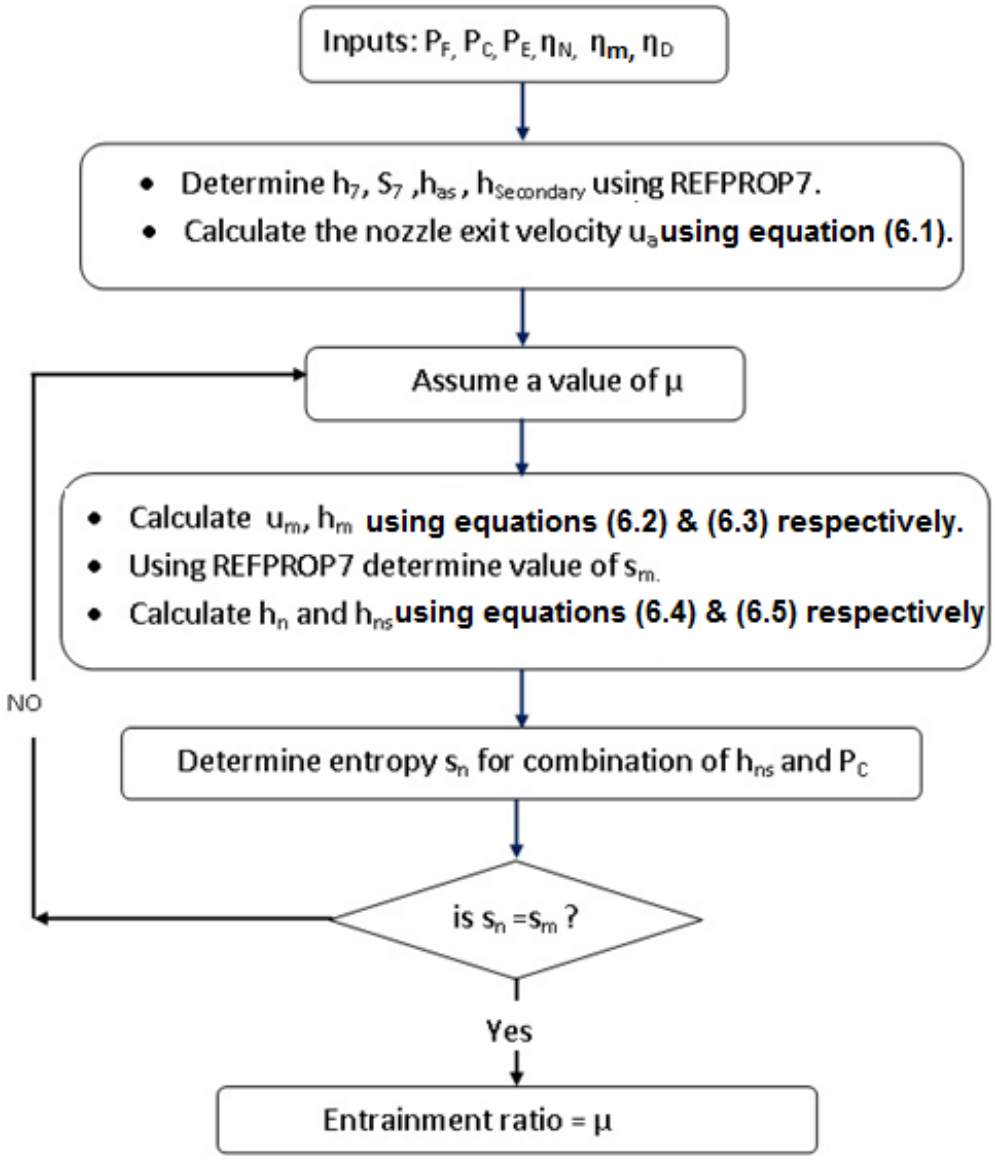

Fig. 6.4: Flow chart for ejector modelling

6.3.2 Thermodynamic modelling

From the heat balance of the heat recovery unit (HRU), the mass flow rate of R245fa is:

$$\dot{m}_f = \frac{\dot{m}_g c_{Pg}(T_{gi} - T_{go})}{h_5 - h_4} \tag{6.6}$$

It should be noted that assuming a 10°C pinch point temperature difference, $t_{go} = t_4 + 10$.

Turbine power output ($\dot{W}_T$), Pump power input ($\dot{W}_P$) and compressor power input ($\dot{W}_C$) (applicable for compressor assisted ejector based OFCO&RC (i.e. Fig. 6.3) only) are calculated using equations (6.7)-(6.9).

$$\dot{W}_T = m_f x(h_1 - h_2) \tag{6.7}$$

$$\dot{W}_P = m_f(h_4 - h_3) \tag{6.8}$$

$$\dot{W}_C = \dot{m}_f(1 - x)\mu(h_{10} - h_9) \tag{6.9}$$

Hence, net cycle power output for all three cycles is:

$$\dot{W}_{NET} = \dot{W}_T - \dot{W}_P - \dot{W}_C \tag{6.10}$$

It should be noted that $\dot{W}_C = 0$ for Ejector based OFCP&RC as there is no compressor in that cycle as shown in Fig. 6.2 (a).

Refrigeration effect produced in the evaporator is:

$$\dot{Q}_{RE} = \dot{m}_f(1 - x)\mu(h_9 - h_8) \tag{6.11}$$

Now 1st law efficiency of the combined power and refrigeration cycle is as follows

$$\eta_I = \frac{\dot{W}_{NET} + \dot{W}_{REF}}{\dot{m}_g c_{Pg}(t_{gi} - t_{go})} \tag{6.12}$$

Where $\dot{W}_{REF}$ represents the requisite compressor power input to run a vapour compression refrigeration cycle between the specified condenser and evaporator temperatures for producing $\dot{Q}_{RE}$amount of refrigeration effect.

2nd law efficiency of the proposed combined power and refrigeration cycles can be represented by the following equation (Yang et al. 2016).

$$\eta_{II} = \frac{\dot{W}_{NET} + \dot{E}_E}{\dot{E}_{ig}} \tag{6.13}$$

Where $\dot{W}_{NET}$ is the cycle power output. $\dot{E}_E$is the exergy of the refrigeration effect produced. This is the difference between inlet and exit exergies of working fluid across the evaporator.

$$\dot{E}_E = \dot{m}_f(1-x)\mu[(h_8 - h_9) - T_0(s_8 - s_9)] \quad (6.14)$$

E_{ig} is exergy associated with the flue gas at the inlet of the HRU as follows:

$$\dot{E}_{ig} = \dot{m}_g c_{Pg}\left(T_{gi} - T_0\right) - \dot{m}_g c_{Pg} T_0 \ln\frac{T_{gi}}{T_0} \quad (6.15)$$

Here T_{gi} and T_0 are the inlet temperature of the flue gas and the atmospheric temperature respectively.

6.4. Results and discussion:

In the present study an organic flash combined power and refrigeration cycle (OFCP&RC) is proposed in which saturated liquid coming out from the vapour separator enters the nozzle of an ejector as the primary flow. The ejector entrainment ratio is such that the total mass flow coming out of the ejector diffuser is at condenser pressure. The cycle can effectively utilize waste heat of sulphur free flue gas for producing simultaneous power and refrigeration effects. In this study effects of flash pressure, condenser and evaporator temperatures on the cycle performance are evaluated.

6.4.1. Ejector based OFCP&RC (EBOFCP&RC)

Effects of varying flash pressure on the net power output and refrigeration effect of EBOFCP&RC for a specified HRU exit temperature of R245fa are shown in Fig 6.5. It is observed that net power output initially increases with an increase in flash pressure, reaches maximum and then shows a decreasing trend above an optimum value of the flash pressure. Initially the net power output increases due to larger specific enthalpy drop associated with the elevated flash pressure. However, with an elevated flash pressure, lesser mass of vapour enters the turbine due to degrading quality of the vapour at the exit of the high pressure throttle valve. Above the optimum flash pressure; this effect dominates the net power output. On the other hand, refrigeration effect monotonically increases with an increase in flash pressure. This can be explained by Fig. 6.6. It is observed in Fig. 6.6 that quality decreases and entrainment ratio increases with an increase of the flash pressure. Entrainment ratio increases due to larger specific enthalpy of primary flow entering the ejector. Thus mass

flowing through refrigeration evaporator also increases. This results in larger refrigeration effect.

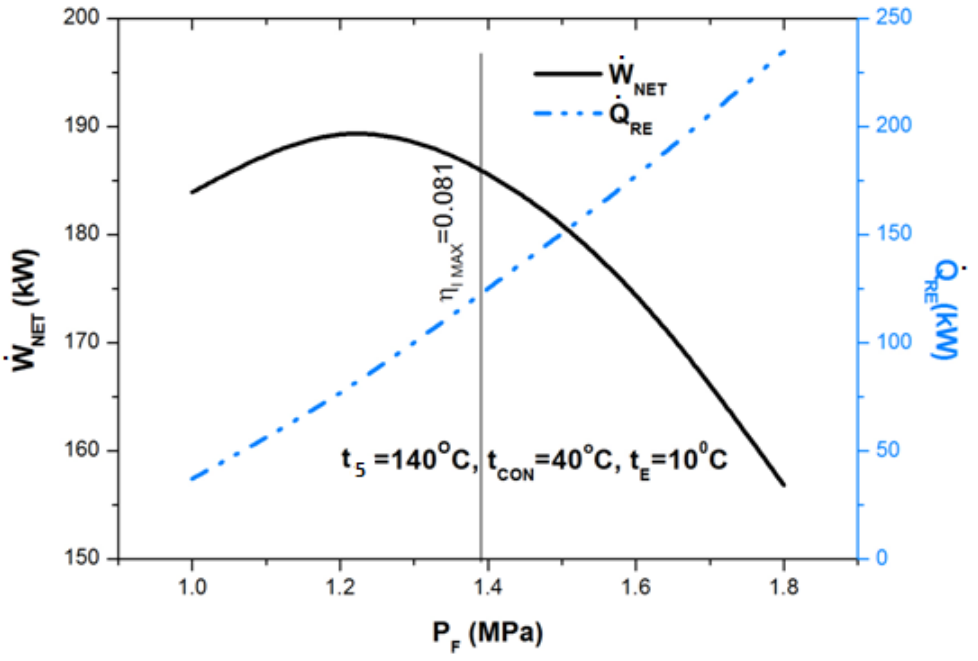

Fig. 6.5: Effects of varying flash pressure on cycle power output and refrigeration effect of an EBOFCP&RC.

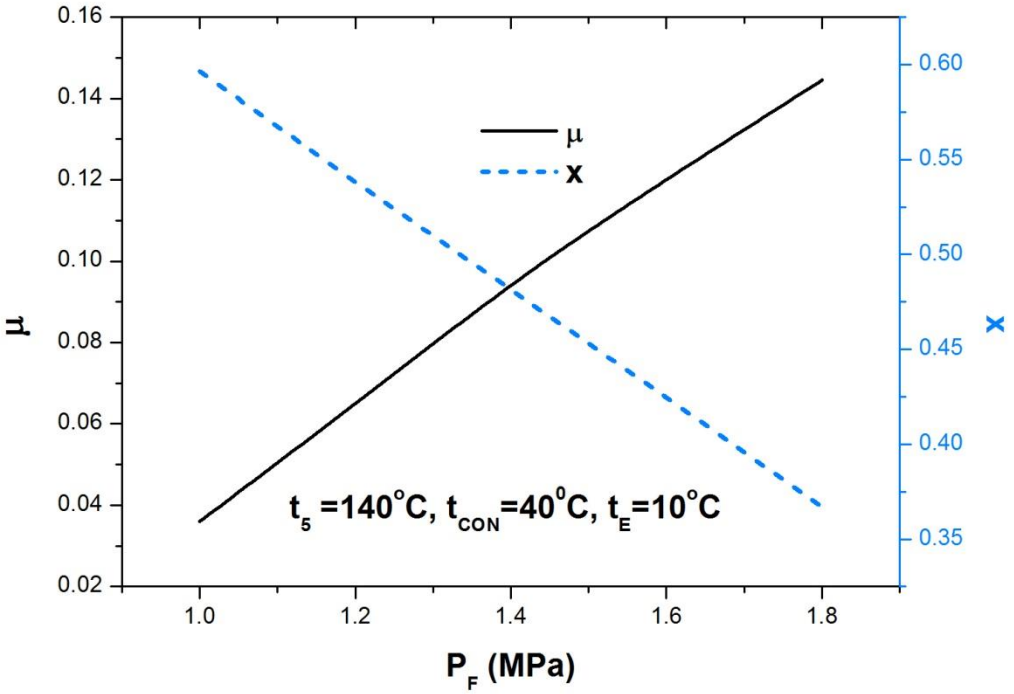

Fig. 6.6: Effects of varying flash pressure on dryness fraction and ejector entrainment ratio of an EBOFCP&RC.

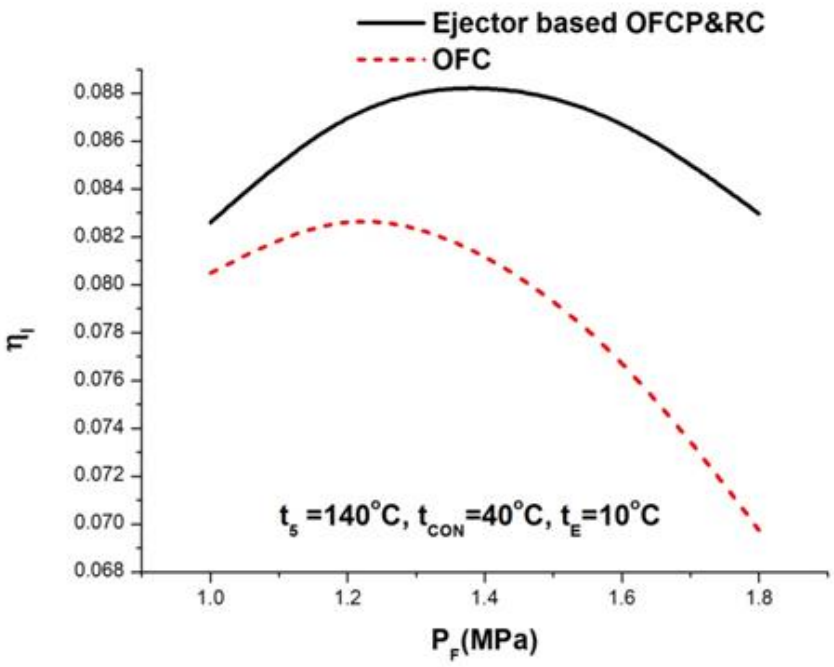

Fig. 6.7: Comparison between 1st law efficiencies of an EBOFCP&RC and OFC

Figure 6.7 shows effects of varying flash pressure on 1st law efficiencies of both the conventional OFC and the EBOFCP&RC. It is observed that the ejector based OFCP&RC yields higher 1st law efficiency due to saving of power that would have been required to produce same refrigeration effect by a vapour compression refrigeration cycle operating between same evaporator and condenser temperatures. Also there exists an optimum flash pressure for maximum efficiency for each of the cycles. The optimum flash pressure line corresponding to maximum 1st law efficiency of the Ejector based OFCP&REC is presented by the vertical line of Fig. 6.5. Corresponding to this maximum flash pressure power output and refrigeration effects are 185.84 kW and 124.08 kW respectively. To get the optimum value of flash pressure corresponding to the maximum 1st law efficiency, a small zone is identified on either side of optimum flash pressure of Fig. 6.7 and for the selected zone 1st law efficiencies are calculated with very small variation of flash pressure (i.e. 0.05MPa).

It should be noted that optimum flash pressure of the EBOFCP&RC is higher compared to that of the conventional OFC due to monotonically increasing trend of the refrigeration effect

produced by the EBOFCP&RC. Also it is observed that the difference between 1st law efficiencies of these two cycles is higher at elevated flash pressure. At an elevated flash pressure 1st law efficiency of the OFC sharply decreases due to a rapid drop in turbine power output as a smaller mass of R245fa enters into the turbine due to degraded quality of vapour at the exit of the HP throttle valve. However, for the modified cycle larger mass of R245fa enters into the evaporator due to improved value of entrainment ratio as well as larger mass flow of the primary fluid into the ejector. Thus higher value of refrigeration effects of the modified cycle associated with higher flash pressure does not allow decreasing the value of first law efficiency as rapidly as that of OFC.

Fig. 6.8 compares 2nd law efficiencies of the OFC and the EBOFCP&RC assuming an ambient temperature as 30°C. Ejector based OFCP&RC is capable of producing higher 2nd law efficiency due to exergy associated with the refrigeration effect. Optimum flash pressure for maximum 2nd law efficiency of the OFC is same as that of the net cycle power output or the 1st law efficiency as exergy associated with power output is only in consideration. Optimum flash pressure for maximum 2nd law efficiency of the ejector based OFCP&RC is higher compared to that of the OFC. It is because exergy of refrigeration effect continuously increases with increasing flash pressure. Above optimum flash pressure, exergy decreases due to the dominating effect of reducing turbine power output.

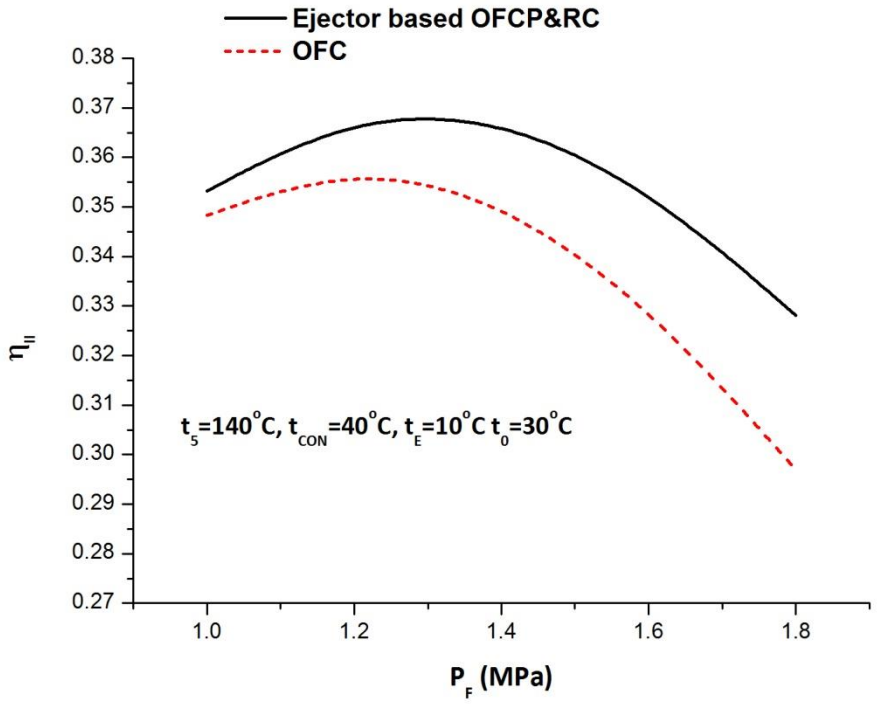

Fig. 6.8: Comparison between 2nd law efficiencies of an EBOFCP&RC and OFC

Effect of varying condenser temperatures on the net cycle power output is shown in Fig. 6.9. It is observed that the net cycle power output decreases with an increase in the condenser temperature due to smaller enthalpy drop across the turbine. It should be noted that varying evaporator temperature does not have any effect on the net cycle power output at a constant condenser temperature.

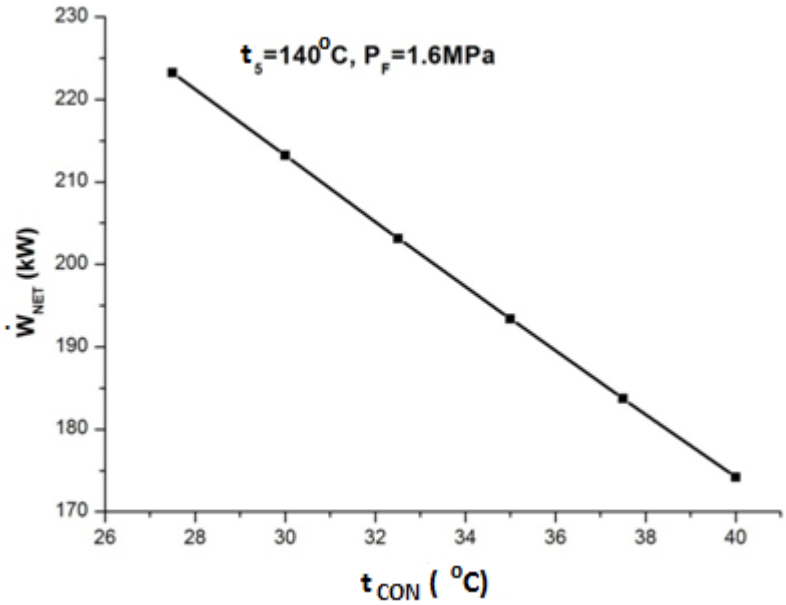

Fig. 6.9: Effects varying condenser temperature on cycle power output of an EBOFCP&RC

Figure6.10 (a) demonstrates simultaneous effects of varying evaporator and condenser temperatures on the ejector entrainment ratio. It is observed that with specified evaporator temperature, the entrainment ratio decreases with an increase in the condenser temperature due to associated higher value of the delivery pressure. On the other hand, ejector entrainment ratio increases with an increase in the evaporator temperature due to a corresponding increase in the evaporator pressure. Thus, as shown in Fig. 6.10 (b), refrigeration effect increases with an elevated evaporator temperature and decreases with an elevated condenser temperature.

It is observed in Fig. 6.11 that 1st law efficiency of the EBOFCP&RC increases with increasing evaporator temperature as refrigeration effect gets improved without affecting the net cycle power output. However, 1st law efficiency decreases sharply with an increase in condenser temperature as this reduces both the net power output and the refrigeration effect simultaneously.

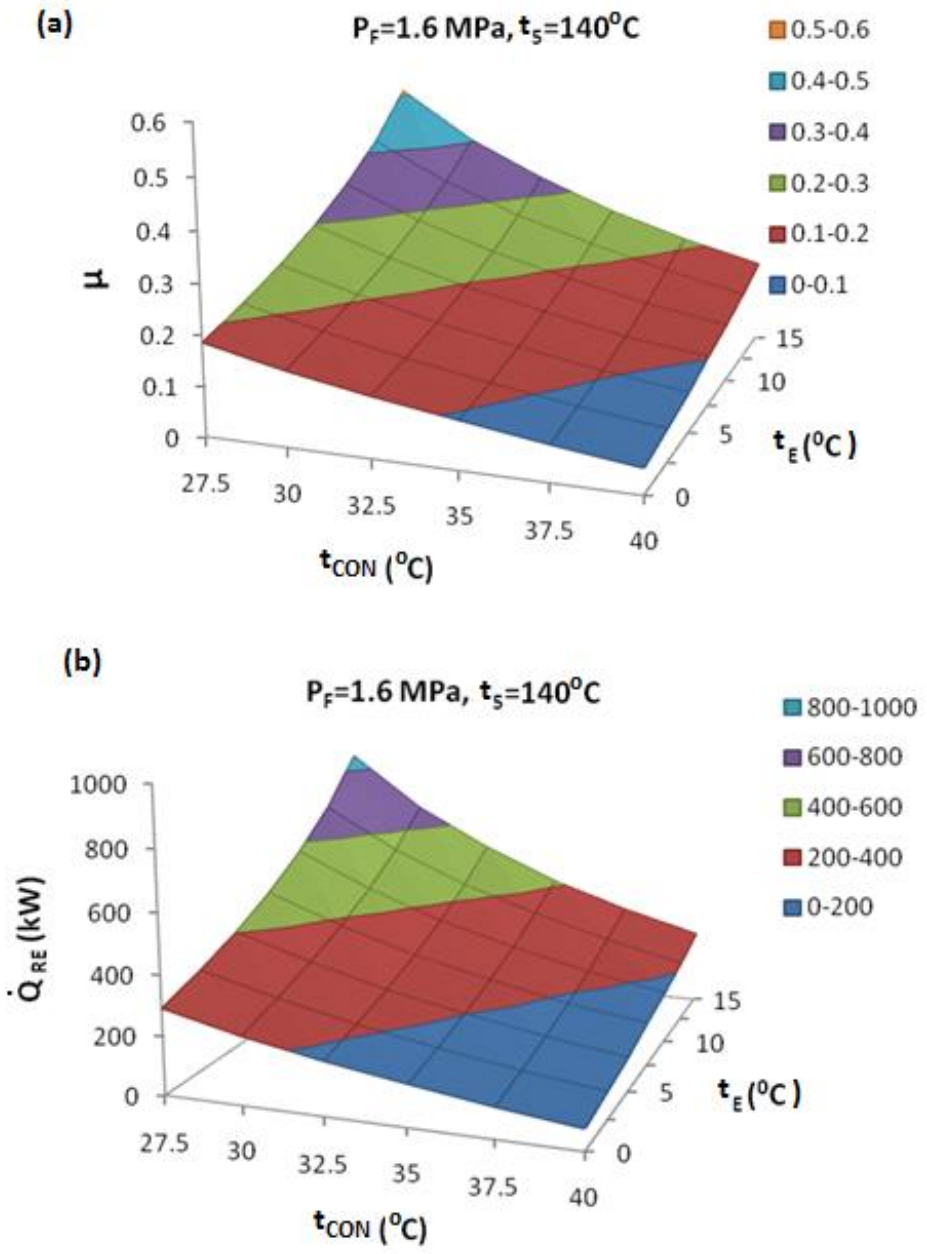

Fig. 6.10 (a): Effects varying evaporator and condenser temperatures on ejector entrainment ratio of an EBOFCP&RC. (b): Effects varying evaporator and condenser temperatures on refrigeration effect of an EBOFCP&RC

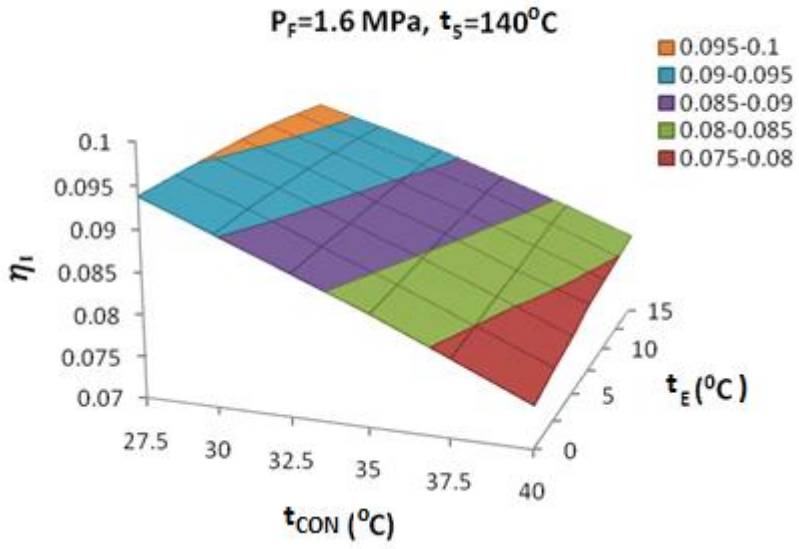

Fig. 6.11: Effects varying evaporator and condenser temperatures on 1st law efficiency of an EBOFCP&RC.

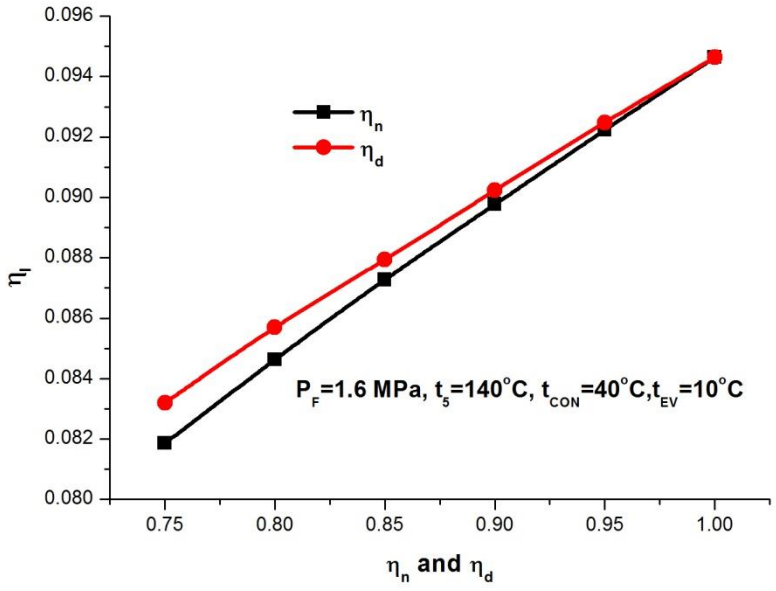

Fig. 6.12: Effects of varying ejector component (nozzle and diffuser) efficiencies on 1st law efficiency of an EBOFCP&RC

Effects of varying ejector nozzle efficiency and ejector diffuser efficiency on cycle performance are demonstrated in Fig 6.12. During showing effects of varying efficiency of any one component on 1st law efficiency, the efficiency of remaining components are assumed to be ideal i.e. 100%. It is observed higher nozzle and diffuser efficiencies yield higher 1st law efficiency as entrainment ratio as well as refrigeration effect increase with increments in nozzle and diffuser efficiencies. It is also evident from Fig. 6.12 that 1st law efficiency is more sensitive to nozzle efficiency variation compared to that of the diffuser.

6.4.2. Compressor assisted ejector based OFCP&RC (CAEBOFCP&RC)

It is evident from Fig. 6.10 (b) that refrigeration effect decreases sharply with increasing condenser temperature and also becomes insignificant for higher values of condenser temperature (say 40°C). In this situation an additional compressor is to be introduced between the evaporator and the ejector to maintain the desired refrigeration effect.

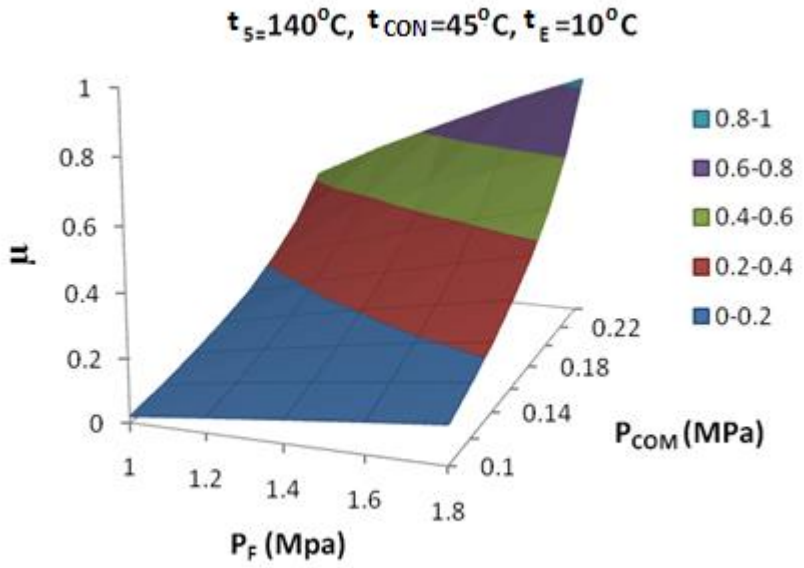

Fig.6.13: Effects of varying flash pressure and compressor exit pressure on ejector entrainment ratio of a CAEBOFCP&RC.

Figure 6.13 is representing simultaneous effects of varying flash pressure and compressor exit pressure on ejector entrainment ratio of the CAEBOFCP&RC. It is assumed that the evaporator temperature is 10°C and the condenser temperature is 45°C. It is observed that entrainment ratio increases with an increase in both flash pressure and compressor exit

pressure. Higher compressor exit pressure reduces difference between inlet pressure of secondary flow and diffuser delivery pressure. Thus, refrigeration effect increases with increasing flash pressure as well as increasing compressor exit pressure due to larger mass of secondary flow as shown in Fig. 6.14.

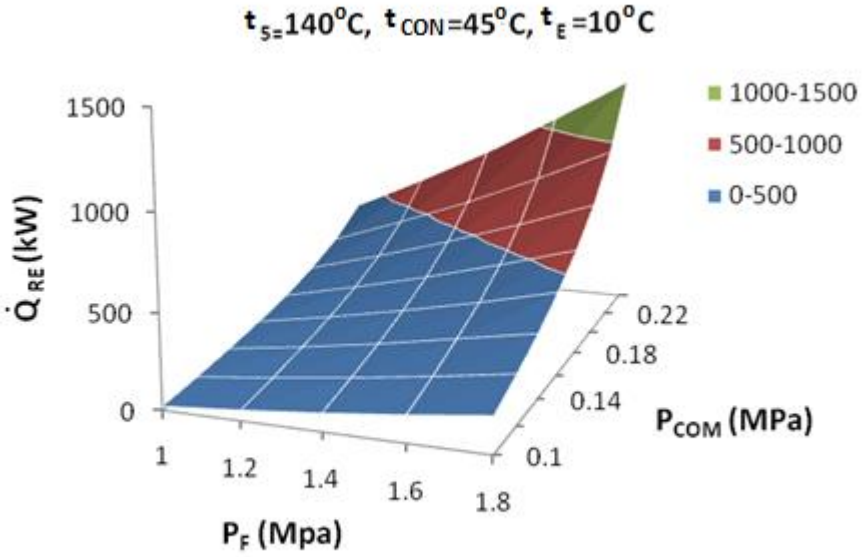

Fig. 6.14: Effects of varying flash pressure and compressor exit pressure on refrigeration effect of a CAEBOFCP&RC.

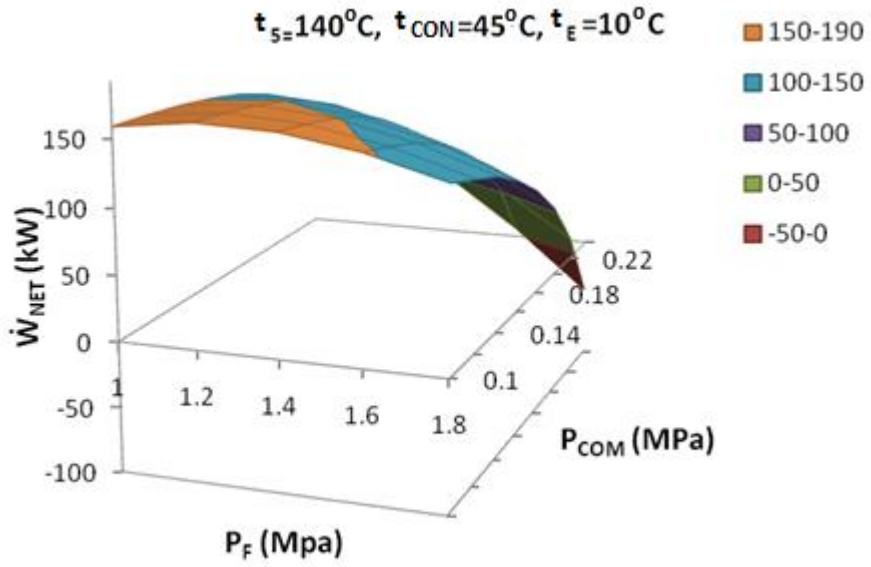

Fig. 6.15: Effects of varying flash pressure and compressor exit pressure on net power output of a CAEBOFCP&RC.

Variation of the net power output of the cycle with varying flash pressure and compressor exit pressure is presented in Fig. 6.15. For a specified compressor exit pressure, there exists an optimum flash pressure for a maximum net cycle power output. The reason behind this is same as that explained for EBOFCP&RC (i.e., Fig. 6.5). On the other hand, for a specified flash pressure net cycle power output decreases sharply with an increase in compressor exit pressure as a part of the cycle power output is consumed by the compressor. It is also observed that above a certain value of the compressor exit pressure, power output becomes negative. This is because the cycle becomes a refrigeration cycle only without any power output, but power input required for the refrigeration cycle.

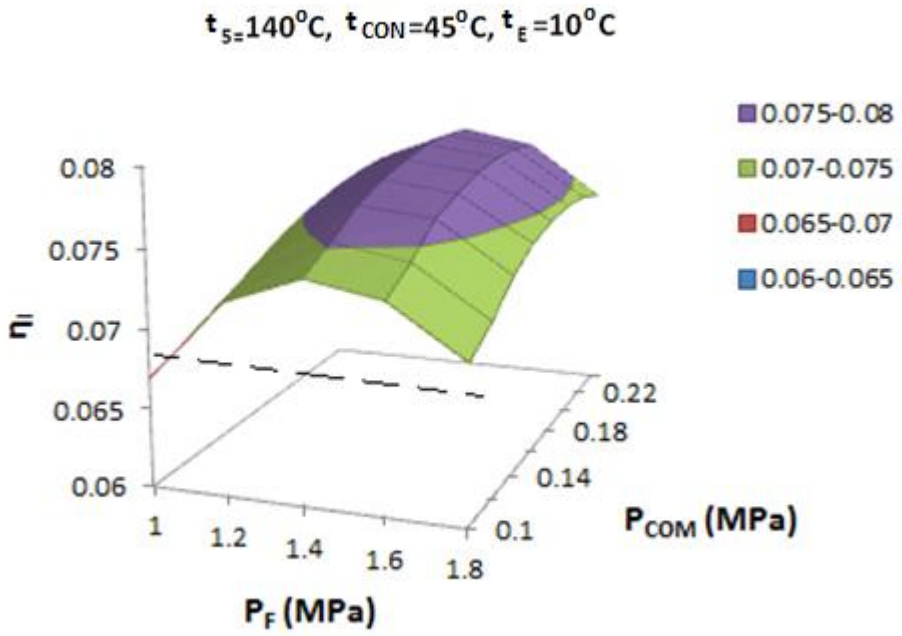

Fig. 6.16: Effects of varying flash pressure and compressor exit pressure on 1st law efficiency of a CAEBOFCP&RC

Effects of varying flash pressure and compressor exit pressure on 1st law efficiency of a CAEBOFCP&RC is shown in Fig. 6.16. It is observed that there exists an optimum combination of flash pressure and compressor exit pressure for a maximum 1st law efficiency. With an increase in compressor exit pressure the net cycle power output sharply decreases and refrigeration effect increases. Larger refrigeration effect will also increases the value of W_{REF} (i.e. the power required for obtaining same refrigeration effect by a vapour compression

refrigeration cycle for specified condenser and evaporator pressures.) The counteracting trends of W_{NET} and W_{REF} result in a maximum 1st law efficiency corresponding to an optimum compressor exit pressure. On the other hand initially 1st lay efficiency increases with an increase in flash pressure as both cycle power output and refrigeration effect increase. However above optimum value of the flash pressure 1st law efficiency decreases due to rapid reduction in cycle power output with increasing flash pressure.

It should be noted that for similar operating conditions the proposed cycle is capable of producing higher 1st law efficiency compared that of an OFC. In Fig. 6.16 the dashed line represents the peak value of 1st law efficiency for an OFC under similar operating condition (i.e., T_5=140°C and T_{CON}=45°C).

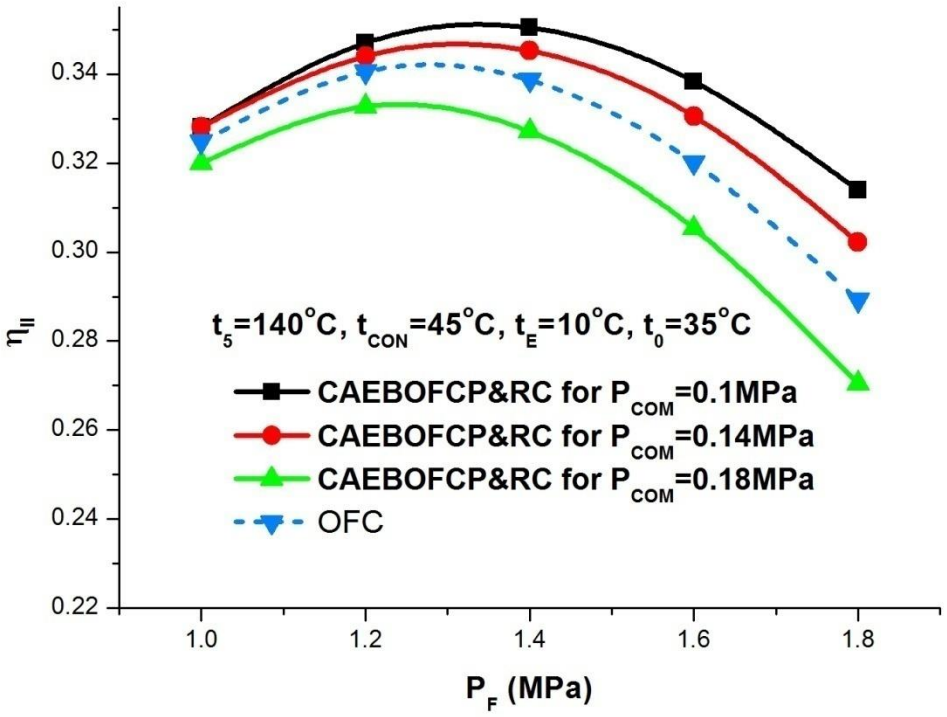

Fig. 6.17: Comparison between 2nd law efficiencies of a compressor assisted ejector based OFCP&RC and organic flash cycle (OFC)

Effect of varying flash pressure on 2nd law efficiency of a compressor assisted ejector based OFCP&RC is demonstrated in Fig. 6.17. Exergy associated with the power output decreases after reaching a peak value. However, exergy associated with the refrigeration effect

monotonically increases due to higher mass flow through the evaporator. Thus an optimum flash pressure exists for maximum 2nd law efficiency. This is the pressure above which exergy associated with cycle power output decreases at a faster rate compared to the corresponding increase in exergy associated with the refrigeration effect. It is also observed that 2nd law efficiency decreases with higher values of the compressor exit pressure due to the decrease in exergy value associated with power output. Also above a certain value of this pressure, exergy efficiency of the proposed cycle becomes even lesser than that of conventional OFC.

6.5. Chapter summary

In the present study, an ejector based organic flash combined power and refrigeration cycle (OFCP&RC) is proposed. The cycle is capable of producing simultaneous power and refrigeration effect using low grade waste heat of sulphur free flue gas. For higher condenser temperature (i.e., say 45°C) an additional compressor has to be introduced for achieving appreciable refrigeration effect.

- It is observed that for both cycles (i.e., cycle with compressor and without compressor) there exist optimum flash pressures for maximum cycle power as well as for 1st and 2nd law efficiencies.
- Refrigeration effects of both cycles (i.e., cycle with compressor and without compressor) increase monotonically with increasing values of flash pressure.
- 1st law efficiencies of both cycles are appreciably higher compared to that of conventional OFC.
- With an increase of compressor exit pressure, cycle power output of the compressor assisted ejector based OFCP&RC decreases. Above a certain value of compressor exit pressure, only refrigeration effect is obtainable from the proposed cycle.
- 2nd law efficiency of compressor assisted ejector based OFCP&RC decreases with an increase in compressor exit pressure and it even become lesser than that of a conventional OFC above a certain value of compressor exit pressure. However, 2nd law efficiency of the proposed cycle is higher in absence of the compressor compared to that of the organic flash cycle (OFC).

7. Conclusions and future scope

7.1 Conclusions

Majority of the industrial waste heat released to the ambient is having a temperature in the range of 100 to 199°C. This available waste heat may be utilized to produce power or cooling effect through some thermodynamic cycles. Due to low quality, conversion of this available waste heat into some energy utilities (mainly power and cooling effects) is very challenging. In the present thesis, a few of the existing power cycles are modified for the efficient utilization of low grade waste heat of industrial flue gas released to the ambient. The findings of different chapters of the present thesis may be summarised as follows:

- 1st and 2nd law efficiencies of a regenerative T-CO_2 power cycle can be improved appreciably by introducing an additional high temperature (HT) regenerator driven by the heat of the bleed CO_2 stream at some intermediate pressure of turbine expansion. Efficiencies of the cycle improve as a larger mass of CO_2 is extracted from the turbine for regeneration. However, the size of the HT regenerator starts to increase exponentially as the bleed mass of CO_2 exceeds a certain value.
- A regenerative T-CO_2 power cycle is capable of producing reasonably good power using low grade heat of flue gas. However, a T-CO_2 power cycle can be executed only if a low temperature heat sink is available. In absence of low temperature heat sink, the cycle is to be executed in supercritical mode.
- The present analysis revealed that an optimized regenerative CO_2 power cycle with two-stage compression and intercooling can yield higher specific work output as well as higher 2nd law efficiency compared to an optimized regenerative supercritical CO_2 power cycle. Minimum cycle temperature is assumed to be 35°C for both of the cycles.
- Specific work output, 1st law and 2nd law efficiencies of a regenerative supercritical CO_2 power cycle can be improved by increasing the number of compression stages. However, beyond a certain number of compression stages improvement achieved becomes negligible.
- Very high operating pressure in the HRU is a major disadvantage of any CO_2 based power cycle. Besides CO2 based power cycle, Organic Flash Cycle (OFC) is another possible option that can avoid the pinch limitation of the conventional ORC. Thus

both of the cycles are very much suitable for producing power from waste heat of flue gas free from SO_2. It is concluded from the thesis that a T-CO_2 power cycle is a better option if the maximum work potential of flue gas is to be exploited with maximum safety and minimum environmental impact. OFCs can provide an economically better solution if smaller work output per unit mass of flue gas is acceptable.

- Due to the absence of pinch limitation in the HRU, an OFC is preferred for waste heat recovery from SO_2 free flue gas. However, this advantage is counteracted by the presence of two throttling process.
- The LP throttle valve of an OFC can be replaced by an ejector. This ensures the expansion of the working fluid in the turbine to a pressure which is lower than the condenser pressure. The working fluid leaving the vapour separator of the OFC at saturated liquid state can be accelerated in the nozzle of the ejector as primary fluid to entrain the working fluid stream exiting the turbine. As condenser pressure is higher compared to turbine exit pressure, the modified cycle can produce higher work output per unit mass of flue gas as well as higher 2^{nd} law efficiency.
- The working fluid leaving the vapour separator of the OFC as the saturated liquid can also be accelerated in the nozzle of an ejector to entrain the mass of working fluid leaving the evaporator of a cooler. This produces an additional cooling effect without affecting the power output.
- For a condenser temperature at or above 40°C, an additional compressor is to be introduced between the evaporator and ejector for maintaining an acceptable level of cooling effect.

7.2 Future scope

- Proposed cycle configurations may be integrated with other energy utilities (such as desalination, heating and cooling, Fuel synthesis, etc.) to develop a low grade heat driven ploygeneration unit. The unit may be driven by locally available low grade heat and may cater to some of the localized energy need.
- The developed ploygeneration system may be accessed for the technological possibility, economic feasibility, environmental vulnerability and partial social impacts, i.e., overall sustainability
- Integrated polygeneration units would lead to future prototype development.

References

Abadi G B, Kim K C (2017) Investigation of organic Rankine cycles with zeotropic mixtures as a working fluid: Advantages and issues. Renewable and Sustainable Energy Reviews 73:1000-1013.

Aljundi I H (2011) Effect of dry hydrocarbons and critical point temperature on the efficiencies of organic Rankine cycle. Energy 36: 1196-1202.

Al-Zuhair S, Almenhali A, Hamad I, Alshehhi M, Alsuwaidi N, Mohamed S (2011) Enzymatic production of biodiesel from used/waste vegetable oils: Design of a pilot plant. Renewable Energy 36:2605-2614.

Baik Young-Jin, Kim M, Chang Ki-Chang, Lee Young-Soo, Yoon Hyung-Kee (2013) A comparative study of power optimization in low-temperature geothermal heat source driven R125 transcritical cycle and HFC organic Rankine cycles. Renewable Energy 54: 78-84.

Bai T, Yan G, Yu J (2015) Thermodynamic analyses on an ejector enhanced CO2 transcritical heat pump cycle with vapor-injection. International journal of refrigeration 58: 22-34.

Bai T, Yan G, Yu J (2015b) Thermodynamics analysis of a modified dual-evaporator CO2 transcritical refrigeration cycle with two-stage ejector. Energy 84: 325-335.

Banik S, Ray S, De S (2016) Thermodynamic modelling of a recompression CO2 power cycle for low temperature waste heat recovery. Applied Thermal Engineering 107:441-452.

Bao J, Zhao L (2013) A review of working fluid and expander selections for organic Rankine cycle. Renewable and Sustainable Energy Reviews 24:325-342.

Benhadid-Dib S, Benzaoui A, (2012) Refrigerants and their Environmental Impact Substitution of Hydro Chlorofluorocarbon HCFC and HFC Hydro Fluorocarbon. Search for an Adequate Refrigerant. Energy Procedia 18:18807-816.

Besagni G, Mereu R, Leo G D, Inzoli F (2015) A study of working fluids for heat driven ejector refrigeration using lumped parameter models. International Journal of Refrigeration 58:154-171.

Besagni G, Mereu R, Inzoli F, Chiesa P (2017) Application of an Integrated Lumped Parameter CFD approach to evaluate the ejector-driven anode recirculation in a PEM fuel cell system. Applied Thermal Engineering 121:628-651.

Braimakis K, Karellas S, (2018) Energetic optimization of regenerative Organic Rankine Cycle (ORC) configurations. Energy Conversion and Management 159: 353–370.

Bina S M, Jalilinasrabady S, Fujii H (2017) Economic and Environmental (3E) Aspects of Internal Heat Exchanger for ORC Geothermal Power Plants. Energy 140: 1096-1106.

Bilir N, Ersoy H K (2009) Performance improvement of the vapour compression refrigeration cycle by a two-phase constant area ejector. International journal of energy research 33:469-480.

Bryant J, Saari H, Zanganeh Kourosh (2011) An Analysis and Comparison of the Simple and Recompression Supercritical CO2 Cycles. Supercritical CO2 Power Cycle Symposium: May 24-25, 2011 Boulder, Colorado.

Cayer E, Galanis N, Desilets M, Nesreddine H, Roy P (2009) Analysis of a carbon dioxide transcritical power cycle using a low temperature source. Applied Energy 86:1055-1063.

Calm J M, Hourahan G C (2011) Physical, safety, and environmental data for current and alternative refrigerants. In: Proceedings of the 23rd International Congress of Refrigeration. Prague, Czech Republic

Cavallini A, Zecchin R (1974) Dimensionless correlation for heat transfer in forced convection condensation. Proceedings of 5th International heat transfer conference: 309-313.

Chen G, Zhang R, Zhu D, Chen S, Fang L, Hao X (2017) Experimental study on two-stage ejector refrigeration system driven by two heat sources. International Journal of Refrigeration 74:295-303.

Chen J, Huang Y, Niu Z, Chen Y, Luo X (2018) Performance analysis of a novel organic Rankine cycle with a vapor-liquid ejector. Energy Conversion and Management 157:382-395.

Chen J, Havtun H, Palm B (2014) Investigation of ejectors in refrigeration system: Optimum performance evaluation and ejector area ratios perspectives. Applied Thermal Engineering 64:182-191

Chen Y and Lundqvist P (2011) The CO_2 power cycle for low grade heat recovery: Discussion on temperature profiles in system heat exchangers. ASME Power Conference 1: 385-392.

Chen Y, Lundqvist P, Johansson A, Platell P (2006) A comparative study of the carbon dioxide transcritical power cycle compared with an organic rankine cycle with R123 as working fluid in waste heat recovery. Applied Thermal Engineering 26: 2142-2147.

Dai B, Li M, Ma Y (2014) Thermodynamic analysis of carbon dioxide blends with low GWP (global warming potential) working fluids-based transcritical Rankine cycles for low-grade heat energy recovery. Energy 64: 942-952.

Dostal V, Driscoll M J, Hejzlar P (2004) A Supercritical Carbon Dioxide Cycle for Next Generation Nuclear Reactors. MIT-ANP-TR-100, Massachusetts Institute of Technology.

D.Q. Kern (1950) Process heat transfer. Mc Graw-hill Publication, Newyork.

Ersoy H K, Yalcin S, Yapici R, Ozgoren M (2007) Performance of a solar ejector cooling-system in the southern region of Turkey. Applied Energy 84:971-983.

Eyerer S, Wieland C, Vandersickel A, Spliethoff H (2016) Experimental study of an ORC (Organic Rankine Cycle) and analysis of R1233zd-E as a drop-in replacement for R245fa for low temperature heat utilization. Energy 103: 660-671.

Ghaebi H, Parikhani T, Rostamzadeh H, Farhang B (2017) Thermodynamic and thermoeconomic analysis and optimization of a novel combined cooling and power (CCP) cycle by integrating of ejector refrigeration and Kalina cycles. Energy 139: 262-276.

Galloni E, Fontana G, Staccone S (2015) Design and experimental analysis of a mini ORC (organic Rankine cycle) power plant based on R245fa working fluid. Energy 90: 768-775.

Garg P, Kumar P, Srinivasan K, Dutta P (2013a) Evaluation of isopenatane, R245-fa and their mixture as working fluid for organic Rankine cycles. Applied thermal engineering 51: 292-300.

Garg P, Kumar P, Srinivasan K, Dutta P (2013b) Evaluation of carbon dioxide blends with isopentane and propane as working fluids for organic Rankine cycles. Applied Thermal Engineering 52: 439-448.

Garg P, Srinivasan K, Dutta P, Kumar P (2014) Comparison of CO2 and Steam in Transcritical Rankine Cycles for Concentrated Solar Power. Energy Procedia 49: 1138-1146.

Ge Y T, Li L, Luo X, Tassou S A (2017) Performance evaluation of a low-grade power generation system with CO2 transcritical power cycles. Applied Energy 227:220-230.

Gnielinski V (1976) New equation for heat and mass transfer in turbulent pipe and channel flow. International chemical engineering 16: 359-368

Guo T, Wang H X, Zhang S J (2010) Comparative analysis of CO2-based transcritical Rankine cycle and HFC245fa-based subcritical organic Rankine cycle using low-temperature geothermal source. Science china 53:1638-1646.

Haddad C, Périlhon C, Danlos A, François M-X, Descombes G (2014) Some efficient solutions to recover low and medium waste heat: competitiveness of the thermoacoustic technology. Energy Procedia 50: 1056 – 1069.

Ho T, Samuel S M, Greif R (2012a) Comparison of the Organic Flash Cycle (OFC) to other advanced vapor cycles for intermediate and high temperature waste heat reclamation and solar thermal energy. Energy 42:213-223.

Ho T, Samuel S M, Greif R (2012b) Increased power production through enhancements to the Organic Flash Cycle (OFC). Energy 45:686-695.

IEA Statistics (2016). Renewables information. OECD/ IEA 2016

IEA Statistics (2017). CO_2 emission from fuel combustion highlights. OECD/ IEA:2017 .

International energy outlook (IEO) (2017). US: US Energy Information Administration.

Invernizzi Costante M, Iora P, Preißinger M, Manzolini G (2016) HFOs as substitute for R-134a as working fluids in ORC power plants: A thermodynamic assessment and thermal stability analysis. Applied Thermal Engineering 103: 790-797.

Kang Z, Zhu J, Lu X, Li T, Wu X (2015) Parametric optimization and performance analysis of zeotropic mixtures for an organic Rankine cycle driven by low-medium temperature geothermal fluids. Applied Thermal Engineering 89:323-331.

Kasperski J, Gil B (2014) Performance estimation of ejector cycles using heavier hydrocarbon refrigerants. Applied Thermal Engineering 71:197-203.

Kenan H, Neumen E P, Lustwerk F (1950) An investigation of ejector design by analysis and experiment. Journal of applied mechanics transaction; ASME 72: 299-309.

Kern DQ (1950). Process heat transfer. Newyork: Mc Graw-hill Publication.

Kehlhofer Rolf H (1991) Combined-cycle gas & steam turbine power plants. Lilburn,Ga, US: Fairmont Press.

Kornhauser A A (1990). The use of an ejector as a refrigerant expander. International Refrigeration and Air Conditioning Conference, Purdue University, USA.

Lee H Y, Park S H, Kim K H (2016) Comparative analysis of thermodynamic performance and optimization of organic flash cycle (OFC) and organic Rankine cycle (ORC). Applied Thermal Engineering 100:680-690.

Lemmon EW, McLinden MO, Huber ML (2002) NIST standard reference database 23: reference fluid thermodynamic and transport properties e REFPROP, version7.0. Gaithersburg: National Institute of Standards and Technology, Standard Reference Data Program.

Le V. L, Kheiri A, Feidt M, Pelloux-Prayer S (2014) Thermodynamic and economic optimizations of a waste heat to power plant driven by a subcritical ORC (Organic Rankine Cycle) using pure or zeotropic working fluid. Energy 78: 622-638.

Li G (2016) Organic Rankine cycle performance evaluation and thermoeconomic assessment with various applications part I: Energy and exergy performance evaluation. Renewable and Sustainable Energy Reviews 53: 477–499.

Li L, Ge Y T, Luo X, Tassou S A (2016) Thermodynamic analysis and comparison between CO2 transcritical power cycles and R245fa organic Rankine cycles for low grade heat to power energy conversion. Applied Thermal Engineering 106:1290-1299.

Li M, Wang J, Li S, Wang X, HE W, Dai Y (2014) Thermo-economic analysis and comparison of a CO2 transcritical power cycle and an organic Rankine cycle. Geothermic 50:101-111.

Li S, Dai Y (2014) Thermo-economic comparison of Kalina and CO2 transcritical power cycle for low temperature geothermal sources in China. Applied Thermal Engineering 70:139-152.

Liu B T, Chien KH, Wang CC (2004) Effect of working fluids on organic Rankine cycle for waste heat recovery. Energy 29: 1207-1217.

Liu F, Groll E A (2013) Study of ejector efficiencies in refrigeration cycles. Applied Thermal Engineering 52:360-370.

Liu Q, Duan Y, Yang Z (2013) Performance analyses of geothermal organic Rankine cycles with selected hydrocarbon working fluids. Energy 63: 123-132.

Lontsi F, Hamandjoda O, Mayi O T S, Kemajou A (2016) Development and performance analysis of a multi-temperature combined compression/ejection refrigeration cycle using environment friendly refrigerants. International Journal of Refrigeration 69:42-50.

Maraver D, Royo J, Lemort V, Quoilin S (2014) Systematic optimization of subcritical and transcritical organic Rankine cycles (ORCs) constrained by technical parameters in multiple applications. Applied Energy 117: 11–29.

Mago P J, Chamra L M, Srinivasan K, Somayaji C (2008) An examination of regenerative organic Rankine cycles using dry fluids. Applied Thermal Engineering 28: 998–1007.

Mansour R B, Ouzzane M, Aidoun (2014) Numerical evaluation of ejector-assisted mechanical compression systems for refrigeration applications. International Journal of Refrigeration 43:36-49.

Mazzelli F, Milazzo (2015) Performance analysis of a supersonic ejector cycle working with R245fa. International Journal of Refrigeration 49:79-92.

Mikielewicz D, Wajs J, Ziółkowski P, Mikielewicz J (2016) Utilisation of waste heat from the power plant by use of the ORC aided with bleed steam and extra source of heat. Energy 97: 11-19.

Milewski J, Bujalski W, Wolowicz M, Futyma K, Kucowski J, Barnat R (2014) Experimental investigation of CO_2 separation from lignite flue gases by 100 cm^2 single Molten Carbonate Fuel Cell. International Journal of Hydrogen Energy 39:1558-1563.

Moullec Y L (2013) Conceptual study of a high efficiency coal-fired power plant with CO2 capture using a supercritical CO2 Brayton cycle. Energy 49:32-46.

Oliveira A C, Afonso C, Matos J, Riffat S, Nguyen M, Doherty P (2002) A combined heat and power system for buildings driven by solar energy and gas. Applied Thermal Engineering 22: 587–593.

Pang Kuo-Cheng, Chen Shih-Chi, Hung Tzu-Chen, Feng Yong-Qiang Feng, Lin Jaw-Ren (2017) Experimental study on organic Rankine cycle utilizing R245fa, R123 and their mixtures to investigate the maximum power generation from low-grade heat. Energy 133:636-651.

Peris B, Navarro-Esbrí J, Molés F (2013) Bottoming organic Rankine cycle configurations to increase Internal Combustion Engines power output from cooling water waste heat recovery. Applied Thermal Engineering 61: 364-371.

Petr P, Raabe G (2015) Evaluation of R-1234ze (Z) as drop-in replacement for R-245fa in Organic Rankine Cycles – From thermophysical properties to cycle performance. Energy 93: 266-274.

Powell R L (2002) CFC phase out; have we met the challenge. Journal of Fluorine Chemistry 114: 237-250.

Pioro I L, Khartabil H F, Duffey R B (2004) Duffey. Heat transfer to supercritical fluids flowing in channels—empirical correlations (survey). Nuclear Engineering and Design 230: 69-91.

Quoilin S, Broek Martijn Van D, Declaye S´ebastien, Dewallef P, Lemort V (2013) Techno-economic survey of Organic Rankine Cycle (ORC) systems. Renewable and Sustainable Energy Reviews 22:168–186.

Rosen Marc A., (2013) Assessing global resource utilization efficiency in the industrial sector. Science of the total environment 461-462:804-807.

Saleh B, Koglbauer G, Wendland M, Fischer J, (2007) Working fluids for low-temperature organic Rankine cycles. Energy 32: 1210-1221.

Sarkar J (2015) Review and future trends of supercritical CO2 Rankine cycle for low-grade heat conversion. Renewable and Sustainable energy review 48:434-451.

Sarkar J, Bhattacharyya S (2009) Optimization of recompression S-CO2 power cycle with reheating. Energy Conversion and Management 50: 1939-1945.

Song Y, Wang J, Dai Y, Zhou E (2012) Thermodynamic analysis of a transcritical CO2 power cycle driven by solar energy with liquified natural gas as its heat sink. Energy 92:194-203.

Tashtoush B, Tashtoush A, Al-Rifai (2015) Performance study of ejector cooling cycle at critical mode under superheated primary flow. Energy Conversion and Management 94: 300–310.

Tchanche B F, Papadakis G, Lambrinos G, Frangoudakis A (2009) Fluid selection for a low-temperature solar organic Rankine cycle. Applied Thermal Engineering 29: 2468-2476.

Tuo H (2013) Thermal-economic analysis of a transcritical Rankine power cycle with reheat enhancement for a low-grade heat source. International Journal of Energy Research 37:857-867.

Turton R, Bailie R C, Whiting W B, Shaeiwitz J A (2009) Analysis, synthesis and design of chemical processes. Prentice Hall PTR, New Jersey

Uusitalo A, Honkatukia J, Turunen-Saaresti T, Grönman A (2018) Thermodynamic evaluation on the effect of working fluid type and fluids critical properties on design and performance of Organic Rankine Cycles. Journal of Cleaner Production 188:253-263.

Varga Z, Csaba T (2018) Techno-economic evaluation of waste heat recovery by organic Rankine cycle using pure light hydrocarbons and their mixtures as working fluid in a crude oil refinery. Energy Conversion and Management 174:793-801.

Wang E H, Zhang H G, Fan B Y, Ouyang M G, Zhao Y, Mu Q H (2011) Study of working fluid selection of organic Rankine cycle (ORC) for engine waste heat recovery. Energy 36: 3406-3418.

Wang F, Li D Y, Zhou Y (2015) Theoretical research on the performance of the transcritical ejector refrigeration cycle with various refrigerants. Applied Thermal Engineering 91:363-369.

Wang J, Dai Y, Sun Z (2009) A theoretical study on a novel combined power and ejector refrigeration cycle. International Journal of refrigeration 32:1186-1189.

Wang J, Sun Z, Dai Y, Ma S (2010) Parametric optimization design for supercritical CO2 power cycle using genetic algorithm and artificial neural network. Applied Energy 87: 1317-1324.

Wang J, Wang J, Dai Y, Zhao P (2014) Thermodynamic analysis and optimization of a transcritical CO2 geothermal power generation system based on the cold energy utilization of LNG. Applied Thermal Engineering 70:531-540.

Wei D, Lu X, Lu Z, Gu J (2007) Performance analysis and optimization of organic Rankine cycle (ORC) for waste heat recovery. Energy Conversion and Management 48:1113-119.

White M T, Oyewunmi O A, Haslam A J, Markides C N (2017) Industrial waste-heat recovery through integrated computer-aided working-fluid and ORC system optimisation using SAFT-c Mie. Energy Conversion and Management 150: 851–869.

World energy council/ resources 2016 summary (2016) .

Xi H, Li Ming-Jia, He Ya-Ling, Zhang Yu-Wen (2017) Economical evaluation and optimization of organic Rankine cycle with mixture working fluids using R245fa as flame retardant. Applied Thermal Engineering 113: 1056-1070.

Xi H, Li Ming-Ja, Xu C, He Ya-Ling (2013) Parametric optimization of regenerative organic Rankine cycle (ORC) for low grade waste heat recovery using genetic algorithm. Energy 58: 473-482.

Xu R, He Y (2011) A vapor injector-based novel regenerative organic Rankine cycle. Applied Thermal Engineering 31:1238-1243.

Yang X, Zheng N, Zhao L, Deng S, Li H, Yu Z (2016) Analysis of a novel combined power and ejector-refrigeration cycle. Energy Conversion and Management 108:266–274.

Yamada N, Mohamad Md Nor Anuar, Kien T T (2012) Study on thermal efficiency of low- to medium-temperature organic Rankine cycles using HFO−1234yf. Renewable Energy 41: 368-375.

Yamaguchi H, Zhang X R, Fujima K, Enomoto M, Sawada N (2006) Solar energy powered Rankine cycle using supercritical CO2. Applied Thermal Engineering 26: 2345-2354.

Yoon H J, Ahn Y, Lee J I, Addad Y (2012) Potential advantages of coupling supercritical CO2 Brayton cycle to water cooled small and medium size reactor. Nuclear Engineering and Design 245:223-232.

Yu J, Li Y (2007) A theoretical study of a novel regenerative ejector refrigeration cycle. International Journal of Refrigeration. 30:464-470.

Yu J, Song X, Ma M (2013) Theoretical study on a novel R32 refrigeration cycle with a two-stage suction ejector. International Journal of Refrigeration 36: 166-172.

Yu J, Ren Y, Chen H, Li Y(2007b). Applying mechanical subcooling to ejector refrigeration cycle for improving the coefficient of performance. Energy Conversion and Management 48:1193-1199.

Zhai H, Shi L, An Q (2014) Influence of working fluid properties on system performance and screen evaluation indicators for geothermal ORC (organic Rankine cycle) system. Energy 74:2-11.

Zhang X, Wu L, Wang X, Ju G (2016) Comparative study of waste heat steam SRC, ORC and S-ORC power generation systems in medium-low temperature. Applied Thermal Engineering 106: 1427-1439.

Zhang X R, Yamaguchi H, Fujima K, Enomoto M, Sawada N (2007) Theoretical analysis of a thermodynamic cycle for power and heat production using supercritical carbon dioxide. Energy 32:591-599.

Zhang X R, Yamaguchi H, Uneno D (2007) Thermodynamic analysis of the CO2-based Rankine cycle powered by solar energy. International Journal of Energy Research 31: 1414-1424

Zheng L, Deng J (2017) Research on CO2 ejector component efficiencies by experiment measurement and distributed-parameter modelling. Energy Conversion and Management 142:244-256.

.

Annexure

A.1 Discussion on effects of frictional pressure drop

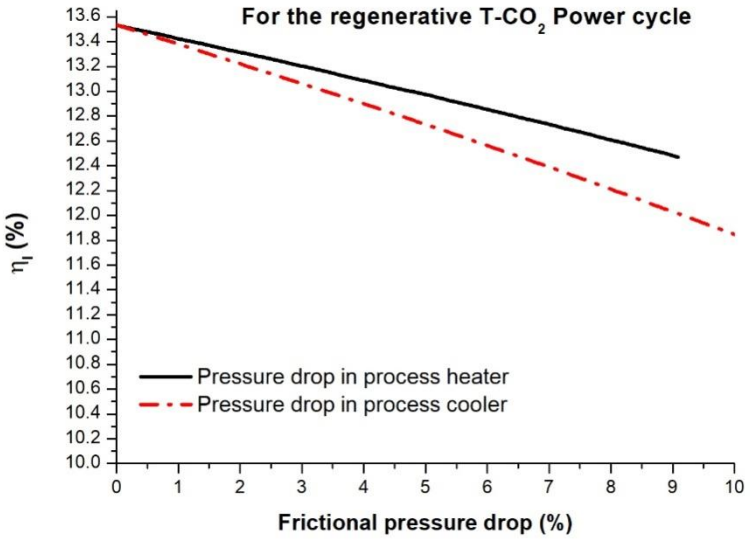

Fig. A1: Effects of varying frictional pressure drop on a CO_2 power cycle

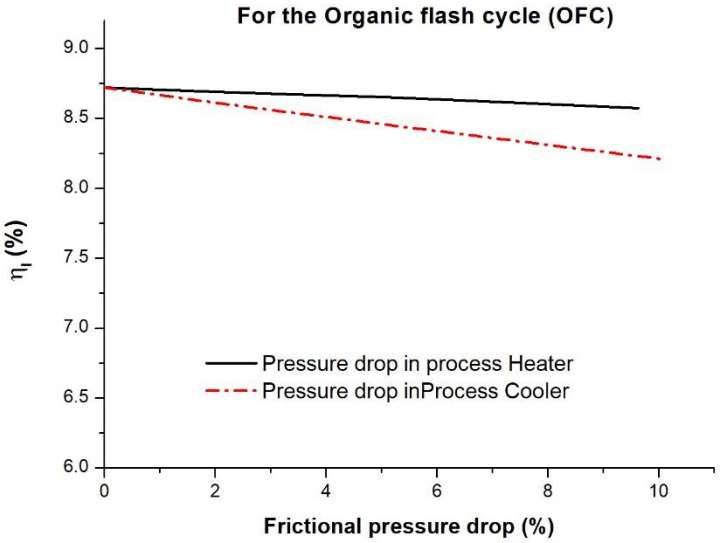

Fig. A2: Effects of varying frictional pressure drop on an OFC

Performances of the most of the power cycles are usually presented in literature by assuming a negligible frictional pressure drop. However, frictional pressured drops during the heat recovery as well as during the heat rejection would affect performance of a power cycle. Effects of varying frictional pressure drops on 1st law efficiencies of a regenerative transcritical CO_2 power cycle and an organic flash cycle are presented in Figs A.1 and A.2 respectively. It is apparent from these figures that with increasing frictional pressure drops, 1st law efficiencies of both cycles reduce. Efficiencies of both cycles are more sensitive to varying frictional pressure drops during heat rejection processes compared to the varying frictional pressure drops during heat recovery processes. If the pressure drop is considered during heat rejection, a higher turbine exit pressure is to be maintained to ensure the requisite condenser exit temperature of the working fluid. It is important to note that the condenser exit temperature is dependent on local ambient temperature. This higher turbine exit pressure results in reduced turbine power output and 1st law efficiency.

A.2 Discussion on effects of varying isentropic efficiencies

Effects of varying isentropic efficiency of each of the turbo machinery on cycle performance are demonstrated assuming ideal operating conditions of the rest of the turbo machineries present in system layouts.

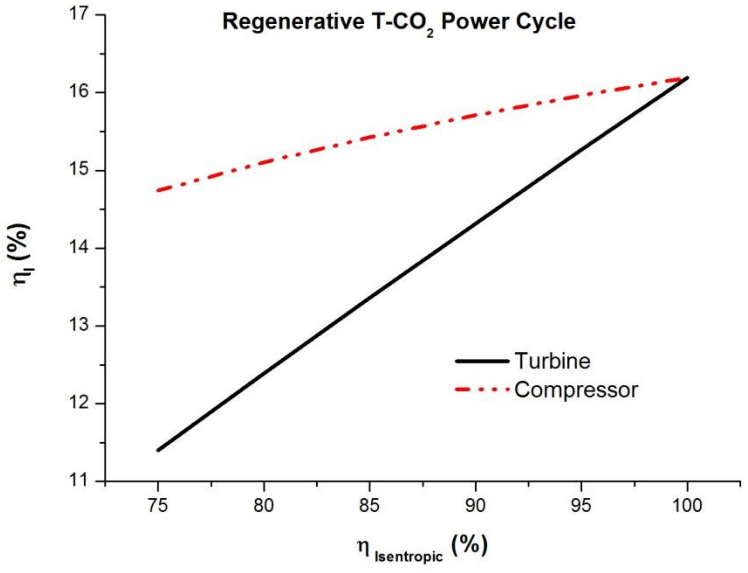

Fig. A3: Effects of varying turbine and compressor efficiencies on 1st law efficiency of a CO_2 power cycle

It is clear from the Fig.A3 that the 1st law efficiency of a regenerative T-CO_2 power cycle reduces with the reduction in both turbine isentropic efficiency and compressor isentropic efficiency. It should be noted that, the 1st law efficiency is more sensitive to the varying turbine efficiency than that with variable compressor efficiency.

It is observed in Fig. A4, that 1st law efficiency of an OFC reduces with a reduction in isentropic efficiency of the turbine. It is also apparent from this figure that the effect of varying isentropic efficiency of the circulating pump is having negligible effects on the OFC performance (i.e. the 1st law efficiency).

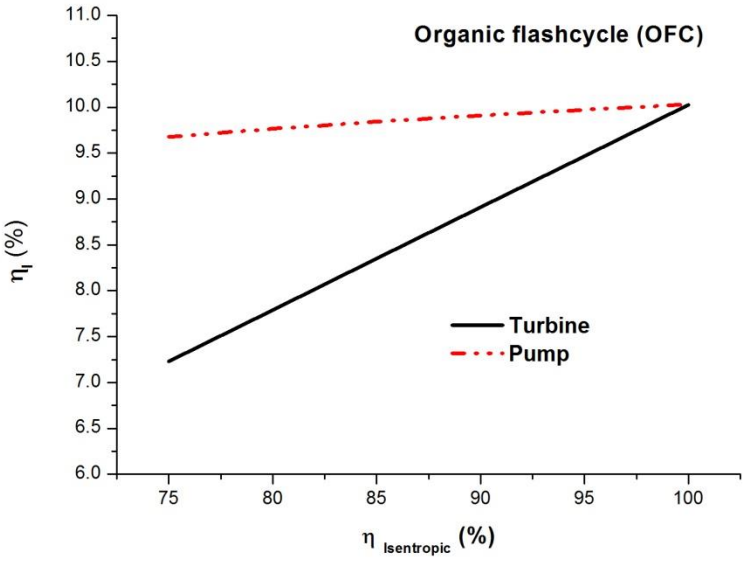

Fig. A4: Effects of varying turbine and Pump efficiencies on 1st law efficiency of an OFC